



University of  
Stavanger

**Faculty of Science and Technology**

## **MASTER'S THESIS**

|   |  |
|---|--|
| Study program/ Specialization:<br>Mechanical and Structural Engineering                           | Spring semester, 2012<br><br>Open                                      |
| Author:<br>André Augestad   | .....<br>(Authors's signature)   |
| Faculty supervisor: Tore Markeset<br>External supervisors: Øystein Bjaanes and Nils Petter Dalstø |  |
| Title of thesis:<br><br>Fatigue of service pipes  |  |
| Credits (ECTS): 30  |  |
| Key words:<br><br>Fatigue<br>Service pipes<br>Damping<br>Vibration<br>Methodology                 | Pages: 111<br><br>+ Appendix: 43 pages<br><br>Bergen, June, 14th, 2012 |

## Preface

This thesis is the final project of my master's degree in Mechanical and Structural Engineering at the University of Stavanger. It was written over the course of the spring semester of 2012.

First of all I would like to thank my supervisors Øystein Bjaanes and Nils Petter Dalstø for giving me the opportunity to write my thesis for Aker Solutions in Bergen. I have greatly appreciated their input and support over the course of this thesis. I would also like to direct my thanks to my supervisor at UiS, Professor Tore Markeset for his advice and inputs along the way.

I finally like to thank Anne Therese, my family and my fellow students for the support they have given me over these five years of studies.

## Table of contents

|  |    |
|--|----|
| Preface.....                                       | 2  |
| Table of contents.....                             | 3  |
| List of figures.....                               | 5  |
| List of tables.....                                | 10 |
| List of abbreviations, terms and nomenclature..... | 11 |
| Abstract.....                                      | 15 |
| 1 Introduction.....                                | 16 |
| 1.1 Motivation .....                               | 16 |
| 1.2 Problem.....                                   | 17 |
| 1.3 Goal .....                                     | 18 |
| 1.3.1 Limitations .....                            | 19 |
| 1.3.2 Method.....                                  | 20 |
| 2 Theory .....                                     | 21 |
| 2.1 Presentation of contractor.....                | 21 |
| 2.2 The principle of fatigue.....                  | 22 |
| 2.3 Analysis of structural damping .....           | 31 |
| 2.3.1 Internal damping.....                        | 31 |
| 2.3.2 Viscoelastic damping .....                   | 32 |
| 2.4 Measurement of damping.....                    | 35 |
| 2.5 Screening for fatigue.....                     | 38 |
| 2.6 Development of screening methodology.....      | 40 |
| 3 Experimental work.....                           | 66 |
| 3.1 Location for testing.....                      | 66 |

|       |  |     |
|-------|--|-----|
| 3.2   | Equipment for testing .....                            | 73  |
| 3.3   | Procedure for testing.....                             | 74  |
| 3.4   | Procedure for analyzing.....                           | 76  |
| 4     | Results.....   | 78  |
| 4.1   | Results of inspection .....                            | 78  |
| 4.2   | Results of testing.....                                | 89  |
| 4.3   | Results of analysis.....                               | 97  |
| 5     | Discussion.....  | 102 |
| 6     | Conclusion .....                                       | 104 |
| 7     | References.....  | 105 |
| 8     | Attachments .....                                      | 111 |
| 8.1   | Deduction of mechanisms for fracture mechanics.....    | 111 |
| 8.2   | Deduction of mechanisms for damping of vibration ..... | 114 |
| 8.3   | Plot Plan.....   | 118 |
| 8.4   | Minutes of Meeting Statoil.....                        | 119 |
| 8.5   | Microsoft Visual Basic macros .....                    | 120 |
| 8.5.1 | BareData__().....                                      | 120 |
| 8.5.2 | NyeElementer() .....                                   | 121 |
| 8.5.3 | GRAF().....  | 123 |
| 8.6   | MatLab datasheet .....                                 | 124 |
| 8.7   | Results from analysis .....                            | 127 |

## List of figures

|  |    |
|--|----|
| Figure 2-1 Logo Aker Solutions (Aker Solutions ASA 2012a).....   | 21 |
| Figure 2-2 Organizational Chart Aker Solutions (Aker Solutions ASA 2012b)...   | 21 |
| Figure 2-3 Hierarchy of steering documents (adapted from International Organization for Standardization, 2006) .....                   | 23 |
| Figure 2-4 Through-thickness crack in an infinite plate ( $\gg 2 \times a$ ) subjected to a remote tensile stress (Anderson 2005)..... | 26 |
| Figure 2-5 Traditional strength of materials approach (Anderson 2005).....   | 27 |
| Figure 2-6 Fracture mechanics approach (Anderson 2005).....  | 27 |
| Figure 2-7 Constant amplitude fatigue crack growth under small-scale yielding conditions (Anderson 2005).....                          | 28 |
| Figure 2-8 Typical fatigue crack growth behavior in metals (Lalanne 2009) .....  | 28 |
| Figure 2-9 Example of generated S-N curve from experimental data (Beardmore 2010) .....  | 29 |
| Figure 2-10 Hysteresis loop of internal damping (Silva 2007).....  | 32 |
| Figure 2-11 Resonance response (Dukkipati 2007).....   | 33 |
| Figure 2-12 Variation of $X$ and $\phi$ with the frequency ratio $r$ (Rao 2010) .....  | 34 |
| Figure 2-13 Impulse response of a simple oscillator (Silva 2007) .....   | 35 |
| Figure 2-14 Comparison of motion with different types of damping (Rao 2010)  | 36 |
| Figure 2-15 Maintenance management Traditional vs. Condition based (Markeset 2012) .....   | 38 |
| Figure 2-16 Extract of P&ID (Statoil 2011c).....   | 41 |
| Figure 2-17 Basic flowchart shapes.....  | 41 |

|   |    |
|---|----|
| Figure 2-18 Flowchart screening report (Adapted from Mathieson 2007).....                                 | 43 |
| Figure 2-19 Potential for valve chatter.....  | 48 |
| Figure 2-20 Potential for acoustic vibration .....  | 49 |
| Figure 2-21 Potential for fluid hammer .....  | 49 |
| Figure 2-22 Potential for slugging flow.....  | 50 |
| Figure 2-23 Potential for mechanical vibrations .....   | 51 |
| Figure 2-24 Potential for flow-induced turbulence.....  | 52 |
| Figure 2-25 Classification of flow-induced vibration (Blevins 1990) .....                                 | 52 |
| Figure 2-26 Geometry effects.....   | 53 |
| Figure 2-27 Weldolet (Bonney Forge Corporation 2012c) .....   | 54 |
| Figure 2-28 Sockolet (Bonney Forge Corporation 2012a) .....   | 54 |
| Figure 2-29 Thredolet (Bonney Forge Corporation 2012b).....   | 54 |
| Figure 2-30 Supporting & static loading of service pipes.....   | 55 |
| Figure 2-31 Screening methodology for fatigue (adapted from Mathieson).....                               | 56 |
| Figure 2-32 Methodology for inspection of service pipes.....  | 62 |
| Figure 2-33 Reduction of risk (Adapted from International Organization for<br>Standardization 2002) ..... | 64 |
| Figure 3-1 Kollsnes gas processing plant (Statoil 2007).....  | 66 |
| Figure 3-2 Influence of thermodynamic inhibitors on the hydrate equilibrium<br>curve (Lien 2010) .....    | 68 |
| Figure 3-3 Area A11 Pig receiver & launchers/ESD valves (Statoil 2011a).....                              | 69 |
| Figure 3-4 Work permit levels and risk triangle (Rogsnvåg et al. 2005).....                               | 72 |
| Figure 3-5 Emerson CSI 2130 Vibration Analyzer (Reliability Maintenance<br>Solutions Ltd n.d.).....       | 73 |
| Figure 4-1 Inspected areas A21 - A23 Turboexpander 1 – 3 (Statoil 2011a) .....                            | 78 |

|   |     |
|---|-----|
| Figure 4-2 Flange Q-B-L—1100-06C connected to CA-21-5111-FS20A in area A21 .....  | 79  |
| Figure 4-3 Detail of socket connected to CA-21-5111-FS20A in area A21.....  | 80  |
| Figure 4-4 Flange Q-B-L—1100-06C connected to CA-21-5110-FS20A in area A22 .....  | 80  |
| Figure 4-5 Detail of socket connected to CA-21-5110-FS20A in area A22.....  | 81  |
| Figure 4-6 Inspected areas A24 NGL Extraction (Statoil 2011a).....  | 81  |
| Figure 4-7 25-8287/1-2 SP2-2 on PV-25-8287-ES20A in A24 .....   | 83  |
| Figure 4-8 Flange on PL-25-8501-BC21A in A24 .....  | 84  |
| Figure 4-9 MX3V2J-J74220 on PV-25-8107-DC11A in A24 .....   | 84  |
| Figure 4-10 Area of inspection A11/A12. (Statoil 2011a).....  | 86  |
| Figure 4-11 Flow orifice monitor 20-FE5228 at 10 <sup>7</sup> -PR-20-5347-EC19AX .....  | 87  |
| Figure 4-12 Flow orifice instrument (Statoil 2010a) .....   | 88  |
| Figure 4-13 Ambient vibration PV-25-8287-ES20A, A24, E-W .....  | 91  |
| Figure 4-14 Ambient vibration PR-20-5347-EC19AX, A11, E-W .....   | 92  |
| Figure 4-15 Ambient vibration PR-20-5347-EC19AX, A11, N-S .....   | 93  |
| Figure 4-16 East-West and North-South mounting on 20-FE5228-1 in A11.....   | 93  |
| Figure 4-17 Ambient vs. forced vibration PV-25-8287-ES20A, A24, E-W .....   | 96  |
| Figure 4-18 Damping ratio of I & II. Range indicated (Side vs. Side).....   | 98  |
| Figure 4-19 Damping ratio of VI & VII. Range indicated (N-S vs. N-S).....   | 99  |
| Figure 4-20 Damping ratio of III. Range indicated (E-W vs. N-S) .....   | 99  |
| Figure 8-1 Characteristic step response of a simple oscillator (Silva 2007) .....   | 114 |
| Figure 8-2 Magnification factor method of damping measurement applied to a single-degree-of-freedom system (Silva 2007) ..... | 116 |

|   |     |
|---|-----|
| Figure 8-3 Bandwidth method of damping measurement in a single-degree-of-freedom system (Silva 2007)..... | 117 |
| Figure 8-4 Plot Plan Kollsnes (Statoil 2011a).....  | 118 |
| Figure 8-5 Result Non-induced vibration CA-25-5111-FS20A, A21, top.....                                   | 127 |
| Figure 8-6 Result Induced vibration CA-25-5111-FS20A, A21, top.....                                       | 128 |
| Figure 8-7 Result Non-induced vibration CA-25-5111-FS20A, A21, side.....                                  | 129 |
| Figure 8-8 Result Induced vibration CA-25-5111-FS20A, A21, side .....                                     | 130 |
| Figure 8-9 Result Non-induced vibration CA-25-5110-FS20A, A22, top.....                                   | 131 |
| Figure 8-10 Result Induced vibration CA-25-5111-FS20A, A22, top .....                                     | 132 |
| Figure 8-11 Result Non-induced vibration CA-25-5110-FS20A, A22, side .....                                | 133 |
| Figure 8-12 Result Induced vibration CA-25-5110-FS20A, A22, side .....                                    | 134 |
| Figure 8-13 Result Non-induced vibration PV-25-8287-ES20A, A24, E-W .....                                 | 135 |
| Figure 8-14 Result Induced vibration PV-25-8287-ES20A, A24, E-W .....                                     | 136 |
| Figure 8-15 Result Non-induced vibration PV-25-8287-ES20A, A24, N-S .....                                 | 137 |
| Figure 8-16 Result Induced vibration PV-25-8287-ES20A, A24, N-S.....                                      | 138 |
| Figure 8-17 Result Non-induced vibration PL-25-8501-BC21A, A24, side.....                                 | 139 |
| Figure 8-18 Result Induced vibration PL-25-8501-BC21A, A24, top.....                                      | 140 |
| Figure 8-19 Result Non-induced vibration PL-25-8501-BC21A, A24, top.....                                  | 141 |
| Figure 8-20 Result Induced vibration PL-25-8501-BC21A, A24, top.....                                      | 142 |
| Figure 8-21 Result Non-induced vibration PV-25-8107-DC11A, A24, E-W.....                                  | 143 |
| Figure 8-22 Result Induced vibration PV-25-8107-DC11A, A24, E-W .....                                     | 144 |
| Figure 8-23 Result Non-induced vibration PV-25-8107-DC11A, A24, N-S .....                                 | 145 |
| Figure 8-24 Result Induced vibration PV-25-8107-DC11A, A24, N-S.....                                      | 146 |
| Figure 8-25 Result Non-induced vibration PR-20-5347-EC19AX, A11, E-W....                                  | 147 |
| Figure 8-26 Result Induced vibration PR-20-5347-EC19AX, A11, E-W .....                                    | 148 |



Figure 8-27 Result Non-induced vibration PR-20-5347-EC19AX, A11, N-S ..... 149

Figure 8-28 Result Induced vibration PR-20-5347-EC19AX, A11, N-S ..... 150

Figure 8-29 Result Non-induced vibration PR-20-5347-EC19AX, A11, E-W.... 151

Figure 8-30 Result Induced vibration PR-20-5347-EC19AX, A24, E-W ..... 152

Figure 8-31 Result Non-induced vibration PR-20-5347-EC19AX, A11, N-S ..... 153

Figure 8-32 Result Induced vibration PR-20-5347-EC19AX, A11, N-S ..... 154

## List of tables

|   |     |
|---|-----|
| Table 2-1 Frequency of occurrence (Mathieson 2007).....   | 44  |
| Table 2-2 Probability of failure (Det Norske Veritas 2010b) .....   | 45  |
| Table 2-3 Consequence of failure ranking scales (International Organization for<br>Standardization 2002; Det Norske Veritas 2010b)..... | 46  |
| Table 2-4 Risk matrix (International Organization for Standardization 2002) ...   | 47  |
| Table 4-1 Test numbering scheme.....  | 89  |
| Table 4-2 Results of vibration testing at ambient conditions .....  | 90  |
| Table 4-3 Results of forced vibration.....  | 94  |
| Table 4-4 Calculated damping ratio .....  | 97  |
| Table 4-5 Estimated results of vibration at resonance.....  | 101 |

## List of abbreviations, terms and nomenclature

|      |   |  |
|------|---|--|
| AI   | - | Asset Integrity                            |
| AIM  | - | Asset Integrity Management                 |
| AS   | - | Aker Solutions                             |
| ATEX | - | Atmosphères Explosives                     |
| BM   | - | Bandwidth Method                           |
| BOP  | - | Blow-Out Preventer                         |
| BS   | - | British Standard                           |
| BSI  | - | British Standards Institute                |
| C&T  | - | Concept & Technology                       |
| CA   | - | Chemical, Methanol                         |
| CBM  | - | Condition Based Maintenance                |
| CM   | - | Condition Monitoring                       |
| CoF  | - | Consequence of Failure                     |
| CTOD | - | Crack-Tip Opening Displacement             |
| DEG  | - | Diethylen Glycol                           |
| DFT  | - | Discreet Fourier Transform                 |
| DNV  | - | Det Norske Veritas                         |
| E-W  | - | East – West (Plant Relative Direction)     |
| ESD  | - | Emergency Shutdown Valve                   |
| ENS  | - | Engineering Numbering System               |
| FoO  | - | Frequency of Occurrence                    |
| FPSO | - | Floating Production Storage and Offloading |
| GVI  | - | General Visual Inspection                  |
| HAZ  | - | Heat Affected Zone                         |

|        |   |  |
|--------|---|--|
| HSE    | - | Health, Safety and Environment                     |
| I&MT   | - | Inspection & Maintenance Technology                |
| ISO    | - | International Organization for Standardization     |
| KENS   | - | Kollsnes Engineering Numbering System              |
| LCI    | - | Life Cycle Information                             |
| LEFM   | - | Linear Elastic Fracture Mechanics                  |
| LDM    | - | Logarithmic Decrement Method                       |
| MEG    | - | Monoethylene Glycol                                |
| MMO    | - | Maintenance, Modification & Operations             |
| N-S    | - | North-South (Plant Relative Direction)             |
| NCS    | - | Norwegian Continental Shelf                        |
| NDT    | - | Non-Destructive Testing                            |
| NGL    | - | Natural Gas Liquid                                 |
| NORSOK | - | Norwegian Continental Shelf's Competitive Position |
| OLF    | - | The Norwegian Oil Industry Association             |
| P&ID   | - | Process & Instrumentation Diagram                  |
| PoF    | - | Probability of Failure                             |
| PSA    | - | Petroleum Safety Authority Norway                  |
| PSV    | - | Pressure Safety Valve                              |
| PT     | - | Process, Two-phase                                 |
| RBI    | - | Risk Based Inspection                              |
| RP     | - | Recommended Practice                               |
| SBS    | - | Strategic Business Stream                          |
| SDOF   | - | Single Degree-of-Freedom                           |
| SJA    | - | Secure Job Analysis                                |
| SRM    | - | Step-Response Method                               |
| STID   | - | Statoil Technical Information Database             |
| TIAS   | - | Technical Integrity Analysis and Studies           |
| TR     | - | Technical Requirement                              |
| USB    | - | Universal Serial Bus                               |

|                  |   |                                      |
|------------------|---|--------------------------------------|
| WP               | - | Work Permit                          |
| System 13        | - | Riser & Well Topside                 |
| System 20        | - | Separation & Stabilization           |
| System 23        | - | Recompression, Cooling and Scrubbing |
| $a$              | - | Crack length                         |
| $A$              | - | Area of surface of crack             |
| $\delta A$       | - | Area increment at crack surface      |
| $C$              | - | Material constant                    |
| $d_v$            | - | Damping capacity of object           |
| $\delta$         | - | Logarithmic decrement                |
| $\delta_{st}$    | - | Deflection under static force $F_0$  |
| $E$              | - | Young's modulus                      |
| $E^*$            | - | Time independent complex modulus     |
| $\varepsilon$    | - | Strain                               |
| $f_{ij}(\theta)$ | - | Function of polar angle              |
| $G$              | - | Energy release rate                  |
| $G_c$            | - | Critical energy release rate         |
| $K$              | - | Stress intensity factor              |
| $K_c$            | - | Critical stress intensity factor     |
| $m$              | - | Material constant                    |
| $M_p$            | - | Peak value                           |
| $n$              | - | 1, 2, 3...                           |
| $N$              | - | Speed (RPM)                          |
| $\eta$           | - | Loss factor                          |
| $\omega$         | - | Vibration frequency                  |
| $p_c$            | - | Breaking load                        |
| $PO$             | - | Percentage overshoot                 |

|                 |   |   |
|-----------------|---|---|
| $Q$             | - | Heat added to the system                                |
| $Q_A$           | - | Amplification factor                                    |
| $\sigma$        | - | Stress  |
| $\sigma_{\max}$ | - | Stress, peak value                                      |
| $r_p$           | - | Period of excitation                                    |
| $t$             | - | Time (sec)  |
| $T_p$           | - | Peak time   |
| $\Delta U$      | - | Change in internal energy                               |
| $U_{\max}$      | - | Maximum internal energy                                 |
| $W$             | - | Work done by the system                                 |
| $\delta W$      | - | Strain energy   |
| $\omega_d$      | - | Damped frequency  |
| $\omega_n$      | - | Natural frequency                                       |
| $\omega_r$      | - | Frequency at peak amplification factor                  |
| $\Delta\omega$  | - | Bandwidth   |
| $X$             | - | Amplitude   |
| $X_i$           | - | Deflection at $i$                                       |
| $X_{i+r_p}$     | - | Deflection at $i+r_p$                                   |
| $\gamma$        | - | Surface energy of crack                                 |
| $\gamma_{eff}$  | - | Effective surface energy of crack                       |
| $\gamma_p$      | - | Contribution to surface energy from plastic deformation |
| $\zeta$         | - | Damping ratio   |

## **Abstract**

The first part of this thesis will present the principle of fatigue, vibration and damping of service pipes on the NCS. This is used for the creation of a screening methodology for prioritizing service pipes with regards to susceptibility to fatigue damage. The methodology provides the user with a toolset for identification and evaluation of the various service pipes in operation.

An acceptance criterion of a damping ratio of 0.3 for service pipes has been identified. Pipes with a damping ratio lower than 0.3 has been shown to experience high amplitudes in the case of resonance frequencies.

# 1 Introduction

## 1.1 Motivation

Production and facilitation of petroleum based products consists of a sequence of different processes. On the Norwegian continental shelf (NCS), the hydrocarbons (a collective term for crude oil, natural gas and the different compositions of petroleum based products in between) are extracted from source rock deep below the sea-bed. The pressure and temperature in the reservoirs forces the content of the reservoir through a flow channel. The flow channel content is a mixture of hydrocarbons, water, injected components and sand in varying concentrations. The flow channel is usually a series of lined steel pipes screwed together and encapsulated with cement. Depending on the category of well, there is usually a valve tree sitting at the sea-bed. This to allow emergency closing and flow regulating by a set of blowout preventers and chokes (Asheim 2011). In a traditional offshore installation processing plant, the multiphase stream is then transported topside by the means of risers.

From the riser tie-in, the first step of the processing of the hydrocarbons is usually the removal of unwanted components. In most cases this includes the produced water, injected components and solid rock, as mentioned above. From the producing wells, the well stream is transported to the individual consumers through a series of pipes. Through separators, scrubbers, slug traps and other equipment, the flow is being moved at varying pressure, speed and inclination.

As pressure and mass flow from the well is choked or decreases throughout the processes, the necessity of pumps and compressors arise. The uni- or multiphase turbulent flow combined with rotating or reciprocating pumps and compressors can introduce vibrations in the system. These vibrations are being transmitted in the pipe walls, supports and the flow itself.

As the flow passes bends, chokes, consumers and valves, the properties of the stream fluctuates. To maintain the overview of the different process parameters at any given time, measuring devices has to come in contact with the stream. In



accordance to standards and technical requirements, there is also the need for instruments, outlets and drains along the line. These can be connected to the main pipe through small-bore pipes known as service pipe.

The introduced vibrations from the main pipe will be transferred to these service pipes. As the dimensions of the small-bore pipes can be significantly smaller in comparison to the main pipe, the vibration can affect these service pipes in a higher degree of severity compared to the main pipe. Depending on a multitude of factors, there is a possibility that the service pipe will start oscillating. These oscillations will again introduce stresses. It is the amplitude and frequencies of the cyclic oscillation of the pipes that affect the magnitude of stresses developed in the service pipes.

## 1.2 Problem

The vibration of service pipes causes stress. Stress can be defined as the measure of the internal forces acting within a deformable body as a result of applied external forces (Callister 2006). According to the basics of mechanics and materials science, the strength of a material is the ability of an object to withstand stress without failure. In the case of the vibration of the service pipes, these stresses are seldom in the range of the material yield or ultimate strength. In stresses of such low magnitude, a different deteriorating process comes in to play.

According to Callister (2006), fatigue can be defined as “[...] *a form of failure that occurs in structures subjected to dynamic and fluctuating stresses*”. Due to the nature of fatigue, a construction can fail at stress levels lower than the yield strength of the material. A small-bore service pipe can be exposed to a random series of loads. In addition to the complexity of mechanics of deteriorating processes in metals, the total number of service pipes, valves, drains and blinded pipe sockets in service on installations on the NCS makes for a difficult development of inspection- and maintenance programs. The results of the failure of just one of the thousands service pipes can lead to a forced partial- or full shutdown of the systems in operation. Unplanned shutdowns and the subsequent

startup of process systems can cost operators millions in lost revenue (Mathieson 2012).

Of the thousands of service pipes in service, only a handful of them experiences complete failure. Identifying which of the pipes that are vulnerable to fail requires a systematic process, and is a complex task. In addition, inspection of the pipes can be problematic due to the limited time range where crack initiation can be identified using non-destructive testing (NDT) methods. This has led to a series of standards and technical requirements intended to help the suppliers of pipes, valves, instruments and structures ((Det Norske Veritas 2010a; Statoil 2012i) among others).

### 1.3 Goal

For this thesis, a series of secondary goals has been identified. Exploring each of these sections, one will be better equipped for handling the gap between the established procedures of today and the best practices for the fatigue of service pipes.

The first secondary goal will be to uncover the literature available for the fatigue of service pipes available today. This will be used as a basis for the development of the next secondary goal; the deduction of the principles of fatigue of service pipes. From these goals, the practices of today will be highlighted; exposing how these practices can be improved on. Within these two secondary goals, the principle of fatigue and damping will be explained.

The third secondary goal will then be testing the practices established in the previous two secondary goals. This is done in the form of an experiment at a process plant of relevance to the contractor. From this, experiences can be extracted and better routines can be created.

Based on the results from the investigation of requirements, one will try to establish a screening methodology for identifying service pipes susceptible to fatigue more systematically compared to the procedures of today. Constructed from these goals, one builds the hypothesis

*“An acceptance criterion based on the damping capability of a service pipe can be found. A screening methodology for prioritizing service pipes with regards to susceptibility to fatigue damage can be developed and implemented applying known and available measuring techniques”*

### 1.3.1 Limitations

It is necessary to limit the scope of the hypothesis. Focus will be put on service pipes of interest to the contractor. In itself, service pipes are a wide category of pipes. This thesis will limit itself to external, small-bore service pipes connected to subsystems at process plants on the NCS. There are today no requirements for amount of damping of oscillation for the small-bore service pipes (NORSOK 2007). This means that there is no specified value of capability for a service pipe to deal with non-defined stresses that might lead to resonance.

It would be interesting to see how the external service pipes compared to the internal thermo wells. This will not be done, as an accept criteria for the vibration of the thermowells already has been identified (Olsnes 2001).

For the inspection and testing of the hypothesis, the onshore process plant at Kollsnes will be used. Most of the service pipes for on the NCS are currently on installations offshore. Access to these installations is regulated and transport costly. Compared to the offshore installations, the onshore processing plants are not as difficult and expensive to visit. As the onshore installations are operated at similar conditions, they are exposed to the same type of problems as the offshore installations. Any accept criteria and/or methodology developed will consequently be valid for both onshore and offshore installations with minor to no modification.

To avoid that the thesis ends up too wide, it will be focused on the theoretical background for the concept of fatigue and how this establishes the expectations for the results of the practical testing. This will again be used for

the creation of a screening procedure for prioritization of service pipes in inspection and maintenance programs.

### 1.3.2 Method

This thesis will split into two separate parts. In the first section, the theory behind the problem with fatigue will be presented. Fracture mechanics will be used to describe how crack initiation and growth will occur at medium to high stress conditions. It will be based on the understanding of how fracture processes function in regards to operating conditions. The principle of dampening of vibrations will also be explained. By introducing a minimum requirement for damping of amplitude within the area of resonance, the service pipes will become more resistant to fatigue. Ending the first section, a suggested methodology for the screening of service pipes will be presented.

The experimental part will utilize the tools of the first part of the thesis for testing the hypothesis. By using the testing equipment and procedures Aker Solutions currently employs, a dataset will be presented. Using this dataset, analyses will be performed for the identification of limit value for the damping of the vibration. Based on the results from the analysis, the data will either confirm or disprove the hypothesis. The handling and manipulation of these measurements will be explained in the part of the thesis labeled “Results”.

Any obstacles or variations of the results will be presented in “Discussion”. Completing the thesis, “Conclusion” will present the finalized findings of the thesis.

## 2 Theory

### 2.1 Presentation of contractor



Figure 2-1 Logo Aker Solutions (Aker Solutions ASA 2012a)

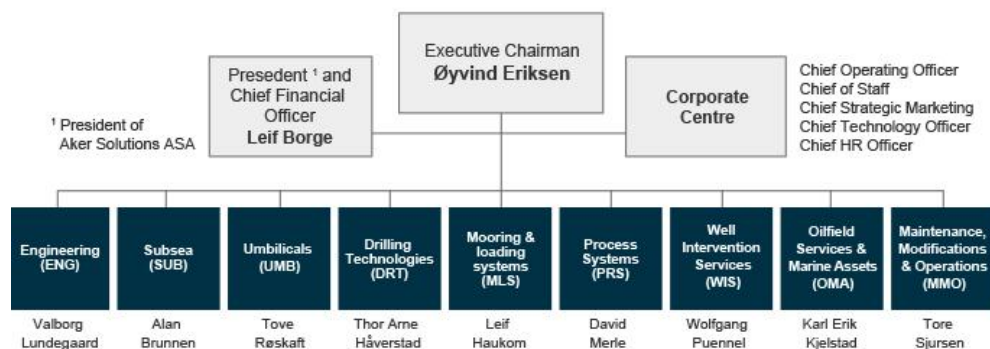


Figure 2-2 Organizational Chart Aker Solutions (Aker Solutions ASA 2012b)

Aker Solutions ASA is a leading global oil service company providing engineering services, technologies, product solutions and field-life solutions for the oil and gas industry. Situated in Bergen, Aker Solutions MMO AS Bergen is the Maintenance, Modification & Operations (MMO) branch of the company. MMO consists of five region independent strategic business streams (SBS).

The roots of Aker Solutions can be traced back to the founding of Kvaerner Brug in Oslo in 1853. From the modest start with working on pulping products, Aker Solutions has grown in to a NOK 35 billion revenue company. It currently employs an estimated 18500 persons in over 30 countries on every continent except Antarctica (Aker Solutions ASA 2012a).

Aker Solutions MMO AS Region Bergen main contracts per May 2012 includes Kristin LPP modification, Mongstad Modification, Oseberg B Drilling upgrade, Gullfaks drilling upgrade, Visund and Troll Brage M&M in accordance to framework agreements with Statoil.

This thesis is written in cooperation with the SBS Asset Integrity Management group (AIM). Working in parallel to the other, mostly Statoil-governed, projects in Bergen, AIM bids and take upon themselves contracts with several operators and installations. Today, AIM are currently working on projects that has to do with fatigue and inspection regimes necessary for maintaining satisfactory uptime and reduced risk when it comes to health and safety requirements on- and offshore (Mathieson 2012).

## 2.2 The principle of fatigue

Fracturing of man-made structures has been a problem since the first buildings were erected. As consequences from structural failure increased over the course of history, there has been a higher focus on understanding the mechanism that causes a given material to fail. An economic study conducted in 1978 estimated that the direct economic cost of fractures in USA were in the range of 119 billion USD (Duga et al. 1983). Calculating the inflation, this number would represent around 390 billion USD and accounted for around 4 % of the gross national product (Central Intelligence Agency 2012).

Anderson does in his book “Fracture Mechanics: Fundamentals and Applications” state that most structural failures falls in to two specific categories.

1. Negligence during design, construction or operation of the structure
2. Application of a new design or material, which produces an unexpected (and undesirable) result

In the case of service pipes on process systems, one can argue that in the case of complete failure, it would most likely fall under the first mentioned category. Oil & gas installations on the NCS must be operated and maintained in accordance with all the laws and regulations within the national border. In addition to the stated laws and regulations, a series of industry standards has been developed for all the operators on the NCS.

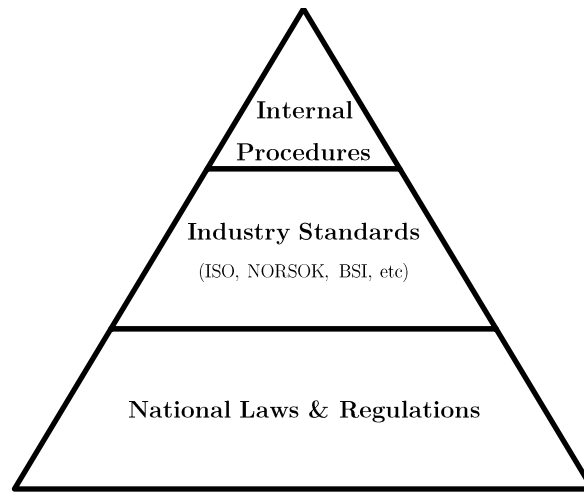


Figure 2-3 Hierarchy of steering documents (adapted from International Organization for Standardization, 2006)

Process systems on- and offshore have to follow very strict regulations for design stated in these standards. One example is the governing requirements for piping on the Norwegian continental shelf (NCS) is based on the American standard *ASME B31.3-2010 Process Piping* (American Society of Mechanical Engineers 2010). This standard contains a series of design specification for the contractor to follow. It is then up to the contractor create internal procedures for their installation specific operation. In the case of installations with Statoil as operator or technical operations manager, the internal procedure for pipe specification is known as the TR2000 (Statoil 2012i).

By accepting and designing after these Life Cycle Information (LCI) requirements, the contractors has a set of standardized and tested guidelines. Although having such strict guidelines means that it cannot cater for every situation. Even though the requirements are considered safe according to the expected operating conditions, one always runs the risk of ending up at a state the technical requirement does not cover. In these cases, fracturing might ensue.

Since the earliest research on fracturing, a qualitatively connection between stress and fracturing has been searched for. The breakthrough came in 1920 when Alan Arnold Griffith published his first work, "The phenomenon of rupture and flow in solids", on the qualitatively connection between the fracture stress

and flaw size (Anderson 2005). Griffith based his fracture theory on work done by the first law of thermodynamics in the application of the conservation of energy principle to heat and thermodynamic processes. It states that; “*The change in internal energy of a system is equal to the heat added to the system minus the work done by the system*” (Nave 2011):

$$\Delta U = Q - W \tag{2.1}$$

- $\Delta U$  = Change in internal energy
- $Q$  = Heat added to the system
- $W$  = Work done by the system

Combined with a simple energy balance, Griffith built his work on that the assumption that the material had an included flaw. This flaw becomes unstable in the form that it grows uncontrollable and thereby invokes the fracturing of the material. To explain this, Griffith assumed that the change in strain energy from the incrementing crack growth becomes larger than the surface energy of the material. The surface energy resists change and tries to close the crack. Because of this assumption, the theory was only valid for the most brittle materials, such as glass. The reason why he chose to work with glass over the other materials had to do with how glass behaves. With very low elasticity, the work of the fracture had to come exclusively from surface energy in the material. In materials with higher elasticity deformation caused by defects and dislocations within the materials structural lattice is also a part of the work done by the system.

$$\frac{\delta W}{\delta A} = \gamma \tag{2.2}$$

- $\delta W$  = Strain energy
- $\delta A$  = Area increment at crack surface
- $\gamma$  = Surface energy

Even with the lack of practical uses, Griffith helped improve the understanding of how fracturing occurs. This led to increased focus on further investigating how the mechanics of fracturing happened step-by-step. A complete deduction of relevant fracture mechanics is attached (ref: Section 8.1). Based on



the work of Griffith, the scientist G. R. Irwin managed to port the specific surface energy method to non-brittle materials. He proposed to add a specific surface energy at the crack tip for the plastic deformation of the crack.

$$\gamma_{eff} = \gamma + \gamma_p \quad 2.3$$

$\gamma_{eff}$  = Effective surface energy

$\gamma_p$  = Contribution to surface energy from plastic deformation

From this, the stress intensity factor,  $K$ , could be deducted from the energy criterion. The energy criterion states that fracture occurs when the energy for crack growth (i.e. stresses) is proportional to a given constant,  $K$ , the stress distribution can be computed. For a crack in an infinite ( $\gg 2 \times a$ ) plate that goes through the thickness the plate with a total crack length of  $2 \times a$  (ref Figure 2-4), the stress intensity factor can be calculated to be

$$K = \sigma\sqrt{\pi a} \quad 2.4$$

$a$  = Crack length

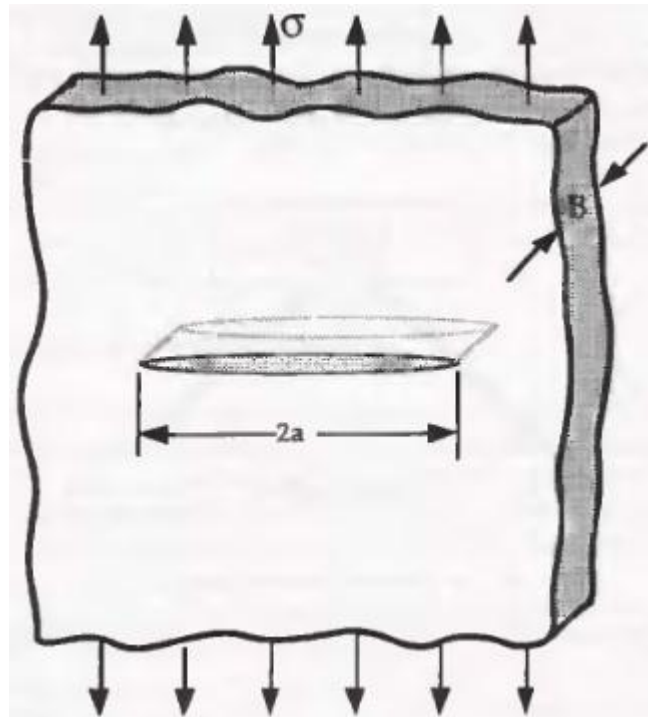


Figure 2-4 Through-thickness crack in an infinite plate ( $\gg 2a$ ) subjected to a remote tensile stress (Anderson 2005)

This gives the simplified relationship between the energy release rate,  $G$ , and the stress intensity factor

$$G = \frac{K^2}{E} \quad 2.5$$

$E$  = Young's modulus

For high strength steels, typical of service pipes, this Linear Elastic Fracture Model (LEFM) is considered the typical fracture behavior for energy release rate (Anderson 2005).

The formula simplified the work necessary to analyse the fracture processes in linearly elastic bodies. What this did was to remove the laborious numerical calculations of strain energy. Earlier, evaluation of the singular part was necessary to finding  $K$ . This could now be replaced by utilizing an already known

distribution of the energy release rate. This approach also makes it possible to describe fracture as a process with stage wise fracturing instead of the all-at-once approach (Yarema 1996).

In design, the better understanding of fracture mechanics has changed somewhat the way new designs are developed. The traditional focus on applied stresses has to a certain degree been replaced by focusing on flaw sizes and fracture toughness. This in combination with applied stresses. The relations are illustrated below.



Figure 2-5 Traditional strength of materials approach (Anderson 2005)

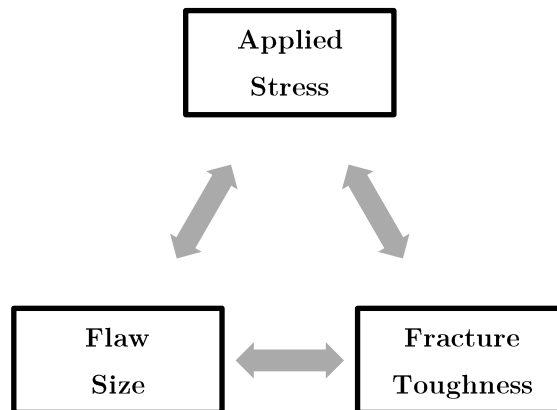


Figure 2-6 Fracture mechanics approach (Anderson 2005)

When a material is exposed for cyclic stresses, fracture mechanics become highly useful. For a complete rundown of the deduction of how the principles are physically explained, the reader is referred to section 8.1. In short, a crack growing under constant cyclic stress intensity experiences the formation of a plastic zone near the crack tip.

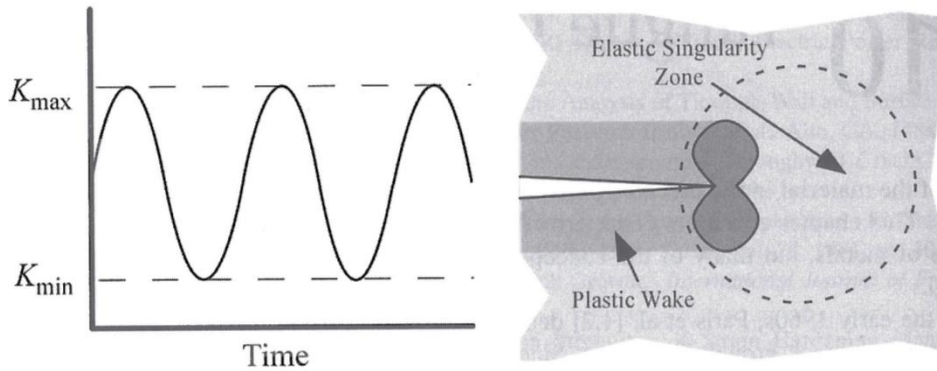


Figure 2-7 Constant amplitude fatigue crack growth under small-scale yielding conditions (Anderson 2005)

Using the  $J$  integral for large scale yielding (ref. section 8.1), the typical crack growth behavior in metals can be illustrated. The crack growth and stress intensity factor is plotted against one another in a log-log plot.

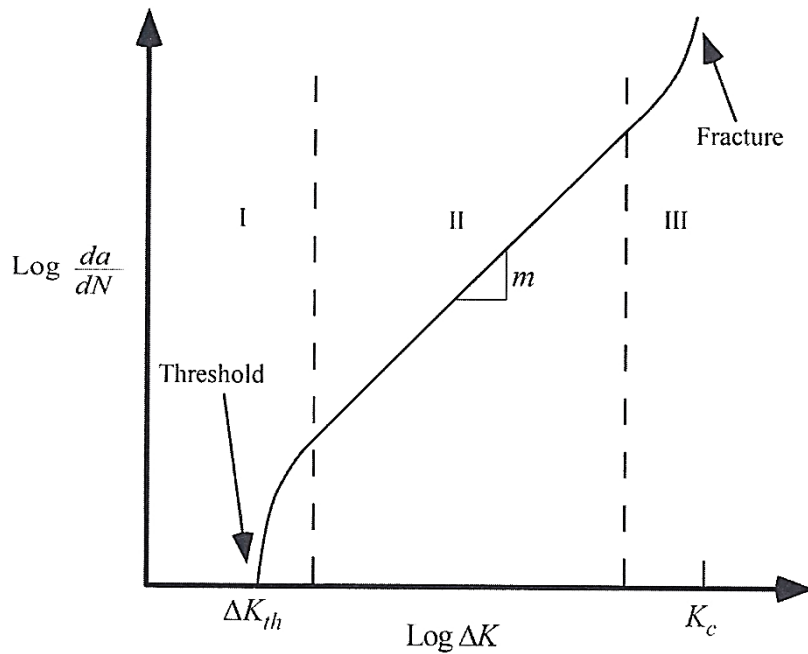


Figure 2-8 Typical fatigue crack growth behavior in metals (Lalanne 2009)

Separated into three specific areas, region I is the region from the left hand side of the tangential curve. This area is where  $\frac{da}{dN}$  approaches zero. This means

that the crack will not grow. In region II, the crack growth will be according to the power law

$$\frac{da}{dN} = C \cdot \Delta K^m \quad 2.6$$

$C$  and  $m$  are material constant determined experimentally. In the case of Figure 2-8, the value of  $m$  is equal to 2.85. It has been shown that  $m$  usually is in the range of 2 – 4 for metals (Lalanne 2009). Equation 2.6 has later been names Paris’s Law after one of its discoverers. Region III is the region where the crack becomes unstable and fracturing occurs.

It is worth mentioning that the procedures of fracture mechanics come as an alternative to the engineering toolset known as S-N curves. The principle of fracture mechanics bases itself on qualitatively explaining crack growth. The S-N curves on the other hand are derived from quantitative analysis (Anderson 2005). By testing material samples with sinusoidal stress until fracture, a curve for expected life time with regards to constant peak loading is extracted. Exposing a set of individual samples for different loads, a curve can be drawn on the basis of linear regression. Probability distributions are then utilized for describing the areas of operation that can be considered reliable for the given material.

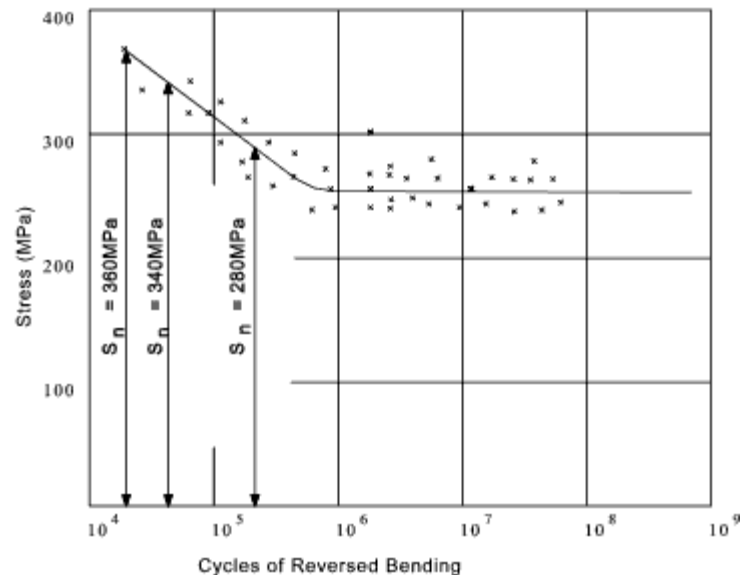


Figure 2-9 Example of generated S-N curve from experimental data (Beardmore 2010)

In service, parts are seldom stressed repeatedly at only one stress level. The cumulative damage effect of operation at various stress levels can be described according to the Mine-Palmgren rule. The rule assumes that the total life of a part may be estimated by adding the percentage of life consumed by each stress cycle (Iowa State University 2009).

If a specimen stressed at  $\sigma_1$  has an expected life of  $N_1$  cycles, the damage after  $n_1$  cycles at  $\sigma_1$  will assumed linearly according to the relation

$$\frac{n_1}{N_1} \tag{2.7}$$

For more than one stress level, the lives at  $\sigma_1, \sigma_2, \sigma_n$  are respectively  $N_1, N_2, N_n$ . For a mult-level test, Mine-Palmgren rule states that

$$\frac{n_1}{N_1} + \frac{n_2}{N_2} + \frac{n_3}{N_3} \dots > 1 \tag{2.8}$$

The component can be expected to fail. The rule is simple to use and has been used to a wide degree in the industry. The problem with the Mine-Palmgren rule is that it is necessary to know the history of the loads. As equipment and service pipes alike rarely are being monitored in real time, the history of the loads is unknown. A series of modified algorithms have thus been created (H. Corten and T. Dolan's method, Henry's method, Modified Henry's method, etc.) (Lalanne 2009).

In the case of service pipes, fracture mechanics is the basis for a series of standards. One example is the Recommended Practice DNV-RP-C203 Fatigue Design of Offshore Steel Structures (Det Norske Veritas 2010a). One thing that should be noted in regards to the DNV-RP-C203 is its area of validity. If one assumes non-cathodic protection in a confined non-corrosive environment, it is valid for a material yield strength of maximum 960 MPa. As Statoil's TR2000 operates mainly within these conditions, one can assume that the recommended practice is valid for installations on- and offshore. In the case of temperature, the recommended practice uses a maximum value of 100 °C. This temperature is higher than the temperature experienced in field. It is therefore not necessary to use the reduction factor stated in the paper (Det Norske Veritas 2010a).

## 2.3 Analysis of structural damping

Damping can be described as the energy dissipation of a material under cyclic stress. This energy is gradually converted in to different forms, such as heat or sound. As the exact cause for damping can be difficult to determine, damping is usually modeled in three main groups. These are known as internal-, structural- and fluid damping. According to Rao (2010), “*a damper is assumed to have neither mass nor elasticity, and damping force exists only if there is relative velocity between the two ends of the damper*”. External dampers can be added to a mechanical system to improve the energy dissipation. Depending on how they operate, the dampers can be of active or passive type. The passive damper dissipates the energy from the induced motion of the system. Example of this can be an added rubber sleeve for adjusting the natural mode of oscillation of the system. An active damper on the other hand depends on external power sourced to dissipate the vibration energy efficiently. For service pipes, the main primary mechanics of the dampening properties can be explained through internal damping.

### 2.3.1 Internal damping

Internal damping is caused by the microstructural defects of the material exposed to vibration. These can be everything from impurities and grain boundaries to thermo elastic effects. The damping is a result of non-ideal movement of the structural lattices within the material. In an ideal metal structure, areas in the lattices known as slip planes are relatively free to move along its own direction. This leads to lower resistance of movement for the material. If a defect is located at, or close to, one, of these slip planes, they increase friction and thereby resist free movement. This friction leads to the dissipation of kinetic energy to other forms of energy and the oscillation is damped. The damped oscillation can be described by a cyclic integral known as the hysteresis loop.

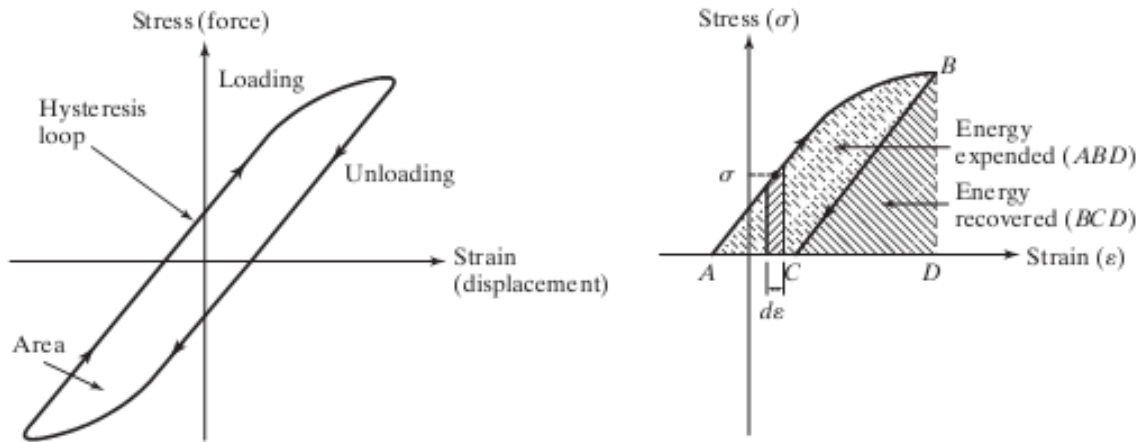


Figure 2-10 Hysteresis loop of internal damping (Silva 2007)

The area within the loop is the energy dissipated per cycle of motion and is equal to the work done against the damping force.

### 2.3.2 Viscoelastic damping

In viscoelastic damping, a subgroup of internal damping, the relation between stress and strain in the material is described by a linear differential equation in the time domain. As the object oscillates, the strain varies accordingly. This oscillation has a given frequency known as the frequency of variation (FoV). The stress in the material follows the FoV and results in varying stress in the time domain. There are several models used to describe how the stress and the damping of the constriction vary. The most commonly used is the Kelvin-Voigt Model. When a service pipe experiences harmonic excitation (movement that can be describes using sine-curves), the damping capacity of the pipe is

$$d_v = \frac{\pi \cdot \omega \cdot E^* \cdot \sigma_{\max}^2}{E^2} \quad 2.9$$

Where

$d_v$  = Damping capacity of object

$\omega$  = Vibration frequency



$E^*$  = Time independent complex modulus

$\sigma_{\max}$  = Stress, peak value

The damping of the vibration of a structure happens at every frequency. It will however have the greatest effect on structures experiencing resonance.

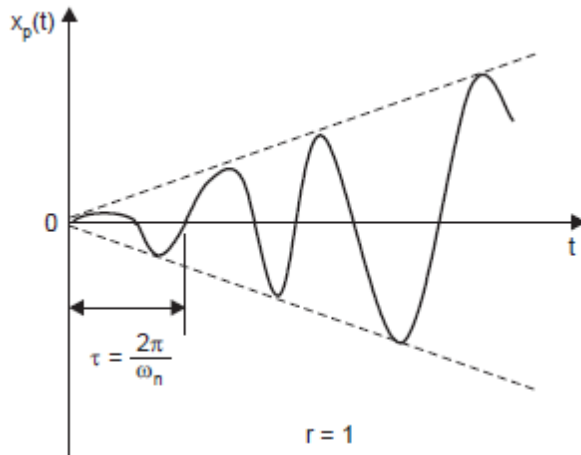


Figure 2-11 Resonance response (Dukkipati 2007)

Resonance is the effect that occurs when  $r = \frac{\omega}{\omega_n} = 1$ . This happens when the circular frequency of the forcing is equal to the circular frequency of the system in motion. When the effect occurs, the displacement  $x(t)$  goes to infinity. This means that the amplitude of the force response grows with time and the amplitude will be very large. As the system continuously is fed energy from the forcing function, excitation will continue to increase. This results in a greatly increased load on the service pipes. As the stress increases, one risk to surpass the defined ultimate limit state of the material, and fracturing is a result

For service pipes on O&G process plants, it is stated that the operational conditions of the system is to be outside of the frequency range of resonance (NORSOK 2007; American Society of Mechanical Engineers 2010). As the operating conditions of the plant may change, this may not always be the case. Conditions change with output and season, leading to an increased risk of ending up in the range where resonance will be the result. This is where the dampening of the system comes in to play. As  $r$  gets closer to 1, it is the dampening of the

system that has to dissipate the increased energy load from the induced vibration.

The amplitude ratio is defined as

$$M = \frac{X}{\delta_{st}} \quad 2.10$$

$X$  = Amplitude

$\delta_{st}$  = Deflection under static force  $F_0$

Comparing the amplitude ratio under different values of dampening of the system, one can visualize how the dampening effect the excitation of service pipes

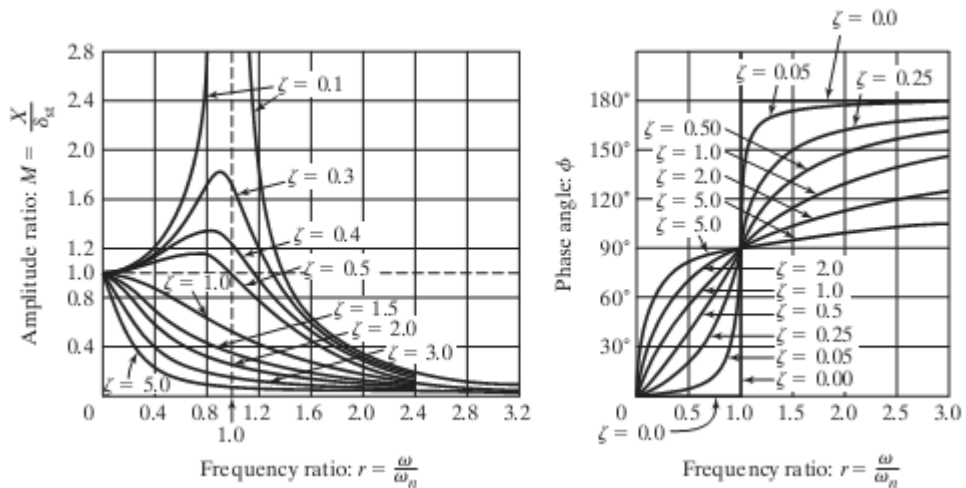


Figure 2-12 Variation of  $X$  and  $\phi$  with the frequency ratio  $r$  (Rao 2010)

At  $r = 1$ , one can see that the systems with poor damping experiences very high amplitudes compared to the static loading. If the circular frequency of the force comes close to the circular frequency of a service pipe with poor damping, the pipe may fail within a short period of time. It is therefore of utmost importance to ensure two things

1. The circular frequency from the loads of the operating conditions must at any time mismatch the circular frequency of the individual service pipes installed
2. The individual service pipe must have sufficient damping to handle an eventual resonance situation if it arises

As there are thousands of service pipes installed on a process plant at any given time, it is difficult to mismatch all the natural frequencies to the varying operating conditions. This gives the need for the second criteria. As previously mentioned, there are currently no accept criteria for the damping of service pipes. It will therefore be a gap between the existing practices and what that can be done to prevent the failure of service pipes. This thesis will try to cover this gap.

## 2.4 Measurement of damping

From a theoretical point of view there are different methods to measure damping. These methods are divided in two main groups depending on if the response of the system is expressed as a function of time or as a function of frequency. Logarithmic Decrement Method (LDM), Step-Response Method (SRM) and Hysteric Loop Method (HLM) are time-response methods, whereas Magnification-Factor Method (MFM) and Bandwidth Method (BM) on the other hand are frequency-response methods.

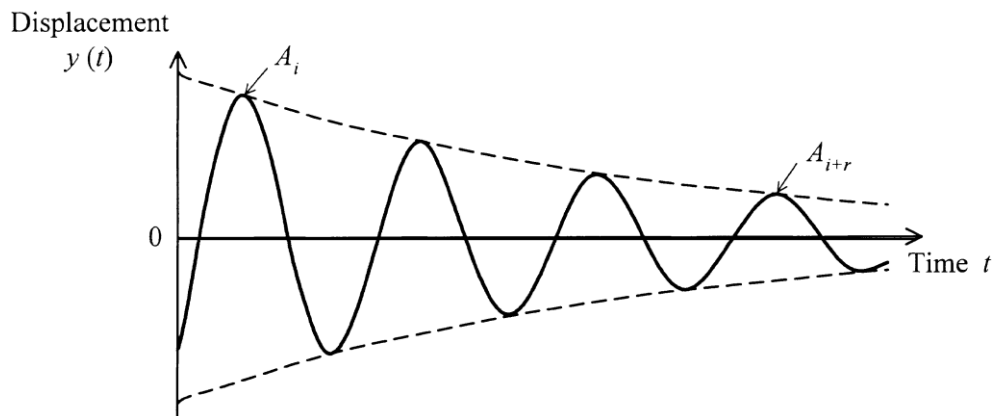


Figure 2-13 Impulse response of a simple oscillator (Silva 2007)

Operating in the time domain, the LDM is the most applied method for measuring damping. This done using an initial excitation to a single degree-of-freedom (SDOF) system. If the response of the system is known, it is possible to determine the value of the logarithmic decrement from the formula

$$\delta = \frac{1}{r} \cdot \ln \left( \frac{X_i}{X_{i+r_p}} \right) \quad 2.11$$

$\delta$  = Logarithmic decrement

$r_p$  = Period of excitation

$X_i$  = Deflection at  $i$

$X_{i+r}$  = Deflection at  $i+r$

The logarithmic decrement can also be found using the damping ratio for the system

$$\delta = \frac{2 \cdot \pi \cdot \zeta}{\sqrt{1 - \zeta^2}} \quad 2.12$$

$\zeta$  = Damping ratio

Restructuring equation 2.12, one can find the value for the damping ratio experimentally

$$\zeta = \frac{\delta}{\sqrt{4 \cdot \pi^2 + \delta^2}} \quad 2.13$$

For a walkthrough of the deduction of the other ways of measuring damping (SRM, HLM, MFM & BM) see attached information (ref. Section 8.2).

Independent of method used for calculating the damping of a system, the damping ratio are within the range of  $0 < \zeta < \infty$ . Depending on the value of the ratio, the system can be separated into four different main types of damping

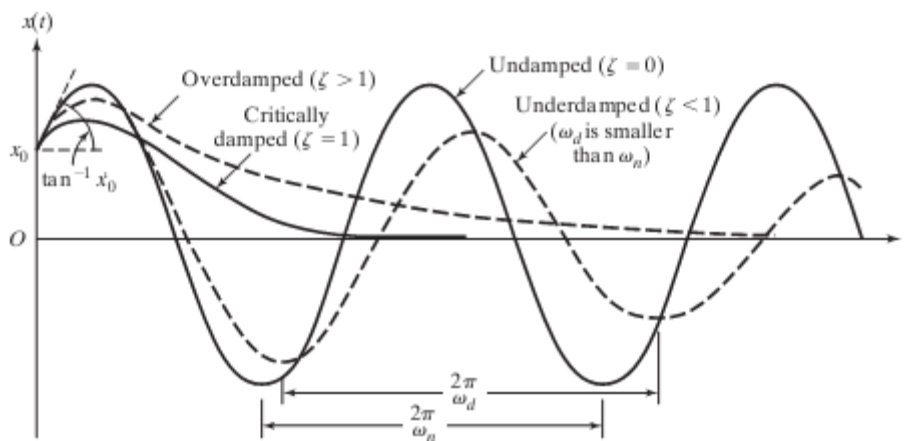


Figure 2-14 Comparison of motion with different types of damping (Rao 2010)

For an undamped system, the dampening ratio is calculated to  $\zeta = 0$ . This means that none of the energy of motion is transferred to other forms. The system will therefor continue oscillating after initial response. In practice, undamped systems do not occur often, as it requires ideal conditions which can only be obtained in a controlled, laboratory environment.

An underdamped system ( $0 < \zeta < 1$ ) is similar to the undamped system, as it takes a longer period of time before one registers a reduction in amplitude. Underdamped systems can be experienced in several situations. One example is a tuning fork vibrating at a frequency that is audible for human ears. If the fork is not damped by introducing additional dampers, the sound will be audible for a long period of time. It is the calculated value of the damping ration which explains for how long the oscillation will continue.

Critically damped systems ( $\zeta = 1$ ) does not have an overshoot as the underdamped system has. This aperiodic motion functions as the optimal way of disposing motion energy in regards to time necessary for asymptotically stabilizing the system. As it is shown in Figure 2-14 the induced forced motion dies out after a half period. Similar to the critical damped system, an overdamped system ( $\zeta > 1$ ) does not have an overshoot. There are thus several similarities between the critical and the overdamped system. Overdamped systems can be considered a critical damped system that reaches the steady state position more slowly. One example is a hydraulic damping system. Compared to an under- or critically damped system, the viscosity of the hydraulic fluid result in a slower return of a piston to its steady state location.

By utilizing these tools, the dampening of the service pipes can be calculated. Depending on the output data of the vibration analysis, the most suitable tool set will be used for calculating the overall dampening of the different service pipes.

## 2.5 Screening for fatigue

Throughout various processing plants on- and offshore, several thousand service pipes are currently in use. In the case of varying loads, unfavorable geometry and insufficient supporting, fatigue may be the result. Described in section 2.2, fatigue may lead partial- or full shutdown of process critical pipelines, with a potential for millions in lost revenue. To counter the effect of the difficult to predict fatigue, operators and their partners are putting more and more effort into the philosophy of reducing downtime. There has always been a desire to have a machine or a process functioning at full capacity without any downtime. Still, this is not always possible. With the understanding of fracturing mechanics, the understanding of several material degrading mechanism where also improved. This lead again to the higher focus on predictive maintenance (PM). The main objective of the predictive maintenance mentality is to foresee possible failures of equipment in use.

In traditional maintenance philosophies equipment was operated till failure. As the understanding of the failure mechanism where not that good, the exact time of failure could only be foreseen a short period of time before the breakdown.

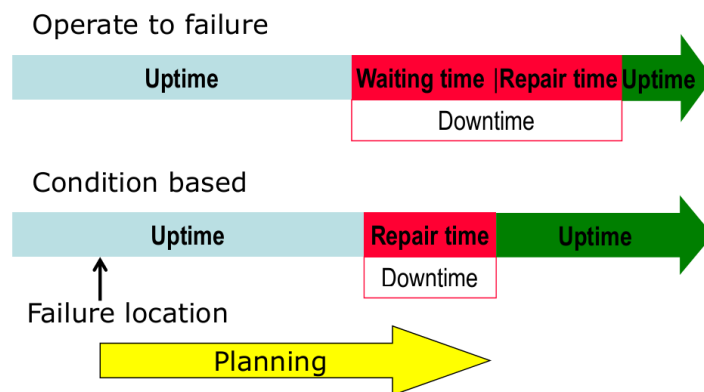


Figure 2-15 Maintenance management Traditional vs. Condition based (Markeset 2012)

Over the years, greater effort has been into increasing of efficiency of every aspect the processing of petroleum. The operate-to-failure maintenance management has been considered to increase the overall downtime of potentially

process critical equipment. In addition to the pure economical gain from increased uptime, condition based monitoring (CM) reduces the personnel risk related to operating equipment at non-optimal conditions (Markeset 2012). Markeset has identified seven separate steps necessary for a successful condition monitoring program

1. Identifying critical systems
2. Selecting condition monitoring technique
3. Setting baselines
4. Data collection
5. Data assessment
6. Fault diagnosis and repair
7. System review

For the identification of critical systems, a methodology for the classification of the individual systems is highly helpful. When the systems are identified, it is necessary to determine how one will monitor the properties of the individual service pipe. As this thesis focuses on the fatigue of service pipes due to vibration, vibration monitoring will be utilized. It is then necessary to determine the accept criteria for the vibration test. One should then perform the vibration testing onsite. Further analysis of the data is then necessary to determine whether the individual pipe is at risk of being exposed to fatigue. If the conclusion is that the pipe is exposed to an unacceptable risk, improvement of the pipe is necessary. When all the pipes identified to be at risk have experiences corrective maintenance, a system review will be performed. This for concluding with the overall condition of the system in question. One can then move to the next system of interest and repeat the program

Due to the amount of service pipes on NCS, one cannot implement CM at every location simultaneously. It is therefore necessary to implement a maintenance strategy. British Standards Institute (BSI) defines maintenance as “*The combination of all technical and associated administrative actions intended to retain an item in, or restore it to, a state in which it can perform its required function.*” This function may be defined as a *stated condition* in the standard BS 3811:1993 (withdrawn, but not yet superseded) (British Standards Institution

1993). Ideally, a maintenance management strategy should be in place during the design phase of any specific construction.

Problems may arise when modifications and upgrades of the process plants changes the basis for which a maintenance strategy has been implemented (International Organization for Standardization 2006). Continuously updating of these plans is thus a necessity. As a part of this updating of strategy, a screening method for service pipes is desirable to implement. After meeting with the operator Statoil (ref. section 8.4), they confirmed that there are currently no other contractor offering a screening method for identifying service pipes vulnerable to fatigue.

For the development of this screening technique, this thesis focuses on the groundwork done by Senior Specialist Engineer Paul Mathieson in Aker Solutions. The screening method bases itself on information accessible for contractors of the installation that is surveyed.

## **2.6 Development of screening methodology**

Before starting the evaluation of the different areas, it is necessary to access the Piping & Instrumentation Diagrams (P&ID) for the installation in question. The P&ID are a set of drawings illustrating the general piping connectivity between the individual process equipment of the installation. The drawings consist of standardized symbols for the different types of equipment. Between the symbols, lines indicate where the piping is located. In addition to the drawings, text information is printed close to the individual equipment. Most of the equipment and pipes in the drawing has their own identifying name, known as a tag. The name of the equipment is built up from the plant-specific engineering numbering system (ENS). This means that the nameplate can be used to identify functions and specifications for that specific piece of equipment or instrument. Piping dimensions are also drawn on the P&ID. If a pipe stretches over longer distances, it may cross the interface between the different areas of the plant. Indicators for these interfaces are added to the P&ID. This to better illustrate in which area one might find the instruments of interest.



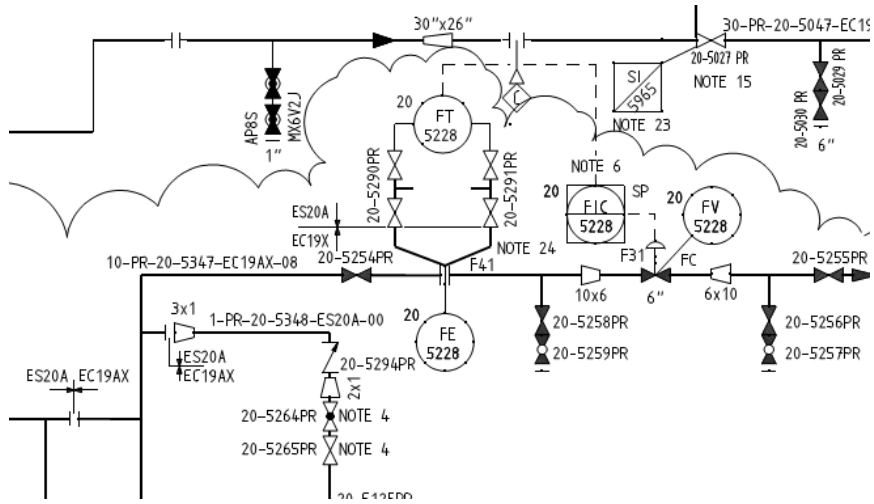

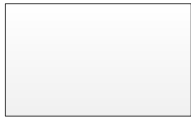

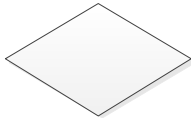



Figure 2-16 Extract of P&ID (Statoil 2011c)

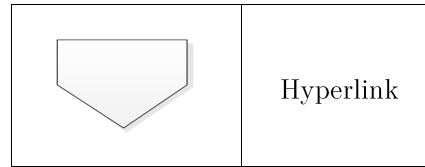
Figure

2-17 Basic flowchart shapes

(Microsoft Corporation 2012)

|  |               |
|--|---------------|
|  | Start/End     |
|  | Process       |
|  | External data |
|  | Decision      |
|  | Sub process   |

For studying service pipes, it is recommended to select first an area of interest (Det Norske Veritas 2010b). One then select a pipe tag. As the P&ID



illustrates how the process moves the sequentially at the plant, service pipes are tagged along the pipe between the individual consumers. One get an idea of what pipes that may be exposed to one or more of the unfavorable conditions evaluated in the flow chart for the creation of the screening report (ref. Figure 2-18). The report consists of basic flow chart shapes of logical operators explained on the right. The location of the service pipe is evaluated in combination with surrounding mechanical equipment. From this, the conditions are evaluated according to the flow chart on the next page. This results in a screening report. The report with then me the basis for the screening methodology developed.

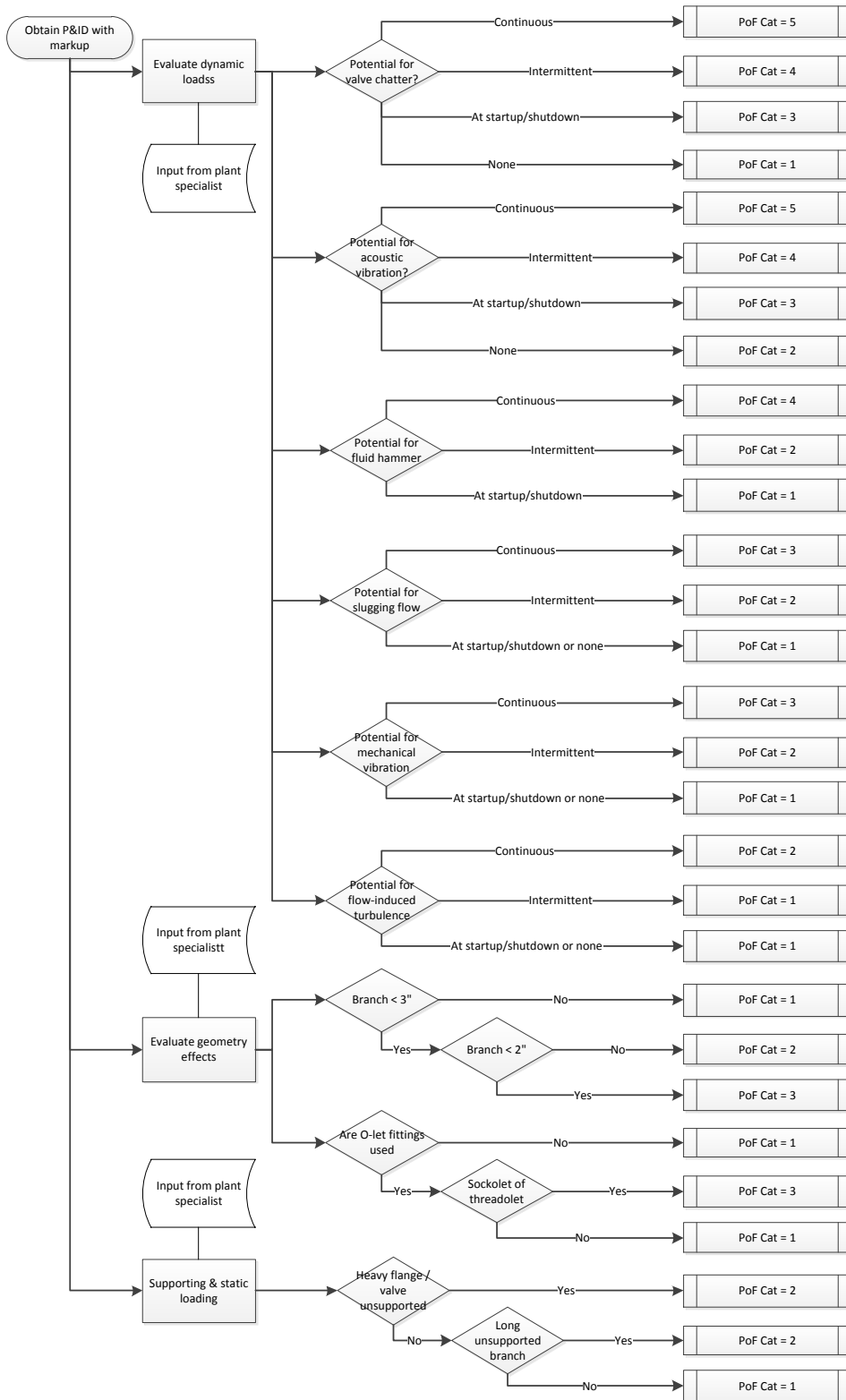


Figure 2-18 Flowchart screening report (Adapted from Mathieson 2007).

The first stage of the screening is the evaluation of the dynamic loads affecting service pipes. By dynamic loads, focus is put on the combination of load type and frequency of occurrence.

Frequency of occurrence (FoO) in this case is defined according to Table 2-1 below

Table 2-1 Frequency of occurrence (Mathieson 2007)

| <b>Frequency of occurrence</b> |   |
|--------------------------------|---|
| Continuous                     | Present more than 10% of operating time   |
| Intermittent                   | Present up to approximately 10% of the operating time                                   |
| Startup/shutdown               | Present during startup & shutdown only, maximum 1% of the operating time or 20 mins/day |
| None                           | Not present or expected   |

With each specific scenario, a Probability of Failure (PoF) has been estimated. DNV defines the PoF as *[...] the probability of an event occurring per unit time* (Det Norske Veritas 2010b). It is estimated on the basis of the degradation of the component. The PoF are described both quantitatively and qualitatively from each of the 5 categories used.

Table 2-2 Probability of failure (Det Norske Veritas 2010b)

| Cat.   | Annual failure probability |                  | Description   |
|--|----------------------------|------------------|---|
|  | Quantitative               | Qualitative      |   |
| 5  | $> 10^{-2}$                | Failure expected | (1) In a small population*, one or more failures can be expected annually   |
|  |                            |                  | (2) Failure has occurred several times a year in location   |
| 4  | $10^{-3} - 10^{-2}$        | High             | (1) In a large population**, one or more failures can be expected annually  |
|  |                            |                  | (2) Failure has occurred several times a year in operating company  |
| 3  | $10^{-4} - 10^{-3}$        | Medium           | (1) Several failures may occur during the life of the installation for a system comprising a small number of components |
|  |                            |                  | (2) Failure has occurred in operating company   |
| 2  | $10^{-5} - 10^{-4}$        | Low              | (1) Several failures may occur during the life of the installation for a system comprising a large number of components |
|  |                            |                  | (2) Failure has occurred in the industry  |
| 1  | $< 10^{-5}$                | Negligible       | (1) Failure is not expected   |
|  |                            |                  | (2) Failure has not occurred in the industry  |
| Notes:                                       |                            |                  |   |
| * Small population = 20 – 50 components      |                            |                  |   |
| ** Large population= More than 50 components |                            |                  |   |

In addition to PoF, the Consequence of Failure (CoF) is also necessary to elaborate. Traditional interpretation of risk states that (International Organization for Standardization 2002; NORSOK 2011)

$$Risk = Probability \times Consequence$$

To estimate the risk of an event, the consequences need to be described. Recommended Practice DNV-RP-G101 operates with a three main categories; Safety, Environment and Business, which each has 5 individual rankings.

Table 2-3 Consequence of failure ranking scales (International Organization for Standardization 2002; Det Norske Veritas 2010b)

| <b>Consequence of failure qualitative ranking scales</b> |                             |                        |                     |
|--|-----------------------------|------------------------|---------------------|
| <i>Rank</i>  | <i>CoF Personnel Safety</i> | <i>CoF Environment</i> | <i>CoF Economic</i> |
| <b>A</b>   | Insignificant               | Insignificant          | Insignificant       |
| <b>B</b>   | Slight/minor injury         | Slight/minor effect    | Slight/minor damage |
| <b>C</b>   | Major injury                | Local effect           | Local damage        |
| <b>D</b>   | Single fatality             | Major effect           | Major damage        |
| <b>E</b>   | Multiple fatalities         | Massive effect         | Massive damage      |

The PoF and CoF can be combined to make up a matrix for estimating of risk. To achieve adequate resolution of details of risk at any given time, it is recommended to use a 5×5 matrix. The matrix will incorporate both category and rank of PoF and CoF respectively.

Table 2-4 Risk matrix (International Organization for Standardization 2002)

| PoF Ranking        | PoF Description   | A            | B                                | C                                   | D                                      | E                                   |
|--------------------|---|--------------|----------------------------------|-------------------------------------|--|-------------------------------------|
| 5                  | (1) Small population; multiple failures annually<br>(2) Multiple failures annually at location                          | YELLOW       | RED                              | RED                                 | RED                                    | RED                                 |
| 4                  | (1) Large population; multiple failures annually<br>(2) Multiple failures annually in company                           | YELLOW       | YELLOW                           | RED                                 | RED                                    | RED                                 |
| 3                  | (1) Multiple failures during life time: Small number of components<br>(2) Failure has occurred in the operating company | GREEN        | YELLOW                           | YELLOW                              | RED                                    | RED                                 |
| 2                  | (1) Multiple failures during life time: large number of components<br>(2) Failure has occurred in the industry          | GREEN        | GREEN                            | YELLOW                              | YELLOW                                 | RED                                 |
| 1                  | (1) Failure is not expected<br>(2) Failure has not occurred in the industry   | GREEN        | GREEN                            | GREEN                               | YELLOW                                 | YELLOW                              |
| CoF Types          | <b>Safety</b>   | No Injury    | Minor Injury<br>Absence < 2 days | Major Injury<br>Absence > 2 days    | Single Fatality                        | Multiple Fatalities                 |
|                    | <b>Environment</b>  | No pollution | Pollution: Minor local effect    | Pollution: Significant local effect | Pollution: Significant regional effect | Pollution: Massive regional effect. |
|                    | <b>Business</b>   | No downtime  | < € 10 000 damage                | < € 100 000 damage                  | < € 1 000 000 damage                   | < € 10 000 000 damage               |
| <b>CoF Ranking</b> |   | <b>A</b>     | <b>B</b>                         | <b>C</b>                            | <b>D</b>                               | <b>E</b>                            |

The overall risk of any operation is then separated into three different levels of risk. DNV has defined these levels as:

- Green - Low risk: *Risk is acceptable. Generally, action needs to be taken to ensure that risk remains within this region; typically this involves operator*

round, cleaning, general visual inspections (GVI) to confirm that there have been no changes in equipment condition.

- Yellow - Medium risk: *Risk is acceptable. Action (such as NDT, functional tests and other condition monitoring activities) should be taken to measure extent of degradation so that action can be taken to ensure risks do not rise into the red high-risk region.*

- Red - High risk: *Risk level is unacceptable. Action must be taken to reduce probability, consequence or both, so that risk lies within the acceptable region.*

These risks are considered valid for all sections of the categories of screening. It has been identified six potential risks for evaluation; valve chatter, acoustic vibration, fluid hammer, slugging flow, mechanical vibration and flow-induced vibration. Depending on how the frequency of occurrence of each of the phenomena, individual PoF has been identified.

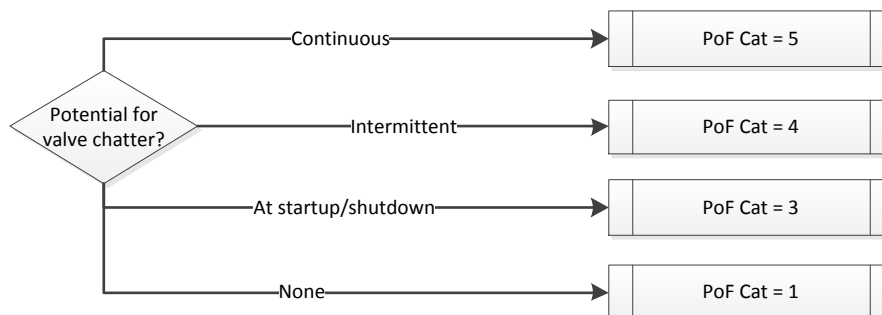


Figure 2-19 Potential for valve chatter

The first dynamic load to be evaluated is the potential for valve chatter on a valve connected to a service pipe. Valve chatter is a phenomenon where partial opening and closing of a valve happens uncontrolled. The process is usually cyclic and the reason can often traced back to improper liner sizing in combination with high pressures in the system (Eng-Tips 2003). The combination of the cyclic movement and the increased loads on the service pipes may induce vibrations, which again may further accelerate the deteriorating processes with continuous crack growth. High pressure gas systems and service pipes close pressure safety valves (PSV) are areas that have a potential for valve chatter. This potential is then again evaluated based on the frequency the phenomenon occurs. As one can



see from the chart, the probability of failure related to valve chatter is considered high. If there is an area that is continuously exposed to valve chatter, one can expect the failure of the component to within a short period of time. If the FoO is reduced, the PoF is somewhat lowered. The system will maintain at risk as long as there are a chance of the chattering of valves during the lifetime of the plant.

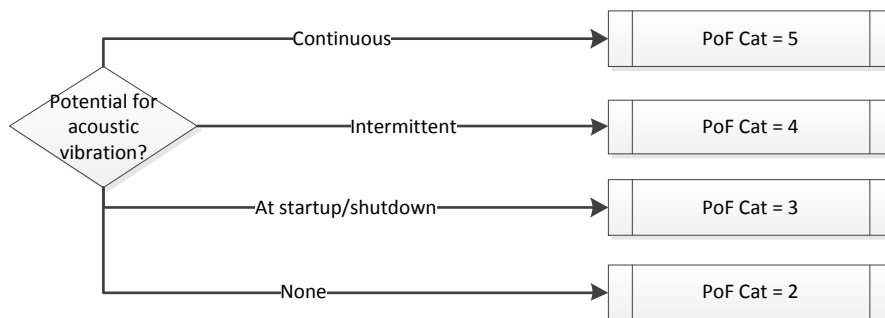


Figure 2-20 Potential for acoustic vibration

The second dynamic load necessary to evaluate is the potential for acoustic vibrations in the system. Suikaih (2002) states in his article “*A practical, systematic and structured approach to piping vibration assessment*” further defines high frequency acoustic excitation as excitation of high energy due to the high broadband frequencies that one can experience in the choking of gas flows. (Sukaih 2002). This is traditionally confined to the areas close to relief valves, control valves and orifice plates. By adding the more general definition by Sukaih, one can also include flow pressure letdowns and gas flow past stubs into this category. Out of the identified dynamic loads, the potential for acoustic vibration will have the highest PoF. It is thus of utmost importance to eliminate elements through the process system that may induce acoustic vibration

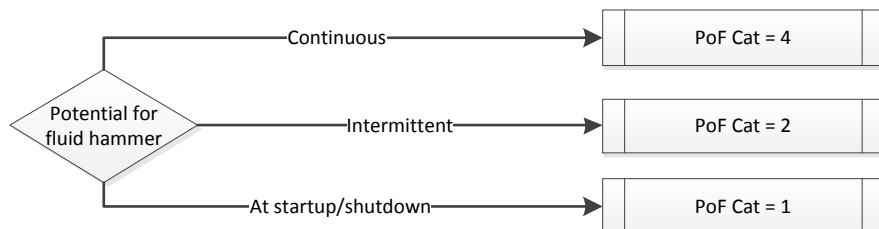


Figure 2-21 Potential for fluid hammer

Potential for fluid hammer can also be considered one of the more important factors for the propagation of cracks and the fatigue of the material. The phenomenon fluid hammering is not part of the steady-state operation condition. Pressure surging in liquid combined with momentum change exposes the service pipes to a pressure wave. The wave may have peak stress values higher than the accepted values for the system. Depending on whether the surge happens up- or downstream of the service pipe, the effects are different. Implosion is one consequence of the closing of valves upstream of the service pipe. Sukaih (2002) does in his procedure exclude the effect of fluid hammering. He argues that hammering is of transient origin. The data- and design guideline for the specific pipeline or service pipe should thus cover these situations. Fluid hammering may occur close to open deadlegs, thermowell probes and reciprocating pumps. Petroleum process plants contain several of each type, fluid hammering will still be considered relevant. Compared to the other dynamic loads, the PoF are only considered a real problem if hammering is experienced during all hours of operation (Mathieson 2007).

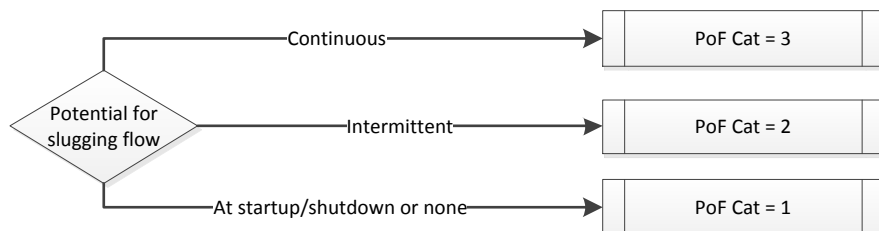


Figure 2-22 Potential for slugging flow

Slug flow is considered one of the flow regimes in multiphase fluid flow. In vertical flow, a slug is a liquid plug in gas pockets that symmetrically occupies up to the entire cross-sectional area of the pipe. Rapid directional change of such plugs introduces shock in the system. Slug flow shocks are similar to the shocks of fluid hammering (Schlumberger 2012). It is this shock that may lead to peak stresses in the system. Throughout the processing plant, the well stream will be increasingly more homogenous in phase. It is therefore more likely to experience slugging close to the plant inlet. Two phase process lines upstream of slug

catcher/inlet separator as areas which are at risk at experiencing these types of loads.

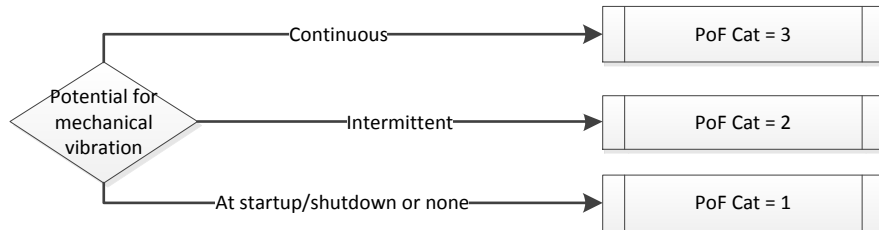


Figure 2-23 Potential for mechanical vibrations

Pumps, turbines and other mechanical equipment may introduce vibrations in systems connected. This usually happens in close vicinity to the equipment. In a process plant, close is defined as a radius equal to twice the maximum length of the skid that contains the mechanical equipment (Sukaih 2002). The source of the vibration is machinery with unbalanced forces and moments. In the vibration spectrum, the excitation force can be of high amplitude while frequencies remain low. The excitation can be identified in the frequency spectrum by the formula

$$f = \frac{n \cdot N}{60} \quad 2.14$$

$n = 1, 2, 3...$

$N = \text{Speed (rpm)}$

The risk of failure is present, but not the same extent as with acoustic vibration and valve chatter. The problem may arise when the condition for mechanically induced vibration are matched with the main operating conditions of the surrounding equipment. One then risk having continuous mechanical vibration, leading to an increased risk of failure. On the other hand, these conditions are usually designed to mismatch the range of mechanical vibration. This leads to a more intermittent FoF

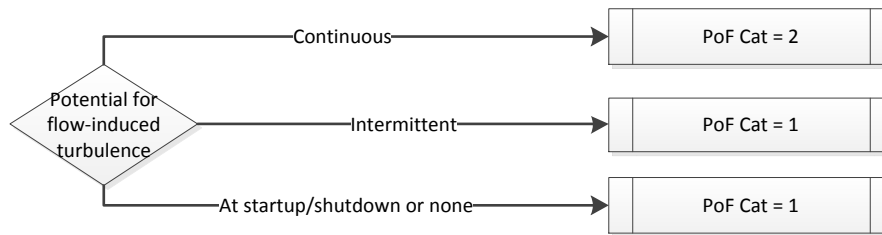


Figure 2-24 Potential for flow-induced turbulence

Flow-induced turbulence is an umbrella term for a series of effect that can occur in pipe flow.

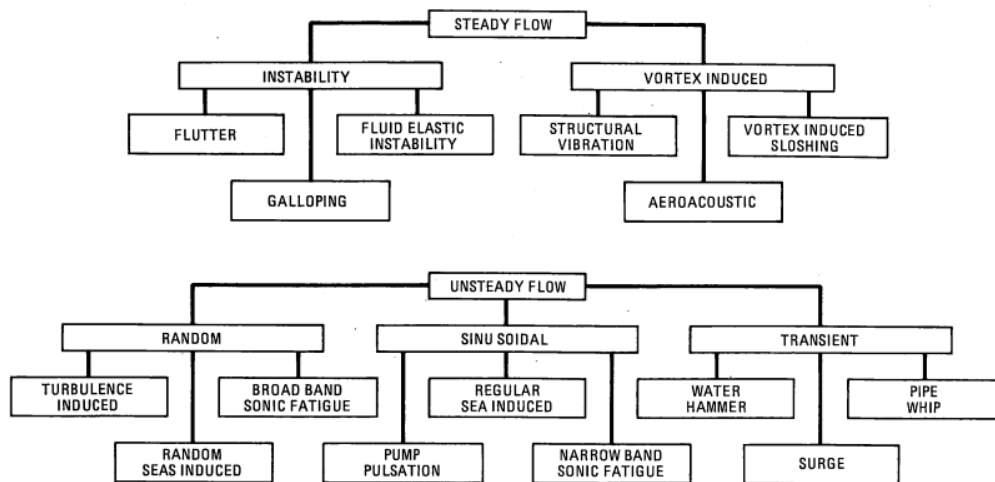


Figure 2-25 Classification of flow-induced vibration (Blevins 1990)

High-velocity flow through a pipe can cause the pipe to vibrate at large amplitudes. This instability of operation can again lead to increased stress on the pipe and fatigue may be of consequence (Blevins 1990). When the flow are of quasi-steady type, it can manifest itself as random vibrations at low frequencies

( $f = 0 - 30 \text{ Hz}$  typically). This is the same range as the ambient vibrations of the service pipes usually occur at. It can therefore be difficult to distinguish the flow-induced turbulence from the white noise readout of a possible vibration-measurement. Unless the vibration is considered continuous, probability can be considered low

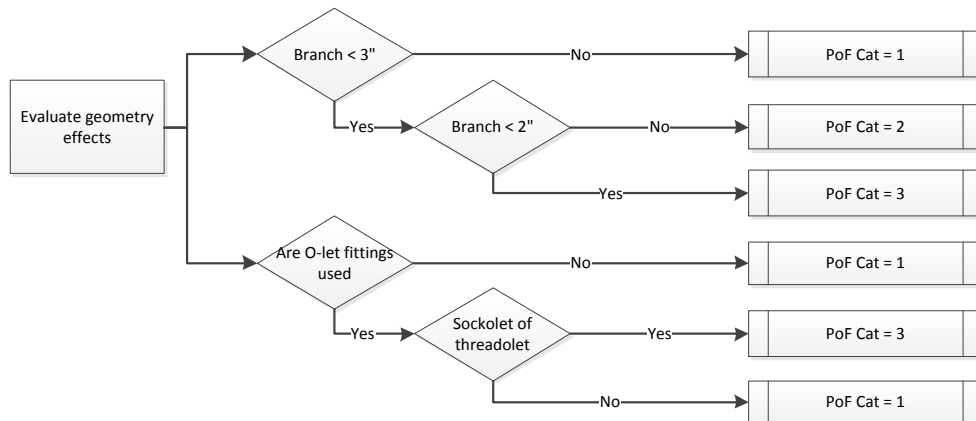


Figure 2-26 Geometry effects

The screening method also evaluates the effect geometry has on the service pipes. According to the international piping standards and Statoil's own technical requirement, TR2000, material thickness increases with an increase of nominal branch size. Service pipes with branches larger than 3" can be considered of lower PoF category compared to the smaller bore service pipes. Using the quantitative definition of the risk of failure, the PoF of fatigue failure of a pipe larger than 3" is negligible. The reason for this has to do with how the piping specification is constructed. Thicker pipes can distribute the vibration force over a larger cross section, leading to an overall lower stress in the fitting and pipe.

In addition to the size of the branches, the branch fittings also influence the overall risk for fatigue of service pipes. O-let fittings are the generic name of several types of weldable outlet fittings. The main purpose of these fittings is to substitute butt weld fittings with more durable fittings. These fittings use fillet welds. On service pipes, O-let fittings such as Weldolet are considered a less favorable compared to the geometry of Sockolet and Thredolets. Comparing the

three mentioned O-lets shows how that the welds at location A are more advantageous when it comes to the dissipation for moments in the Sockolet and the Thredolet.

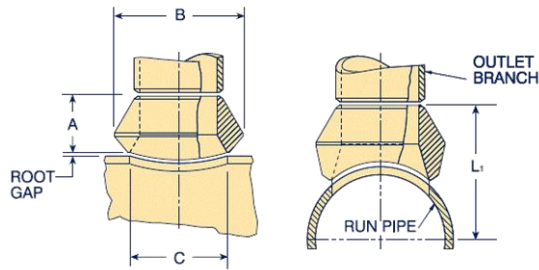


Figure 2-27 Weldolet (Bonney Forge Corporation 2012c)

Economical butt-weld branch connection. Designed to minimize stress concentrations and provide integral reinforcement.

Unfavorable compared to Sockolet or Thredolet

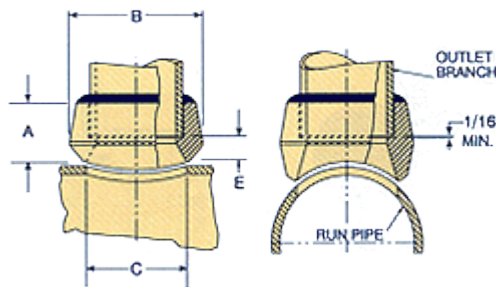


Figure 2-28 Sockolet (Bonney Forge Corporation 2012a)

Based on design of the basic Weldolet, but incorporates a socket-weld outlet

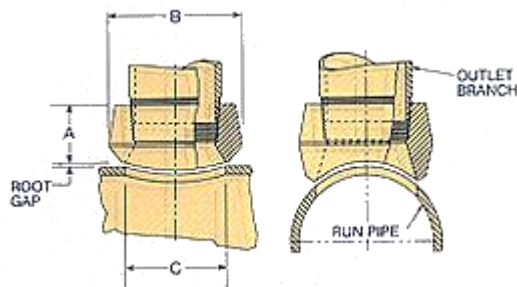


Figure 2-29 Thredolet (Bonney Forge Corporation 2012b)

Based on the design of the Weldolet with a threaded branch connection.

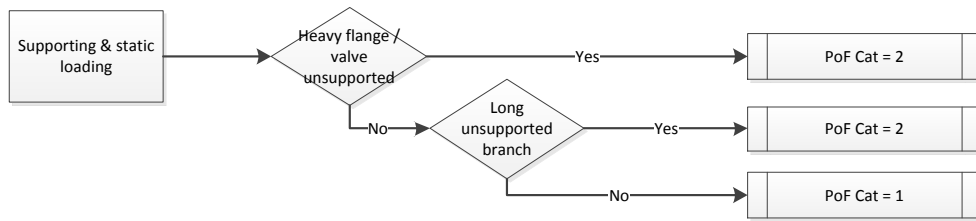


Figure 2-30 Supporting & static loading of service pipes

The last category of evaluation consists of how the supporting structures of the service pipe are constructed. Some of the flanges and instruments may be of some weight. Unsupported, lumped masses exposed to vibration with dampening of unknown character are considered somewhat of a more disadvantageous category of PoF. If one of the mentioned load types forces the pipe to vibration without support, the centered mass may enter resonance frequency. Real life experiences has illustrated the problem with constructions and equipment vibrating at resonance frequency (Billah 1991). At these frequencies, the overall life span can be reduced to mere hours. As equipment often has a design life of over 25 years, this is a dramatic reduction. If one can properly support the heavy valves and flanges, the overall dampening of the construction improves. Support reduced the possible deflection of a vibrating construction and thereby effectively reduces stress from the lower amplitudes. By supporting a construction, one also gets the chance to break up the vibration. The natural frequency the flange/valve is combined with the natural frequencies of the support. The energy is then dissipated to several frequencies instead of the frequency of just the service pipe.

When the initial screening report has been prepared, the results are to be evaluated according to the screening methodology.

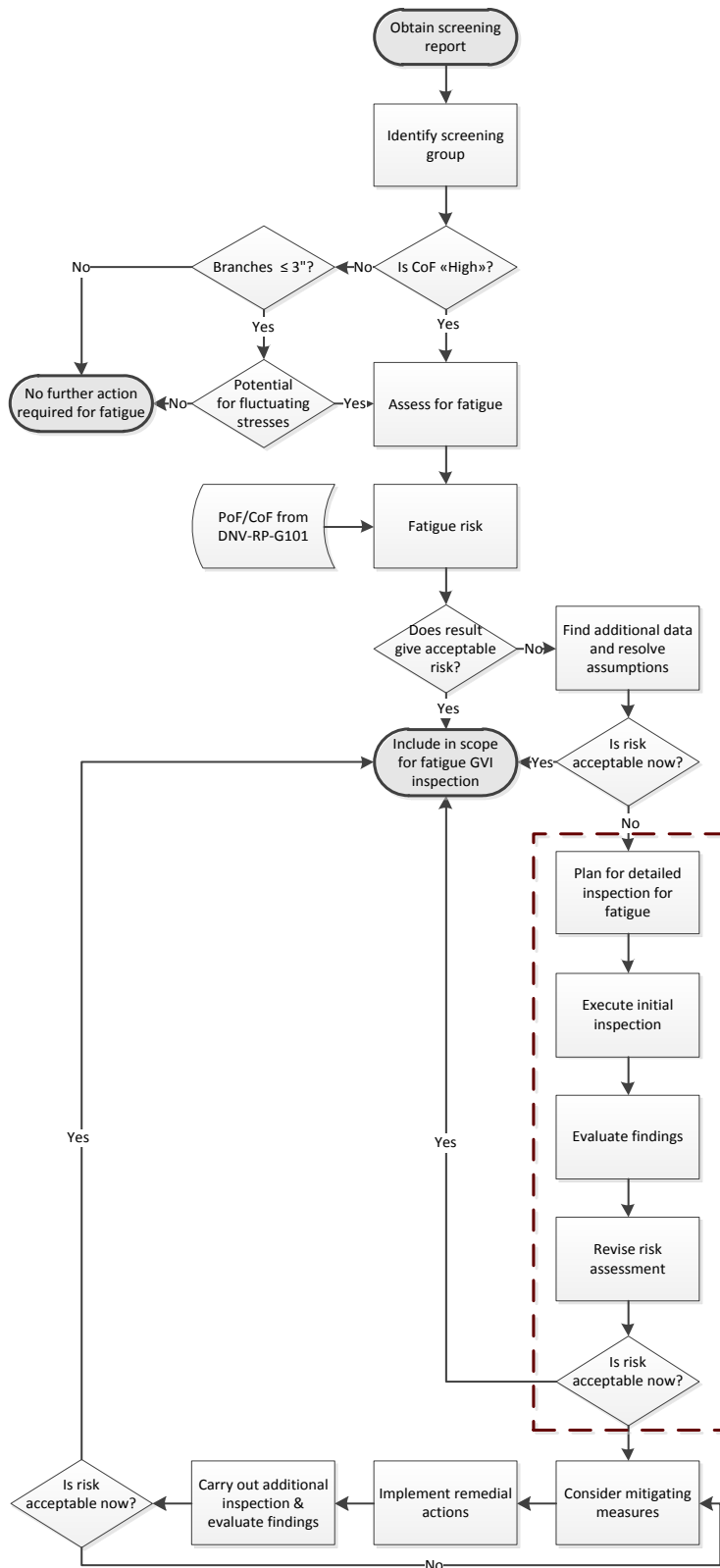


Figure 2-31 Screening methodology for fatigue (adapted from Mathieson)



As presented on the previous page, the first step is to create a screening report for the installation of interest. Even though it bases itself on P&ID's accessible offsite the installation of interest, input from plant specialists can assist in prove/disprove suspicion of fatigue on site. Information within the electronic databases one can access is not always up to date. Input will thus be preferable. The specialist can give information whether or not actions already have been taken. It is also worth mentioning that information from the P&ID does not include information about the supporting constructions that may or may not be in place. It is therefore necessary to study the isometric drawings (shortened ISO's) to gain information about routing of piping throughout the process plant. In addition to regular ISO's, stress ISO's can also be inspected. Stress ISO's are design document containing the loads throughout the process system. Stress ISO's are also not always available. Older processing plant's does not always have their collection of design documentation digitized and readily accessible for the creation of screening report.

When the necessary effort has been put finishing the screening report, the next step is to identify the group of service pipes one want to screen. As stated in section 1.2, a process plant usually houses thousands of individual and unique service pipes. Limiting the scope of the screening methodology to a restricted numbers of predefined service pipes, more effort can be put into improve up the original screening model. After the second step, one should have limited the amount of service pipe to a number which can be handled within the work group.

Process plants are divided in to various sections. These sections have their own main purposes. As both the systems and areas are of varying importance to the main process train, the CoF for the different equipment varies. One example can be the export compressor train on installations offshore. Failure of piping close to a compressor can result in leakage of hydrocarbons. This may result in a complete shutdown of the plant, similar to the one at Oseberg Field Centre (ref. Section 8.4). Comparing the failure of the compressor to failure of a utility system, the CoF can be assumed to vary.

The third step takes the CoF into consideration so that the most important areas are being screened first. Still, all systems need to work together so that the facility can run at optimum efficiency. A decision gate is thus installed in the flowchart. The gate opens for the screening of pipes of lower estimated CoF. In the case of low CoF, the dimensions of the individual pipe are deciding for whether or not to perform actions in regards to fatigue.

As stated, branches of larger dimensions have an increased wall thickness over the branches of smaller dimensions at identical pressure rating. In addition to the increased thickness, the dampening properties of thicker pipes are considered better. Hence, another decision gate is installed, whether or not the branch thickness are higher or lower than the predetermined 3" diameter. For branches of low CoF and dimensions over 3", it is not necessary to perform any proactive or reactive actions in terms of fatigue.

For service pipes with dimensions smaller than 3", one has to know the properties of the stress regimes the branch may or may not be exposed to. Fluctuating stresses can be of different character. For installations offshore, wind-, waveloads and operating conditions can lead to stresses that fluctuate over time. In the case of no potential for fluctuating stresses at branches < 3", one come to the same conclusion as with the larger branches; it is not necessary to perform actions to reduce the risk of fatigue.

When the conclusion is that there is either fluctuating stresses or high estimated CoF, it is necessary to perform an assessment for the risk for fatigue. The first assessment is to calculate the overall fatigue risk. Here, one combines the information about the CoF with the PoF that are both collected from DNV-RP-G101. This gives a result based on the 5×5-matrix also collected from the DNV's recommended practice.

For the risk of fatigue to be acceptable, the combined CoF and PoF need to be considered of risk category *Green*. Actions necessary for these low risks are few. They generally are just to include service pipes of identical CoF and PoF in the operators GVI program. When the risk is categorized as *Yellow* or *Red*, more drastic actions are necessary. For *Yellow*, the risk is still considered acceptable.

Performing GVI is no longer sufficient for concluding with that the overall condition of the service pipe is satisfactory. Common actions for the measurement of degradation for the service pipe includes, but does not limit to, condition monitoring activities and NDT. *Red* risk category is not accepted. Located in the upper rightmost corner, both consequences and probabilities are of such a character that the risk is considered high. It is necessary to reduce the overall risk, either by lowering PoF or CoF, so that the overall risk is reduced to *Yellow*, or more desirable *Green*.

In the methodology, the assessment of the acceptability of the risk for fatigue is done in a series of steps. In the case of Green risk, the methodology ends by including the service pipe in the GVI. For Yellow or Red service pipes, additional data gathering is necessary to improve initial assumptions about the pipes in question. Examples of initial assumptions can be how the PoF has been interpreted. According to the risk matrix, the frequency of failures of service pipes is highly influential on the PoF Ranking. Putting more effort into dissecting available data for the failures of the specific service pipes may result in a more accurate view of the risk situation. Databases openly available to the public can include data from, for example, HSE.co.uk or OLF.

According to the laws and regulations on the NCS, the operators are legally obliged to report situation of hazard and accidents offshore and onshore to the Norwegian Petroleum Safety Authority (PSA). After PSA's initial investigations, a report is to be exhibited online. Causes and actions are there presented and can be of interest in regards to the initial assumptions on the service pipes that are being screened. In addition to the open databases, operators themselves may sit on internal databases. Inspection and maintenance history for the pipes of interest may be available. If the results of the data gathering conclude with a risk that is considered acceptable (*Green* or *Yellow*), the service pipe can be included in the scope for fatigue GVI. No additional actions are then necessary. If the risk don't improve adequately from the additional data, it is necessary of create a more detailed plan for the inspection of the service pipes of interest.

The findings of these reports are then evaluated. Combining the improved assumptions with the findings of the inspection at the plant itself, one gets an overview of how the overall condition of the service pipe. NDT testing of the pipes in question are most commonly used. The usage of X-ray will show defects such as initiated microcracks, inhomogeneity and dislocation of lattices within the material itself. External testing measures such as eddy-current and die penetrant will give a result if the cracks are of external character. Depending on the results of these inspections, one has a more detailed view of the overall condition of the pipe in general.

For the Oseberg installation cluster, a large scale program for the swapping of the service pipe fittings are currently in progress (ref. Section 8.4). The 20 and 23 system on Oseberg C has been shown to experience induced vibration of unknown origin. These vibrations may be induced from the acoustic vibration. This is combined with lock-in properties of the systems themselves. Acoustic vibration is highly dependent on the length of the main pipes the flanges are installed on. If the main pipe vibrates at frequencies close to the natural frequency of the flange, the frequency may jump to the resonance frequency, leading to resonance in the system.

Aker Solutions has presented a solution to this. Temporarily reducing the production of the relevant system to a near halt for a short period of time kills the lock-in phenomenon. The production can then be taken back to normal levels. It is then most likely that the flow will take a different vibration regime.

Installations that also experiences unfavorable vibrations are Åsgård (FPSO), Kollsnes, and Visund. On Kollsnes, a dead leg close to the pig launcher (area A11) was vibrating. The solution to this problem was to open a bypass. This effectively increased the loop length by 3 meters. This resulted in flow in anti-phase, effectively eliminating the problem.

The program for swapping of fittings on the Oseberg-cluster has resulted in the inspection of 6000 individual service pipes. When the installation Oseberg Field Center was under revision stop in 2011, the fittings on 59 service pipes was

swapped. The welded Weldolet fittings were replaced by the more favorable Sockolet.

An extended loop for the handling of non-accepted risk has been developed. Noted in Figure 2-31 on page 56, the generic loop does not cater for the individual findings of the inspection. The improved methodology is as follows

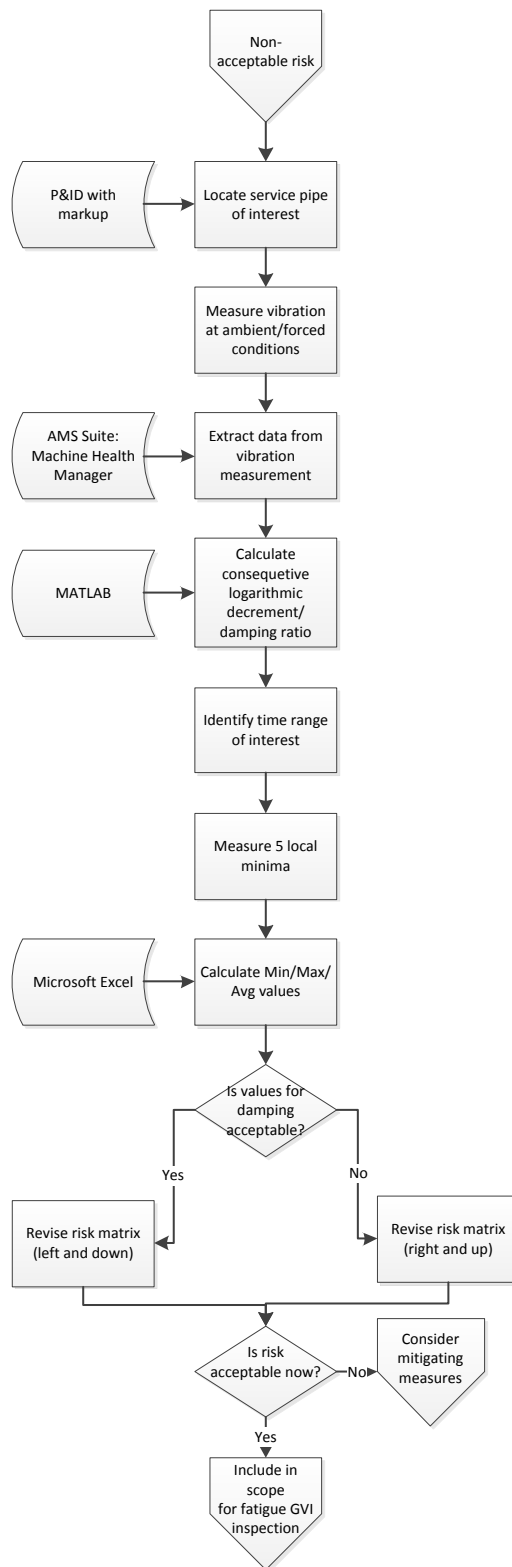


Figure 2-32 Methodology for inspection of service pipes

The loop involves the inspection of the service pipes at installations of interest. When it has been shown that a service pipe does not meet the conditions in regards to fatigue, inspection is necessary. As the overall objective of the methodology is to ensure that a service pipe won't fail due to fatigue, the condition of the pipe is necessary to examine.

On site, the vibration of the individual service pipe is measured. This is done both at ambient vibration and forced induced vibration. The measured vibration then needs to be further analyzed. For a complete breakdown of the steps in the analysis of the measured data, one refers to section 3.4. Using a developed MATLAB-script, one can then calculate the logarithmic decrement and dampening ration throughout the dataset.

In the case of estimating an average dampening ratio, only a section of the dataset is of relevance. It is thus necessary to identifying the time range which one will use for the estimation. When the range is identified, local minima's within this range is identified. In the case dampening, conservative calculations are used. Based on the 5 lowest minima's in the range, one can find the max/min/average value of the damping. These calculated values will then be used to revise the risk assessment.

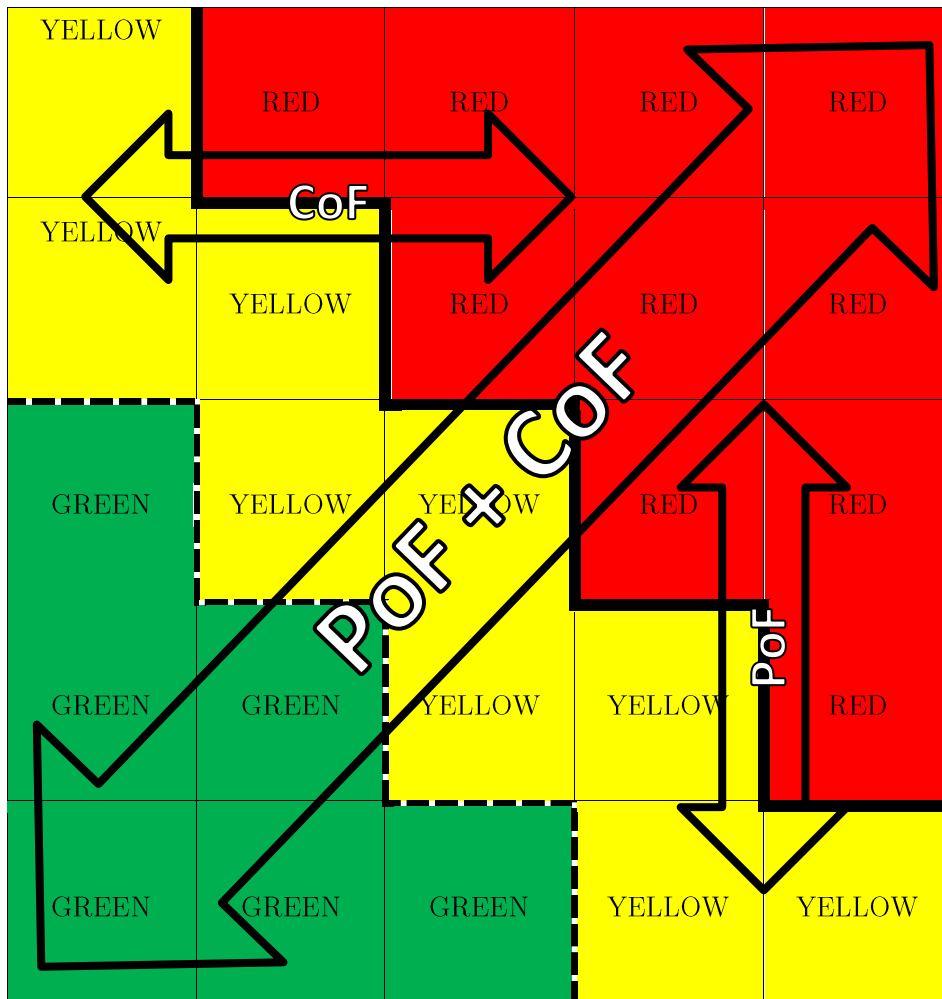


Figure 2-33 Reduction of risk (Adapted from International Organization for Standardization 2002)

If the dampening of the individual service pipes is considered sufficient, the PoF can be reduced. This means that the risk will be lowered vertically in the risk matrix. As a result of the inspection, the CoF may also be lowered. The combination of lowered PoF and CoF will help with reducing the risk categorized as *RED* to *YELLOW* or *GREEN*.

Risk reducing measures are necessary to remedy the unfavorable operating conditions on any installation. A period after completing the remedial action, additional inspection is necessary. This to ensure the improvement of the condition of the pipe. If the findings can be considered satisfactory and the risk can be considered lowered, the next natural step will be to incorporate the area in the scope for GVI. If the risk is not lowered from the remedial action,



additional measures are necessary to take to ensure the security of personnel, the environment and the business. The loop will continue to run until the risk of failing service pipes is satisfactory.

## 3 Experimental work

### 3.1 Location for testing



Figure 3-1 Kollsnes gas processing plant (Statoil 2007)

For testing of the hypothesis, the processing plant of Kollsnes was chosen. Situated in Øygarden, 65 kilometer North West of Bergen, the plant was put in production in 1996. The plant was a part of the expansion of the Troll-field. After its opening, the process plant has been modified to handle gas from Kvitebjørn (2004) and Visund (2005). After the last of its fourth upgrades was completed in 2006, the daily capacity for the export of natural gas exceeded 143 million  $\text{Sm}^3$  (Økland 2010). The gas is transported to both the British Isles and the European continent, where the primary consumers are located.

As of today, Gassco AS is the operator of the plant. Statoil functions as the technical operations manager. Upon construction, it was originally A/S Norske Shell which had the operator role. At completion, Statoil took over. As the ownership of the plant was transferred from the Troll-group to Gassled in 2003, Gassco took then the operator role from Statoil.

At the Troll gas-inlet, it is necessary to separate the wet gas from the stream. As Gassco is contracted to deliver gas according to specified parameters, undesired elements have to be removed. In the case of the multiphase wet stream, it is necessary to remove water (liquid and gas phase), heavier hydrocarbons (condensate) and other unwanted components (such as sour components). The individual tasks of preparing the gas for export are done in a series of various numbered systems. One example is the 20 – system. This system is called “Separation and stabilization”. The 20 system and is the first system the gas comes in contact with upon entering the plant. Each of the individual systems has interfaces to the other systems throughout the loop. One of the interfaces of the inlet 20 system is the CA-pipeline system (Chemical, Methanol). Methanol is added to the stream offshore before the well stream enters the pressurized pipeline towards Kollsnes.

The reason for this is because the multiphase mixture of gas, water and other components under the high pressure creates an environment ideal for the forming of hydrate.

Per definition, hydrate is an umbrella term for any solid substance containing water. In the case of well streams, it is used to describe the formation of a solid plug in consistency comparable to wet snow. The reason for the forming of these plugs has to do with how the hydrocarbon molecules, in most cases methane in gas phase, are trapped in the much larger water molecules. By adding components such as MEG (monoethylene glycol), DEG (diethylene glycol) or methanol, the properties of the well stream changes. This is illustrated below.

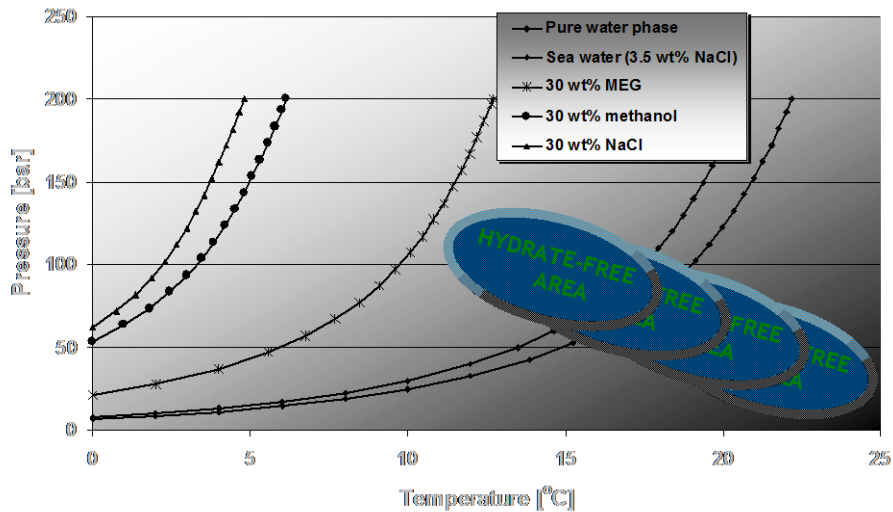


Figure 3-2 Influence of thermodynamic inhibitors on the hydrate equilibrium curve (Lien 2010)

A methanol and glycol additive change the thermodynamics of the liquid phase and lowers the solubility of salts. It also changes the pH value and the solubility of gas in water. Compared to glycol, methanol is less regenerative (Brustad et al. 2005). This is a trade-off necessary for obtaining the inhibiting properties of methanol illustrated in Figure 3-2.

After the gas has been dried and scrubbed according to specifications, it is compressed in six compressors. Three of these are driven electrically, while the other three are connected to turbo expanders. The compressors increase the pressure of the gas while reducing the specific volumetric properties. This for a more efficient transport of the gas through the export pipes. From Kollsnes, the gas is transported offshore to the installations Draupner and Sleipner in two individual pipes. From these installations, the gas is divided into four main export pipes; Statpipe, Zeepipe, Franpipe and Europipe I (Gassco 2012).

From the plot plan of Kollsnes (ref. Figure 8-4) (Statoil 2011a), one can see that the different systems and functions are spread over different areas mapped A11 – A83. Inspecting the entire plant for service pipes is time consuming. This is where the value of a screening method comes in play. Utilizing the defined categories of section 2.5, one can study the individual P&ID's for areas that might be of interest. In addition to the parameters of the screening method, one

has to evaluate the ability to both visually and physically gain access to the individual areas.

Focus in this thesis has been on the areas A11, A12, A21, A22, A23 and A24. In the upcoming section of the thesis, all directions are related to the plant-specific system of coordinates, illustrated by the compass rose on the figures.

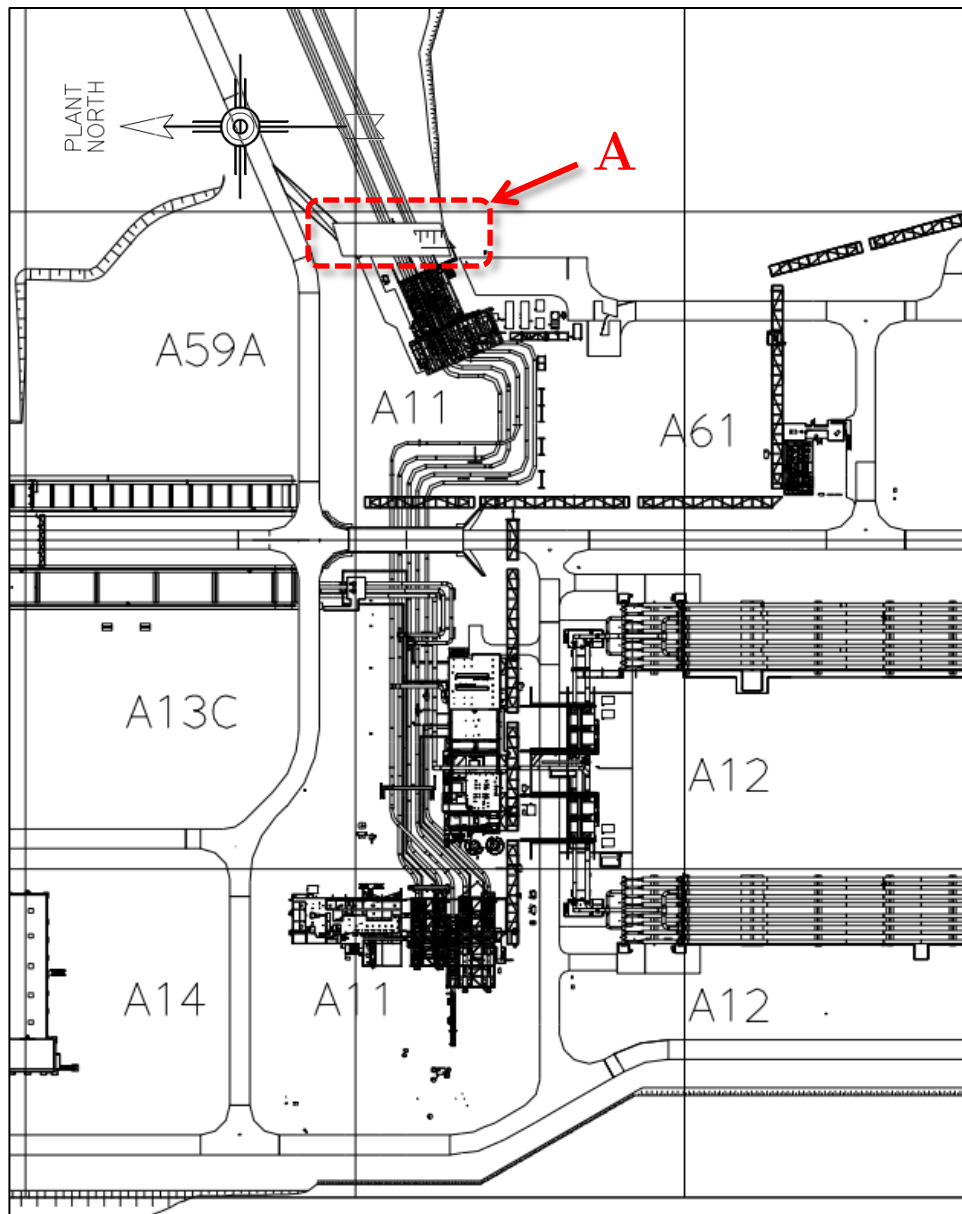


Figure 3-3 Area A11 Pig receiver & launchers/ESD valves (Statoil 2011a)

Area A11 is named “Pig Receiver & Launcher / ESD Valves.” Figure 3-3 illustrates how the area is located between the areas A14, A13C, A61 and A59A. A11 covers both the pipe inlet in the east and the pig receiver further west. One area of importance is the anchor, noted A in Figure 3-3. This is formally the interface between offshore pipeline and the process plant. From the offshore installation to the tie-in at Kollsnes, it is the transport pipeline specification that is prevailing. West of the anchor, it is Statoil’s pipe specification TR2000 that are considered valid. Situated on top of the anchor, the emergency shutdown valves (ESD) are located. These function on the same premises as blow-out preventers (BOP) on the well heads offshore. In case of an emergency shutdown, these valves close. This effectively cuts the flow of hydrocarbons from the offshore installations. For reasons of redundancy, each of these valves has series of bypasses. For access to this area, there are very few items hindering inspection. Most of the instruments are close to established pathways and do not require the construction of scaffolding.

Within the same area designation, the system for pigging is located. Pigging of pipelines of these dimensions is performed on a regular basis. There are several pipelines in place for the bypassing of the superfluous process stream when pigging is in progress. Since the tie-in of the newest pipeline (P12), the pigging area has been expanded to also incorporate the process stream from this line. Parts of these lines have yet to be inspected in regards to fatigue. They are interesting to compare to the service pipes connected to P12 to the older pipelines P10 and P11 (Økland 2010).

Area A12 is designated to the slug catcher. Slugs are non-gaseous objects in the process stream. By eliminating the slugs as close to the inlet as possible, one does not run the risk of obstruction of the pipes. This reduces the unwanted pressure loads in the systems post slug catcher. According to the flowchart for screening of fatigue on service pipes, most of the pipelines in this area are well over the criteria of the 3” diameter pipeline. The catcher itself consists of 8 pipes, each with a dimension of 48”. Focus will consequently be on the connected pipelines of a smaller diameter. Inspecting the P&ID C030-PH-A00--PE-101-03

(Statoil 2011b) using both the Kollsnes Engineering Numbering System (KENS) and the legends accessible from STID, one can identify the service pipes in the P&ID's (Statoil 2010b; Statoil 2012a; Statoil 2009b; Statoil 2012b; Statoil 2008; Statoil 2009a; Statoil 2004; Statoil 2012c; Statoil 2012d; Statoil 2012h; Statoil 2012f; Statoil 2012e; Statoil 2012g).

Focus has therefor been on service pipes located at the utmost south of the plant. Further inspection will uncover whether there are service pipes in that area that should be tested and analyzed for vibration and fatigue.

The areas A21, A22 and A23 are the locations of the three process trains. Inside individual housings, turbo expanders are connected directly to compressors. From the drawings and P&ID's, one can see that the piping in the regions is, for the most part, properly insulated. The insulation functions as dampener for both mechanically and flow-induced vibrations. One do run the risk of fluid hammering this close to the compressor, and it will therefore be an area worth inspecting. Outside the housing, more dead legs and service pipes are identified. Combining the inspection of the turbo expanders with visually inspecting the outside area will give a good indicator on the variation in regards to amount and type of service pipes. The piping outside of the turbo expander is not insulated, making for a reduced damping of the system.

The extraction of natural gas liquid (NGL) is done at the area A24. This vertical column is connected to several support systems. The reason why area A24 is chosen over other areas is because of the history of fatigue in this zone. During the latest capacity upgrade of the plant, inspection discovered cantilever flanges vibrating at relative high frequencies. The increased frequency led to higher stresses in the service pipes. Normally, this is improved by adding support for the flanges in question. The problem with these higher frequencies is that they don't respond that good to the added support. This led again to the need for replacing the flanges and fittings. Some of the flanges experiencing higher frequencies were taken out of service (Dalstø 2012).

Working within the gates of the process area at Kollsnes requires the usage of work permits (WP). Work permits are written approval issued by Statoil. It

authorizes on-site work on within a specific area. The validity of a WP demands that the work is done in accordance with the details that one applied for.

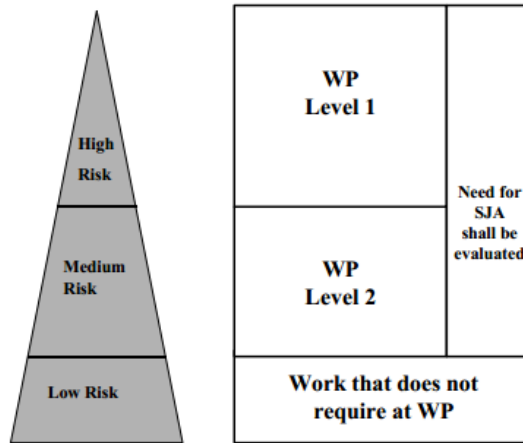


Figure 3-4 Work permit levels and risk triangle (Rogsvåg et al. 2005)

In this case, it is necessary to apply for a work permit for the usage of both non-Ex classified camera (Canon S100) and the Emerson CSI 2130 Vibration Analyzer within the areas mentioned above. Working around hydrocarbons require all equipment to be Ex-certified to the Atmosphere Explosible (ATEX) directive (Det Norske Veritas 2012).



### 3.2 Equipment for testing



Figure 3-5 Emerson CSI 2130 Vibration Analyzer (Reliability Maintenance Solutions Ltd n.d.)

For testing the vibrations on the pipelines in Kollsnes, an Emerson CSI 2130 Machine Health Analyzer is used. Measuring 203x260x48 mm at 2.04 kg, the unit itself is small and rugged (IP65-rated) enough to be used in field testing. This includes work both on- and offshore.

The CSI 2130 is a vibration data collector capable of vibration-, cross-channel- and transient analysis onsite (Emerson Process Management 2011). For analyzing vibration, a dual-channel option can be chosen for improving operating speed and overall efficiency for data monitoring. In addition to collecting vibration data, the CSI 2130 can be used to decide the overall health of the machinery which is being tested. Through the internal firmware, the CSI 2130 can be programmed and updated with for the specific usage at the customer. For in-field analysis, the CSI 2130 has built in software based tools for waveform autocorrelation. This help separating periodic from random wave frequencies. As

the machine originally was developed for use on rotating equipment, it can identify the trending of narrowband parameters over longer periods of time.

Optimal use of the sensors can result in a complete set of data after a period of 7 - 10 seconds. As previously mentioned, it is possible to perform analyses on the unit in the field. In the case of the testing on Kollsnes, the data will be exported to a dedicated computer. This is done using a USB cable for moving the file of proprietary file type from the unit. For analyzing the data, Emerson Process Management delivers a software suite called “AMS Suite: Machine Health Manager” (Emerson Process Management 2010). The program consists of an integrated solution for multiple predictive diagnostic technologies. Example of diagnostics that can be run through the suite is portable vibration analysis, continuous online machine monitoring, lubrication analysis and infrared thermography. Each of the diagnostic tools has one or more modules for analyzing raw data from the sensors. Plotting of the data is done in-suite and can be visualized and analyzed in different ways. For this thesis, the software suite will be utilized to extract the raw data from the unit. The data will then be exported into a file type that can be read on other commercially available pieces of software. The export is done via a column formatted .txt-file. The file is then imported into Microsoft Excel, where it is necessary to properly format the value. Due to the size of the datasets, macros are developed for a more automated process. The data is then prepared for further analyzes.

### **3.3 Procedure for testing**

When testing vibrations on site, there are several ways of gathering data. For this thesis, focus was on using accelerometer to output the excitation of the individual pipes

The procedure for testing was developed in to two separate stages. When a service pipe of interest has been identified, an accelerometer will be mounted. Oscillation of non-supported service pipes is assumed to be free in two directions. With access to just one accelerometer, the testing will be performed in series. For the first measurement, the accelerometer will be attached on top of the flange on

horizontal equipment. By preprogramming the vibration analyzer, one can decide on the range, time and amount of data points for which the tests are to be performed by.

For the first vibration test, the accelerometer is mounted on the flange and the background vibration (ambient conditions) of the flange itself is measured. This will be done so that one can identify white noise and hopefully remove this from the measurement of the dampening. This test is to be performed using the analyzers auto-range function. Auto-range determines the best range of amplitude to be measured. It will then be plotted over a period of 12800 ms (12.8 s) capturing a total of 32768 individual points. The results from these measurements will then be analyzed further.

When the test with ambient vibration is completed a second set of measurements are taken without moving the accelerometer. As the second measurement is started, one strikes the service pipe with the hand. As opposed to the ambient testing, the gathering of the data will be performed within a predetermined range. Whenever the auto-range function is used, the equipment needs to correctly calibrate the range to fit the input from the accelerometer. This process takes some seconds, meaning that data close to the initial strike will be lost. By striking the flange, one will have the possibility to test how long it takes the system to return to asymptotically stable conditions. Using the peaks from these measurements, one can calculate the dampening of the service pipe in accordance with the formulas presented in section 2.3. These two separate measurements are then repeated with the accelerometer mounted normal to the original location. This is done to compare the dampening in two separate directions. It will result in redundancy in the measured data, resulting in four individual datasets per service pipe.

### 3.4 Procedure for analyzing

When the data are extracted from AMS Suite, it is in a .txt file container as written text. This file is then imported to Microsoft Excel for conversion from the proprietary data layout to a two-column data set containing Time (ms) and Amplitude (mm/s). Due to the type of the original layout, it is necessary to manually move datapoints for the two-column layout in addition to formatting the values to a format that Microsoft Excel can read and write to natively. A macro is written in Microsoft Visual Basic for Applications for adjusting the data. The macro itself is attached in section 8.5 and illustrates the individual steps necessary for handling the data.

As the data are correctly formatted according to Microsoft Excel, a MatLab script is written. Using the `xlsread()` function of MatLab, the data are stored in a user defined vector space, in this case `Time` and `Amplitude`. The first plot is then created. Here, the amplitude is plotted against the registered time in the time-domain in a regular x-y plot.

For transferring the data from the time-domain to the frequency-domain, a Fast Fourier Transform is performed. The MatLab function `fft(x, n)` implement the transform given for vector of length  $N$  by

$$X(k) = \sum_{j=1}^N x(j) \omega_N^{(j-1)(k-1)} \quad 3.1$$

Where

$$\omega_N = e^{(-2\pi i)/N} \quad 3.2$$

The `fft(x, n)`-command returns the discrete Fourier transform (DFT) of vector `x`, computed with MatLab's fast Fourier transform algorithm. If the length of `x` is greater than `n`, `x` is padded with trailing zeros to length `n`. Fourier transforms are often used to find frequency components of a signal buried in a noisy time domain signal. It will be used for identifying main frequency for vibration.

When the single sided amplitude spectrum has been identified, the calculation focuses on finding the damping properties for the service pipe. For discrete data sets, the Logarithmic Decrement Method is often utilized. Derived in section 2.4, the method utilized local maxima to calculate decrement of the interpreted signals in the time domain. In MatLab, this calls for the function `findpeaks(PosAmp, 'minpeakdistance', n)` for the identification of local maxima's. Here, the variable "PosAmp" equals only the positive amplitude in the time domain, where the negative values has been set to 0. Using the parameter 'minpeakdistance' in collaboration with `findpeaks()`, one get the ability to determine the minimum distance between peaks for MatLab to loop through. If a peak is discovered in a range smaller than the preset distance, it will be skipped. This continues until a maximum peak outside of the distance is found throughout the available data. A logical `for`-loop runs through the data and calculates the varying logarithmic decrement for each identified peak.

Based on the output of the LDM-calculations, each value for the decrement gets a corresponding value for the damping ratio. Depending on the size of the dataset and the amount of identified peaks, many individual damping ratios are found. The results are then plotted into four different subplots, showing amplitude in time domain, single-sided amplitude spectrum of signal, logarithmic decrement and damping ratio.

## 4 Results

### 4.1 Results of inspection

Using the developed screening methodology combined with the information from the P&ID's, several service pipes of interest were identified. After the initial coursing necessary for plant access, a survey throughout the entire plant was done.

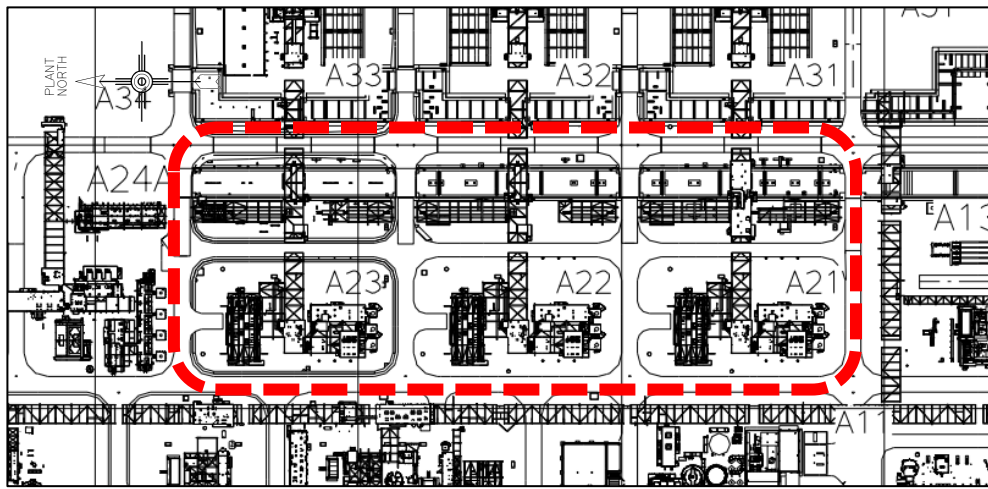


Figure 4-1 Inspected areas A21 - A23 Turboexpander 1 – 3 (Statoil 2011a)

Upon examining the P&ID's prior to the inspection, a set of flanges in the areas A21 – A23 were identified. Situated just outside the housing for the turbo expanders, the line tags CA-21-5111-FS20A and CA-21-5110-FS20A in areas A21 and A22 respectively had been identified as of interest. Both of the flanges are the identical type and carried the identifying valve tag Q-B-L—1100-06C. The flanges themselves are branches from the outlet of the process train connected to the methanol system. In the immediate proximity, a Joule-Thomson valve is located. According to the screening method, it has been identified that the flanges can be exposed for fluid hammer that can occur close to centrifugal compressors. Mechanical vibration can also take place.

In the period of the field testing, a planned partial revision stop of the process plant was in progress. The area A21 was affected by this revision stop.

This led to an above-average level of activity in the area surrounding process train 1. It was still possible to gain access to the area and visually inspect the line tag CA-21-5111-FS20A.

The free-hanging flanges are welded to a T-piece transporting methanol from process train 1. It was identified that the dimensions of the service pipe and the mass of the flange can result in high loads at the weld. As the socket itself is not of Socketlet or Weldolet type, the overall geometrical shape is not of most favorable type.

As the area A21 where shut down, there could not be visually observed any oscillation in the system. Any vibration would therefore be as a result of resonance of vibration in a different area, or, as a result of external excitation. This would mean that the conditions were different from the flange in area A22, which were of identical type.



Figure 4-2 Flange Q-B-L—1100-06C connected to CA-21-5111-FS20A in area A21



Figure 4-3 Detail of socket connected to CA-21-5111-FS20A in area A21



Figure 4-4 Flange Q-B-L—1100-06C connected to CA-21-5110-FS20A in area A22





Figure 4-5 Detail of socket connected to CA-21-5110-FS20A in area A22

As stated, the area A22 had a valve of identical type connected to the same type of system. The difference was that the process train 2 was currently running. Inspection uncovered an oscillating flange. Comparison of how this affected the damping properties will be presented in a later section of the thesis.

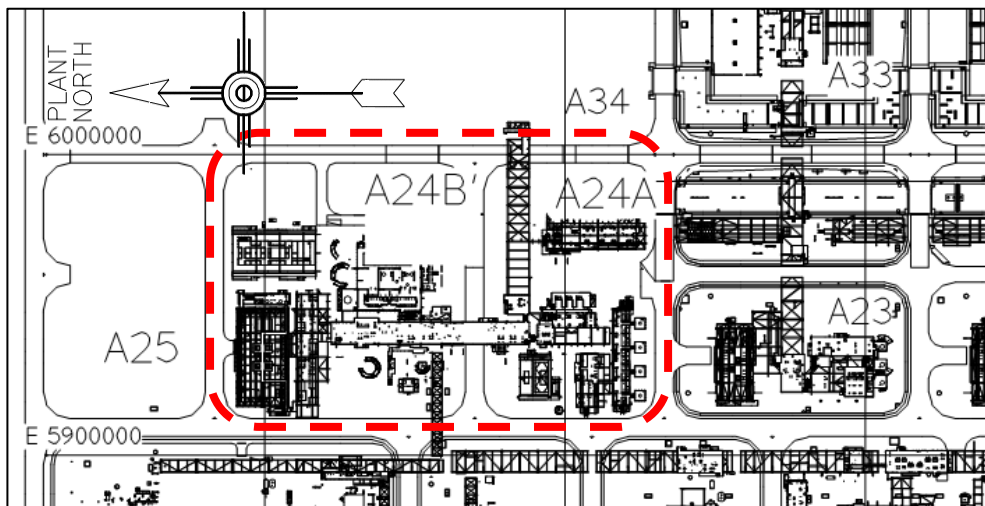


Figure 4-6 Inspected areas A24 NGL Extraction (Statoil 2011a)

In addition to the areas A21 and A22, section 3.1 concluded with that the area *A24 - NGL Extraction* also was of interest. Visual inspection of the area identified three separate service pipes for further analysis. The first flange is connected to the PV-25-8287-ES20A pipe. This pipe transports dried gas from the NGL stripping column to the torch. The flange, 25-8287/1-2 SP2-2 has previously been replaced for fatigue (ref. Figure 4-7). The new design incorporates many of the changes reflected in more modern flanges. The socket is of type Weldolet which has been stated as a more favorable geometry compared to the sockets of the flanges in area A21 and A22. The fitting leads to less stress on the heat affected zone (HAZ). Even with the newer geometry, vibration can be seen from the visual inspection. As the flange is situated roughly 20 meter above ground, vibration from lower levels can be amplified in the structures. This leads to increased amplitude at the flange tip.

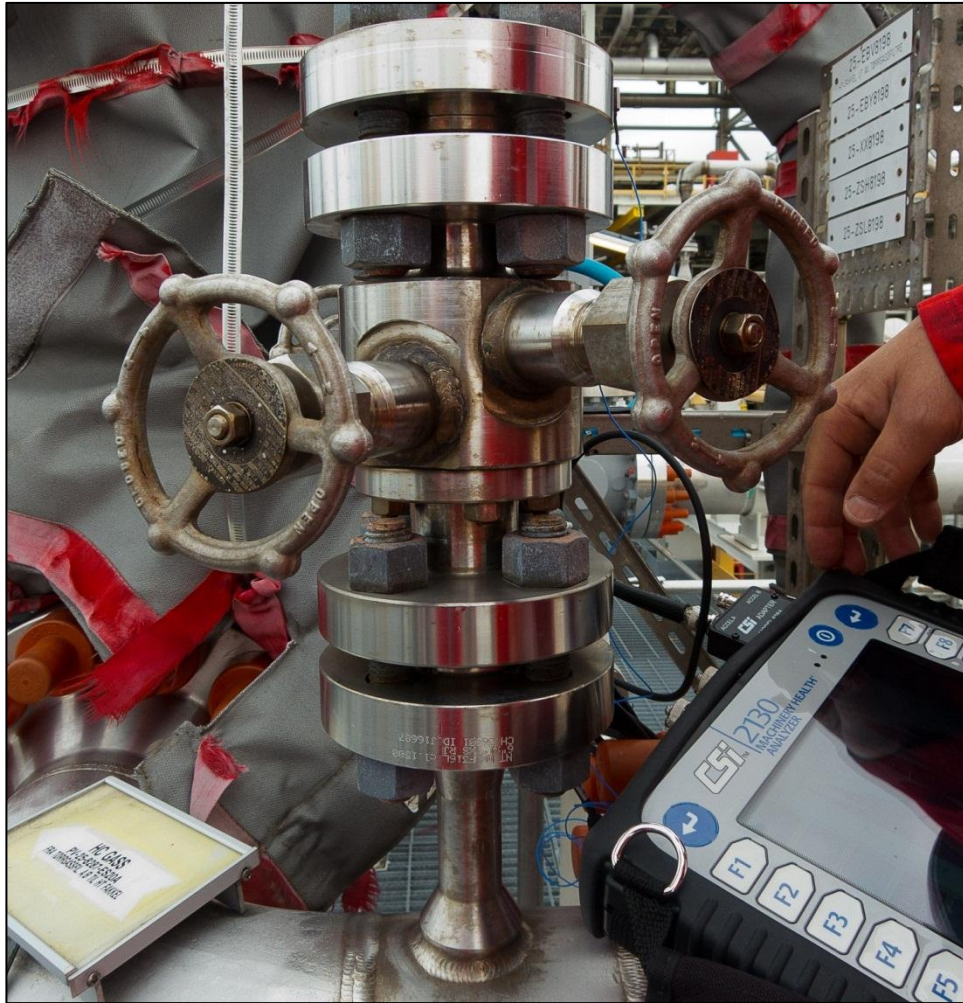


Figure 4-7 25-8287/1-2 SP2-2 on PV-25-8287-ES20A in A24

Within in the same area of operations, two other relevant service pipes are located. The first one are of the older type, directly connected to the pipeline PL-25-8501-BC21A. This pipe leads hydrocarbons from the NGL cooler (ref. Figure 4-8). Since the flange functions as a concentrated mass, the combination with the low, nominal pipe diameter means the according to the screening procedure, the flange is in risk of fail due to fatigue. The flange cannot be seen to vibrate from the visual inspection. Putting the hand on the outer flange, one can clearly feel the vibration of the structure



Figure 4-8 Flange on PL-25-8501-BC21A in A24

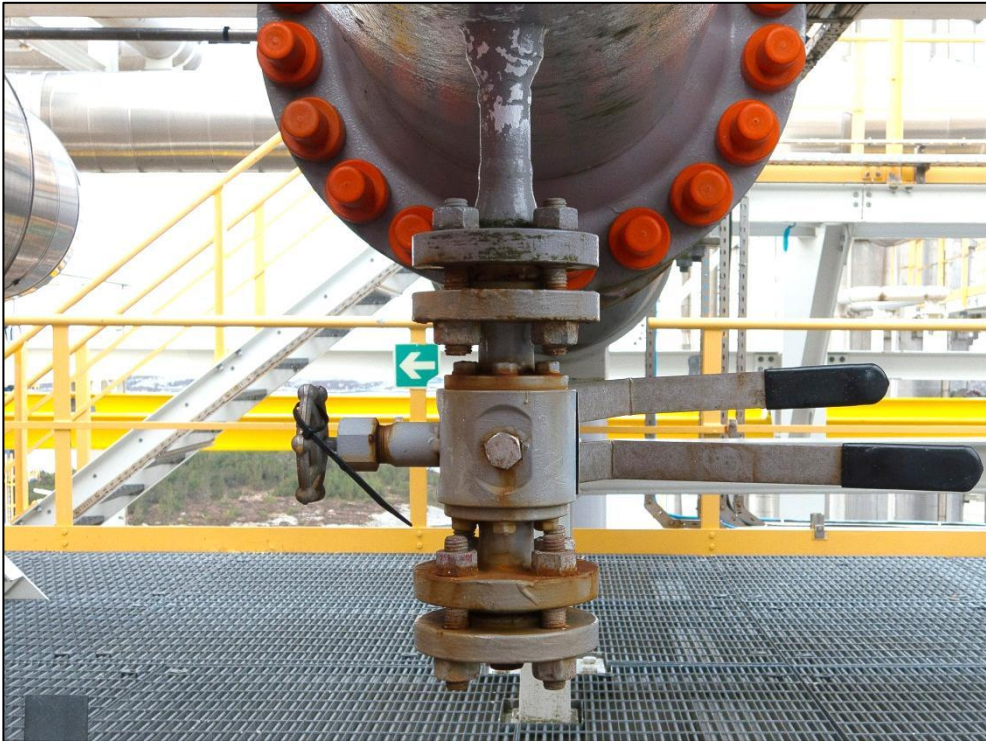


Figure 4-9 MX3V2J-J74220 on PV-25-8107-DC11A in A24

The last service pipe in area A24 is connected to the much larger PV-25-8107-DC11A on the fourth floor of the structures in the area (ref. Figure 4-9 MX3V2J-J74220 on PV-25-8107-DC11A in A24). The main pipeline itself is currently in revision in regards to the lack of support. The pipeline leads dried gas from to the gas/gas heat exchangers on ground level of A24. This means that the potential for both flow induced turbulence and acoustic vibration are present.

The last area of interest is the location where the tie-in from the pipeline (ref. Figure 3-3 Area A11 Pig receiver & launchers/ESD valves (Statoil 2011a)). Being the newest extension to the process plant, the piping from the tie-in of the pipeline P12 have yet be inspected. Without proper inspection, unwanted geometrical effects won't be discovered. According to the screening methodology and the available P&ID's, there were not identified any service pipes with high PoF. When the area was visually inspected as a part of the general survey at the plant, service pipes of interest were identified

During the stay at Kollsnes, there where pigging of the pipeline from Troll in progress. This led to periodic unstable operating conditions and increased pressure at the plant inlet. It was thus necessary for the operator to reduce access to the areas A11 and A12. Application for admission combined with radio communication with the responsible operating team was needed to gain access of the area and perform the visual inspection of the service pipes.

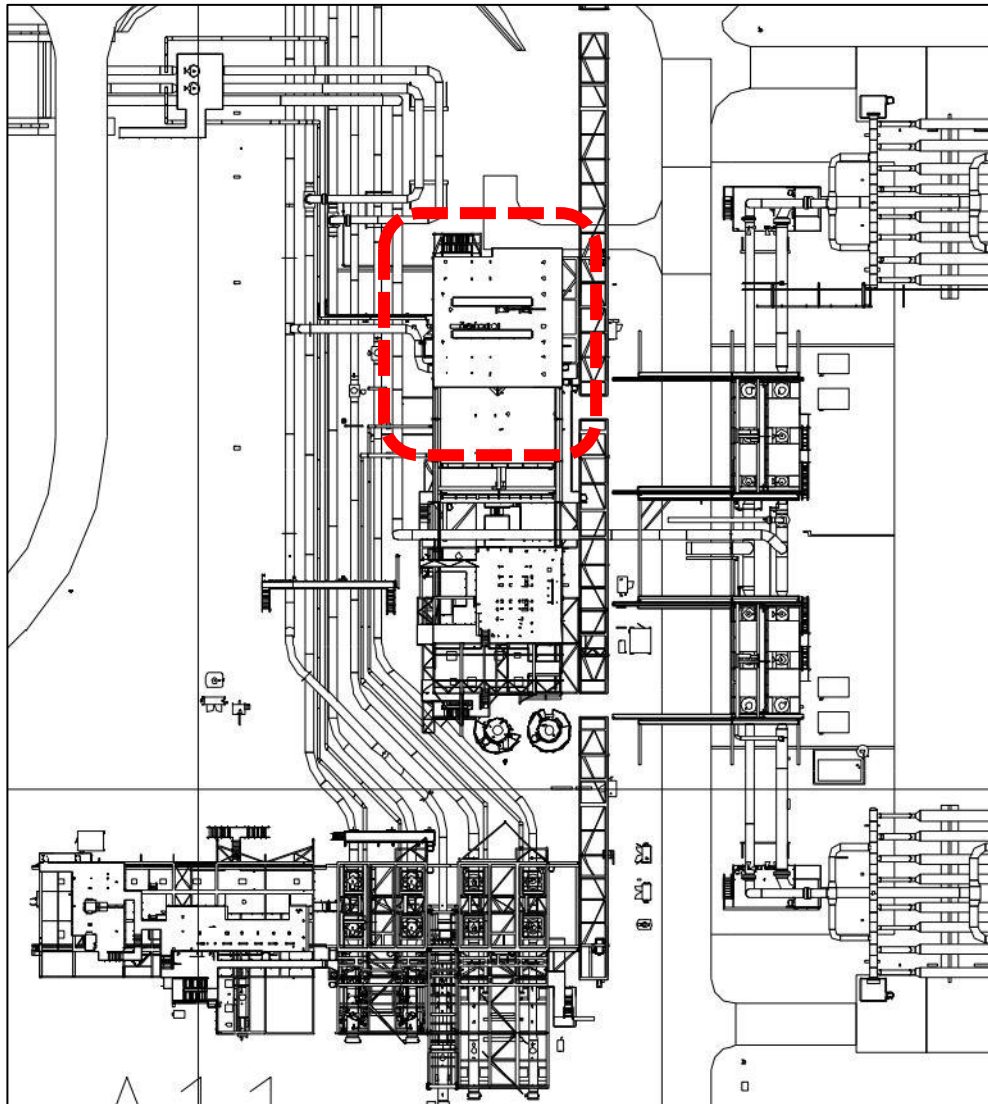


Figure 4-10 Area of inspection A11/A12. (Statoil 2011a)

On top of the structures that marks the interface between the areas A11 and A12 sits instruments connected to the new inlet pipeline (P12). Among them, an orifice flow meter for the multiphase process stream to the slug catcher is located. Connected to 10"-PR-20-5347-EC19AX, the flow meter are exposed to several of the conditions stated in the methodology. Slugging flow and flow induced turbulence are conditions the pipe can experience. This can lead to the vibration of the pipe itself and this can spread to the auxiliary equipment connected to the same pipe. In the case of the flow orifice instrument, the branches are thinner than 2" criteria stated in the screening methodology. This is

combined with a non-ideal fitting and a heavy instrument on an unsupported branch.

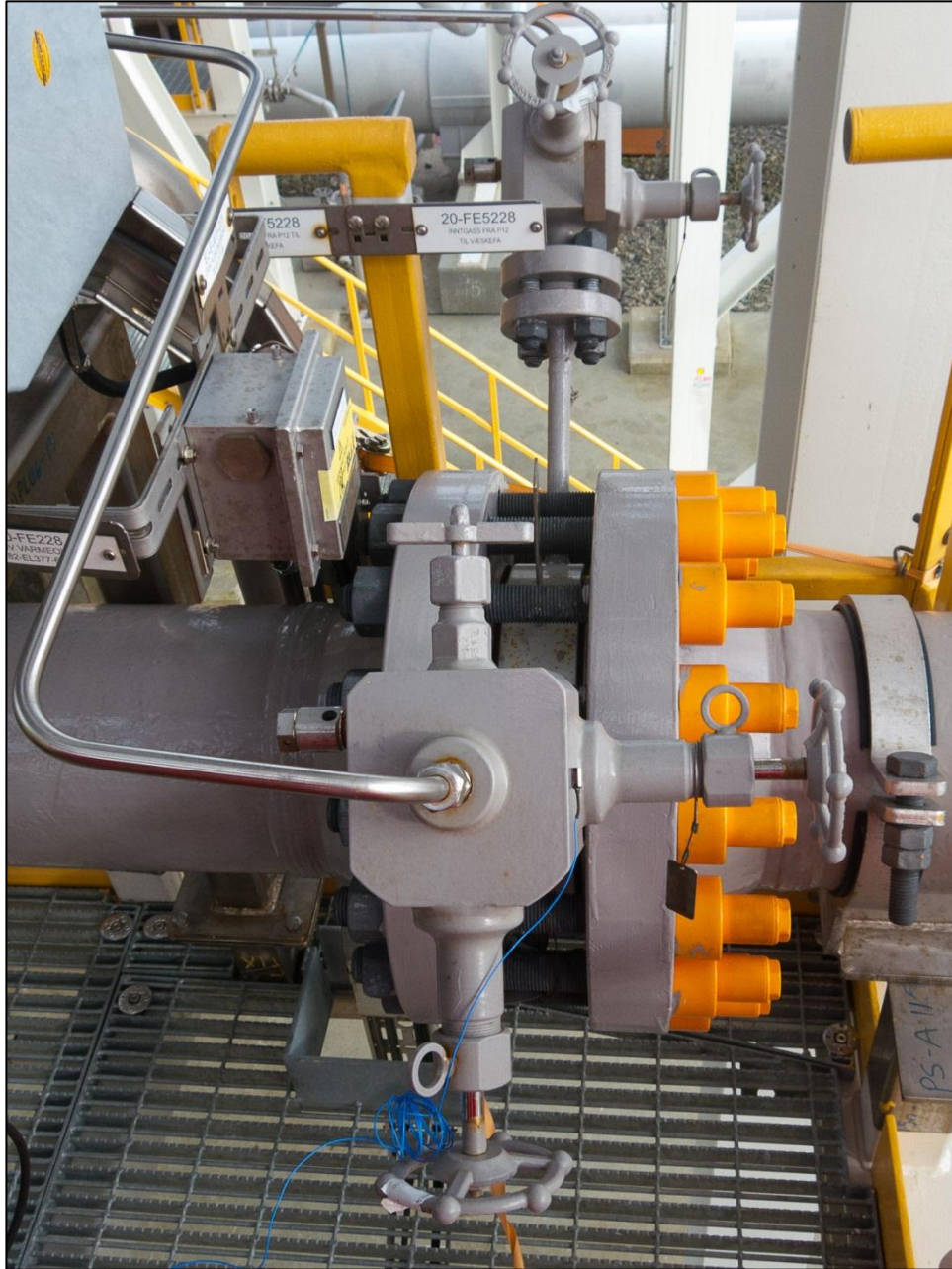


Figure 4-11 Flow orifice monitor 20-FE5228 at 10"-PR-20-5347-EC19AX

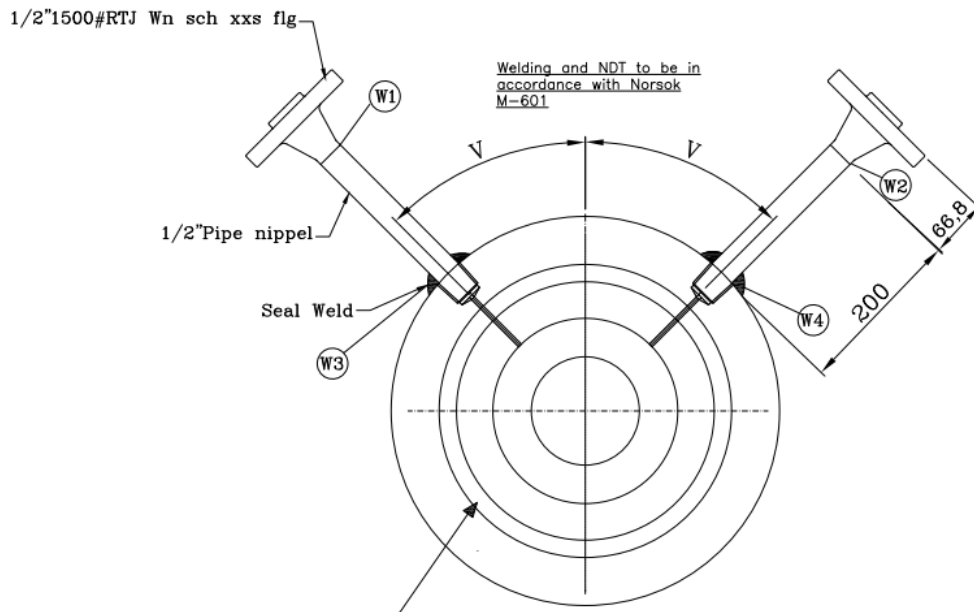


Figure 4-12 Flow orifice instrument (Statoil 2010a)

A 200 mm, 0.5” nipple sits between the flange and the piping orifice. Compared to the masses of the valves and flanges, it can be considered a slim construction. The material of orifice, flange and nipple are all of the designation 316L and are according to Statoil’s pipe specification. Since none of the valves are supported, it is only the 0.5” nipple that is to provide dampening of the service pipe. At the time of the inspection, the no vibration could be identified. When striking the valves, oscillation is induced in the system. One can see that the system takes a long time before the movement is reduced to an asymptotically stable motion. This does again indicate that the dampening of the system is of underdamped character. As described in section 2.4, underdamped systems takes longer to dissipate the motion energy into its surroundings and then stabilize itself. If the amplitude of the vibration is maintained high for longer periods of time, the stresses will make existing microcracks propagate and thereby make for non-ideal for fatigue resistance.

From the drawing of accessible STID, the instruments are confirmed to have been fully tested using radiographic testing. Dye penetrant inspection to verify the integrity of the seal weld is also performed. As the equipment is new and it has already been confirmed to be of acceptable quality in accordance with



NORSOK M-601 Welding and inspection of piping (NORSOK 2008), one can assume that the overall condition of the instrument is similar to when installed. From this the assumption means again that one, from the tests performed at these service pipes, can predict how the dampening properties of identical instruments installed at different installations will be. Two separate service pipes are directly connected to the pipe 10"-PR-20-5347-EC19AX. Performing the vibration test on the both of them will give a total of eight sets of data to perform the analyses on.

## 4.2 Results of testing

The first results of the vibration testing focuses on the amplitude in the time domain. The clean output signal was plotted against the time axis, giving an indication of vibration of the individual service pipe behaved. This was done both with ambient conditions and when it is forced to vibrate from striking the service pipe. This section presents and comments on the time-domain signal. The results from the additional analysis will be presented in the upcoming sections.

The order of testing was performed in accordance to the order of which the candidates were described in section 4.1. The results are split up in two separate tables. This for identifying the results from the ambient vibration and comparing these to the test with excited motion. The results are numbered in accordance with the following table.

Table 4-1 Test numbering scheme

| <i>Line tag</i>     | <i>Test no. (ambient)</i> | <i>Test no. (excited)</i> |
|---------------------|---------------------------|---------------------------|
| CA-25-5111-FS20A    | 1                         | I                         |
| CA-25-5110-FS20A    | 2                         | II                        |
| PV-25-8287-ES20A    | 3                         | III                       |
| PL-25-8501-BC21A    | 4                         | IV                        |
| PV-25-8107-DC11A    | 5                         | V                         |
| PR-20-5347-EC19AX-1 | 6                         | VI                        |
| PR-20-5347-EC19AX-2 | 7                         | VII                       |

Each of the individual service pipes was tested four separate times. The tests at ambient conditions resulted in 32768 individual points. This was done over the course of 12800 millisecond. The sampling rate under these conditions was preset to 2560 Hz. As no vibration was forced on the service pipe, it was only the vibration picked up from the surrounding equipment that was tested. There was no predefined range of amplitude set in the testing under ambient conditions. The machine would therefore calibrate itself according to the measured excitation. Results from the vibration and the following fast Fourier transform is found in the table below. The frequencies are organized in the order of magnitude.

Table 4-2 Results of vibration testing at ambient conditions

| <i>Test no.</i> | <i>Peak value [mm/s]</i> | <i>Dominant frequencies [Hz]</i>  | <i>Direction</i> |
|-----------------|--------------------------|-----------------------------------|------------------|
| <b>1</b>        | -4.045                   | 0.937; 1.840; 2.038; 3.281; 4.375 | Top              |
|                 | 10.55                    | 19.38; 4.766; 10.08; 1.250; 17.27 | Side             |
| <b>2</b>        | 16.30                    | 17.03; 15.94; 14.45; 14.22; 25.55 | Top              |
|                 | 10.04                    | 16.02; 14.14; 19.30; 18.44; 5.625 | Side             |
| <b>3</b>        | 117.2                    | 36.09;                            | E-W              |
|                 | -13.28                   | 36.09;                            | N-S              |
| <b>4</b>        | 17.74                    | 10.63; 2.656; 5.625; 31.56; 34.53 | Side             |
|                 | -11.75                   | 5.625; 10.94; 34.14; 13.67; 20.00 | Top              |
| <b>5</b>        | 27.69                    | 497.2; 56.80; 1.406; 49.45; 69.22 | E-W              |
|                 | 26.84                    | 56.88; 497.2; 1.406; 50.23; 68.75 | N-S              |
| <b>6</b>        | 41.59                    | 0.781; 1.563; 2.500; 3.125; 4.141 | E-W              |
|                 | 5.320                    | 1.787; 14.53; 1.172; 2.578; 11.56 | N-S              |
| <b>7</b>        | -8.089                   | 1.094; 6.563; 13.20; 4.672; 10.94 | E-W              |
|                 | 7.697                    | 1.875; 0.093; 11.56; 12.50; 4.766 | N-S              |

The measured peak values of the vibration at ambient conditions can be considered low. Still, there are two values that stand out.

Test number 3 was performed on the service pipe 25-8287/1-2 SP2-2 on the NGL extraction column. This pipe was again connected to the line PV-25-8287-ES20A. It was the only service pipe showing only one dominating frequency.

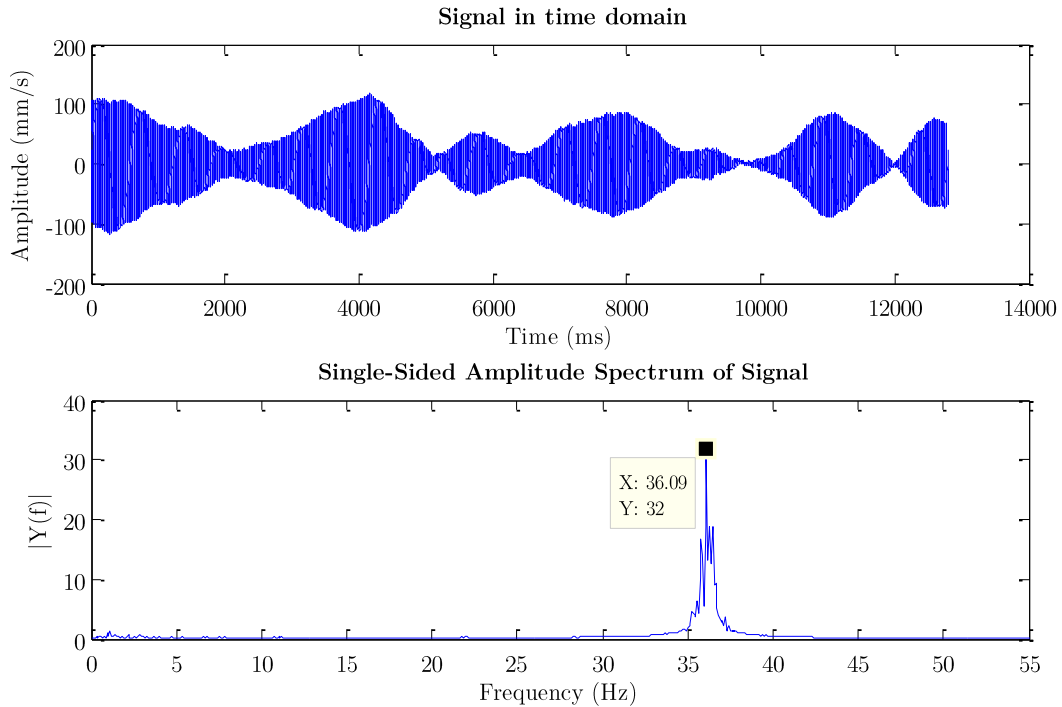


Figure 4-13 Ambient vibration PV-25-8287-ES20A, A24, E-W

The motion in the E-W direction gives rather high amplitudes over the course of testing. It also shows the phenomenon called beating. This happened when the forcing frequency is close to the natural frequency of the system (Rao 2010). The amplitude builds up and then diminishes in a semi-regular pattern. With little-to-no background noise to break up the vibration, it is only the damping properties of the system that prevent lock-in of frequency and consequently resonance in the system. The effect is also noticeable, but not as distinct, as the motion in N-S direction. (Ref. Figure 8-23 Result Non-induced vibration PV-25-8107-DC11A, A24, N-S). The beating of the motion in the N-S direction is broken up by some additional minor frequencies not present in the E-W direction.

For comparison, the results from the ambient vibration measurement of test number 6 do not show signs of beating.

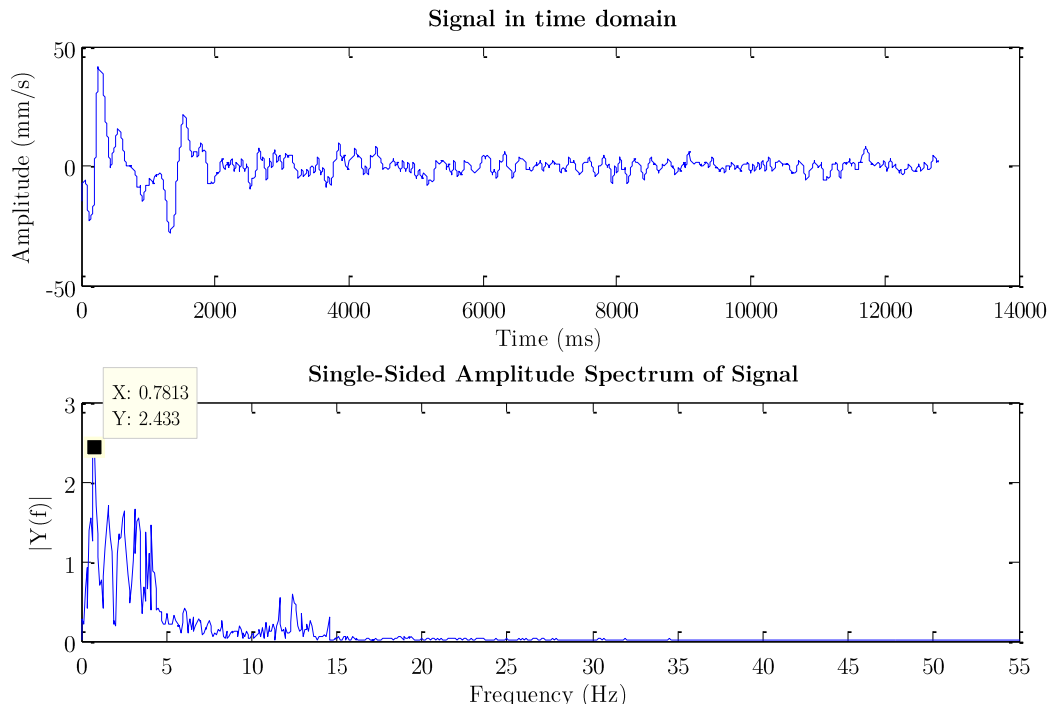


Figure 4-14 Ambient vibration PR-20-5347-EC19AX, A11, E-W

Besides test number 3, the test performed in E-W direction of the flange labeled test number 6 has the highest ambient amplitude. The large amplitude only occurs in the start of the measurement. This indicates that one has come in contact with the flange prior to starting the test. Post the 2 second mark, the motion asymptotically stabilize itself in the range of  $\pm 10$  mm/s. This is similar to the other service pipes at ambient conditions

From the frequency spectrum, one can also see that the motion oscillates in the range of 0.5 – 5 Hz. Two additional minor peaks are found at 11.64 Hz and 12.42 Hz respectively.

From the results of the inspection, the service pipes labeled number 6 and 7 was shown to be of interest. From the figure below, one can see that test number 6 in N-S experiences the amplitude of similitude to the other tests. It is in other words not that exposed to fatigue at the operating conditions at the time of the testing.

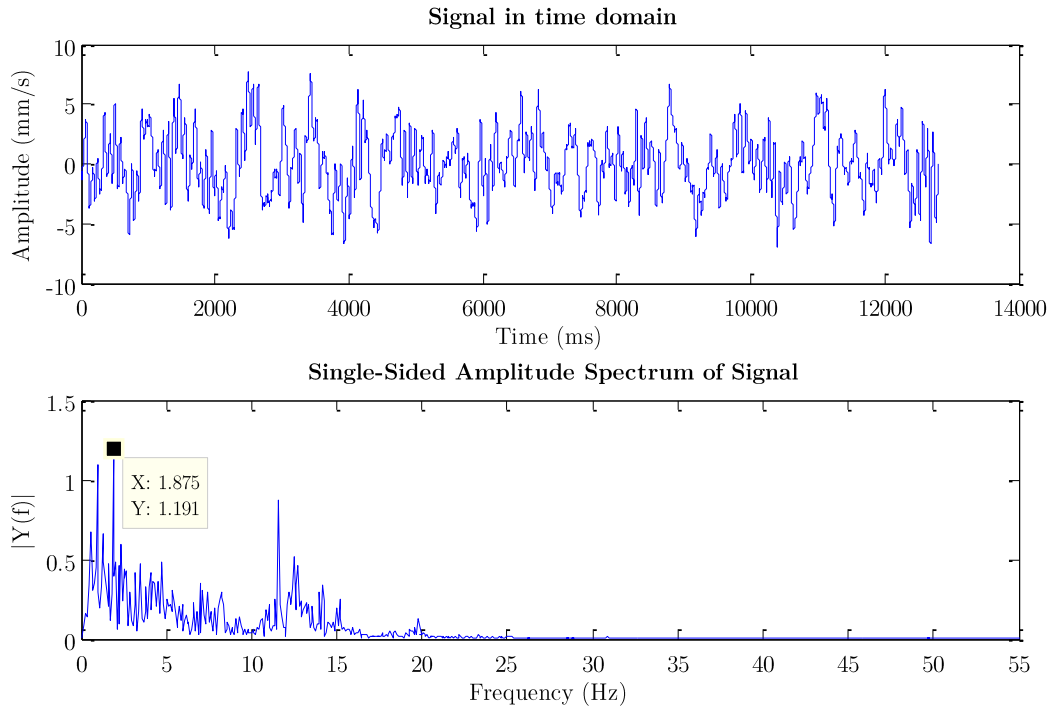


Figure 4-15 Ambient vibration PR-20-5347-EC19AX, A11, N-S

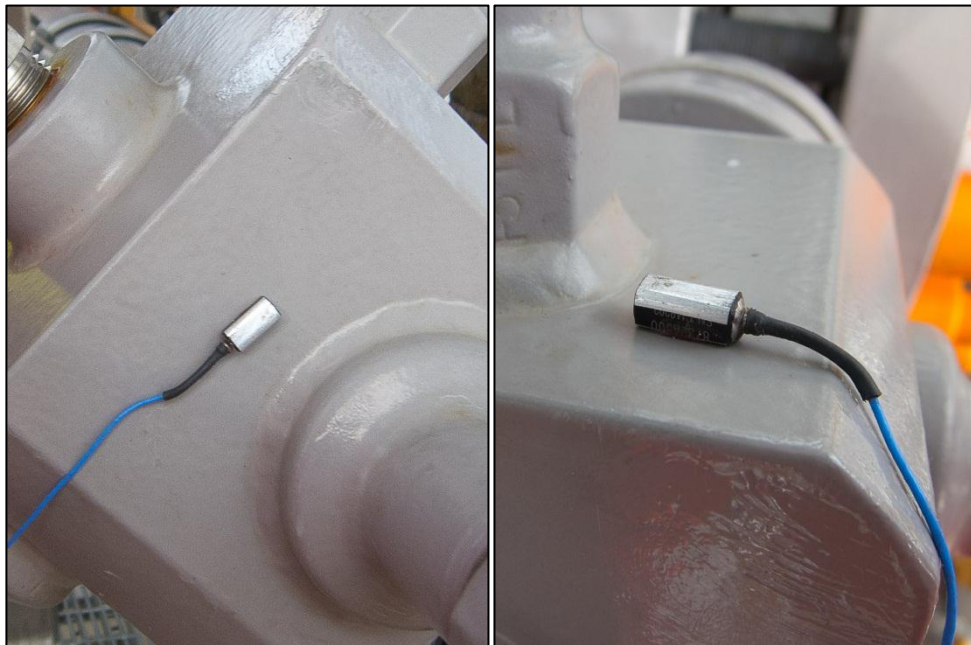


Figure 4-16 East-West and North-South mounting on 20-FE5228-1 in A11

After the testing of the ambient conditions, the individual service pipe was exposed to a forced vibration. Results are shown in table below.

Table 4-3 Results of forced vibration

| <i>Test no.</i> | <i>Peak value [mm/s]</i> | <i>Dominant frequencies [Hz]</i>  | <i>Direction</i> |
|-----------------|--------------------------|-----------------------------------|------------------|
| <b>I</b>        | -149.8                   | 12.30; 12.21; 26.25; 14.53; 32.97 | Top              |
|                 | -113.0                   | 19.38; 10.00; 14.53; 17.19; 21.25 | Side             |
| <b>II</b>       | -156.4                   | 25.16; 15.94; 5.625; 14.22; 17.03 | Top              |
|                 | -135.1                   | 19.38; 14.06; 5.625; 15.94; 20.94 | Side             |
| <b>III</b>      | 283.7                    | 36.25                             | E-W              |
|                 | 244.5                    | 33.44; 36.56                      | N-S              |
| <b>IV</b>       | 137.7                    | 5.625; 42.66; 10.16; 7.344; 42.66 | Side             |
|                 | 150.8                    | 5.625; 34.53; 34.06; 37.81; 10.94 | Top              |
| <b>V</b>        | 300                      | 57.50; 1.406; 497.2; 65.47; 458.1 | E-W              |
|                 | 272.6                    | 57.81; 497.2; 47.81               | N-S              |
| <b>VI</b>       | 129.8                    | 12.50; 14.53                      | E-W              |
|                 | 206.7                    | 14.53; 12.50                      | N-S              |
| <b>VII</b>      | -198.9                   | 14.22; 12.66; 2.813; 1.719        | E-W              |
|                 | -201.8                   | 14.22; 12.66; 1.563; 2.969        | N-S              |

In the case of the forced induced vibration, a smaller set of data was extracted. The logging of the vibration was performed at a lower sampling rate (1280 Hz vs. 2680 Hz) at a shorter period of time (6400 ms vs. 12800 ms). This resulted in a dataset 8192 points in size. The reason for this had to do with the firmware available at the vibration monitor at the time of testing. In the case of the forced vibration in area A21, the range was set to be within  $\pm 200$  mm/s. For the testing of the forced vibration on the rest of the pipes, this was changed to  $\pm 300$  mm/s.

The peak values the individual service pipes experiences does obviously change when force is applied. As there was no way of effectively measuring the magnitude of the force, the value will only be used for calculating the dampening of the pipe at a later stage. More interesting will be to see how the frequency of the oscillation changes.

For service pipe connected to turbo expander 1 that was out of operation, the top mounted accelerometer registers a shift in dominant frequencies (ref Figure 8-5 vs. Figure 8-6). The registered frequency peaks are also more distinct in the forced oscillation. In the side mounted accelerometer, the shift is not as distinct. The most dominant frequency remains at 19.38 Hz. The shift of frequencies does also occur in test labeled 2/II, 5/V, 6/VI and 7/VII.

In the case of test 3/III and 4/IV, the dominant frequencies remain at the frequencies of the ambient vibration. Comparing the motion of test number 3 with test number III, one can see how the frequency of motion affirms what can be considered the natural frequency of the system

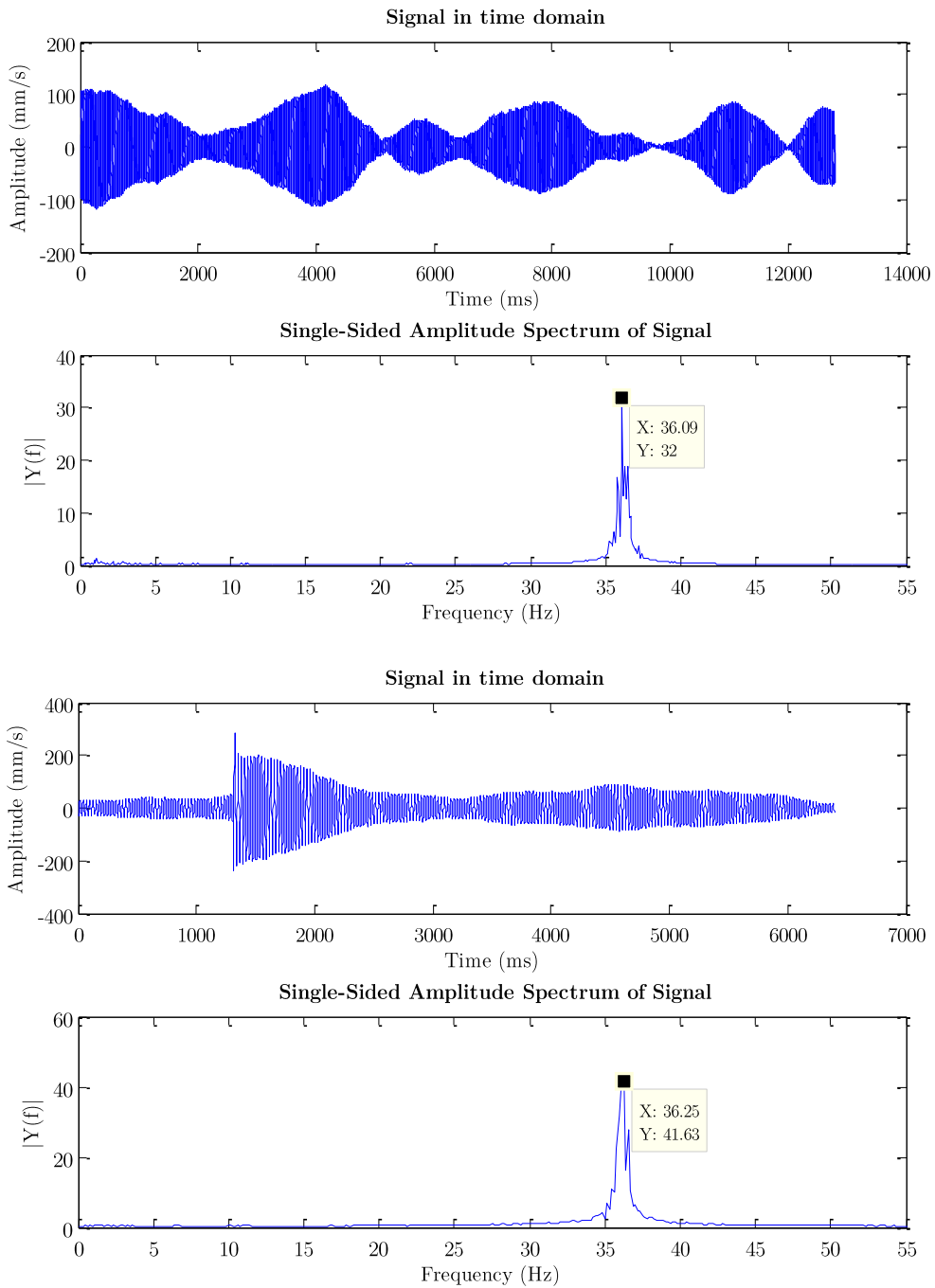


Figure 4-17 Ambient vs. forced vibration PV-25-8287-ES20A, A24, E-W



### 4.3 Results of analysis

For the analysis of the output data, effort has been put into making the analyzing procedure as universal as possible. As the size of the datasets varies for the different measurements, the scripts are written so that the output will suit the available data at current date. The process can also take into account data in the case of future usage.

For calculating the damping of the individual service pipe, the logarithmic decrement has been calculated. The LDM has then been used to calculate the discrete damping ratio throughout the measurement of the vibration (ref. section 8.2). This gives a series of discrete values for the damping ratio. To find the average value for the damping coefficient, the five lowest peaks within the specified time range are used. Based on this average, one gets an expected value for the dampening of the given service pipe.

Table 4-4 Calculated damping ratio

| <i>Test no.</i> | <i>Max value</i> | <i>Min value</i> | <i>Avg. value</i> | <i>Time range [ms]</i> | <i>Direction</i> |
|-----------------|------------------|------------------|-------------------|------------------------|------------------|
| <b>I</b>        | 0.6894           | 0.08818          | 0.418336          | 1302 - 2062            | Top              |
|                 | 0.9315           | 0.08371          | 0.538542          | 552.3 - 961.7          | Side             |
| <b>II</b>       | 0.7565           | 0.10090          | 0.476000          | 563.3 - 2192           | Top              |
|                 | 0.7995           | 0.18190          | 0.494220          | 443.8 - 1360           | Side             |
| <b>III</b>      | 0.1340           | 0.00482          | 0.054176          | 1326 - 2876            | E-W              |
|                 | 0.7883           | 0.11160          | 0.306920          | 914.8 - 1789           | N-S              |
| <b>IV</b>       | 0.4507           | 0.06722          | 0.172748          | 1348 - 2048            | Side             |
|                 | 0.2783           | 0.01077          | 0.144402          | 1500 - 2372            | Top              |
| <b>V</b>        | 0.5162           | 0.03392          | 0.242612          | 1146 - 1820            | E-W              |
|                 | 0.2165           | 0.01221          | 0.105434          | 1486 - 2246            | N-S              |
| <b>VI</b>       | 0.0515           | 0.00265          | 0.026363          | 1169 - 6381            | E-W              |
|                 | 0.1958           | 0.00956          | 0.095014          | 875.0 - 5768           | N-S              |
| <b>VII</b>      | 0.0588           | 0.00776          | 0.027511          | 1206 - 4510            | E-W              |
|                 | 0.2035           | 0.09411          | 0.155163          | 906.3 - 3997           | N-S              |

Based on the tabulation of the results, one can see that the damping ratio varies. In the case of the service pipes connected to turboexpander 1 and 2, the

average dampening ratio is calculated to be considerable higher compared to the other results.

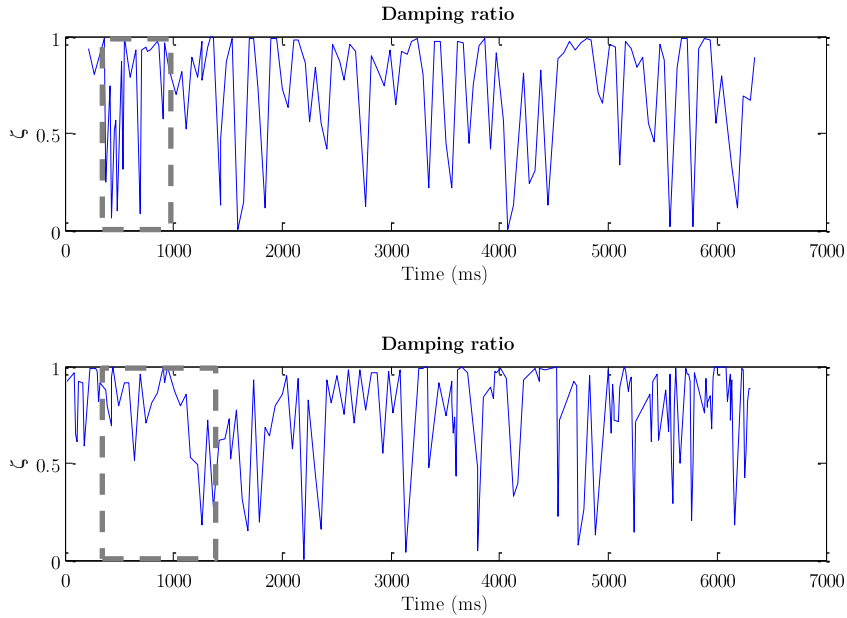
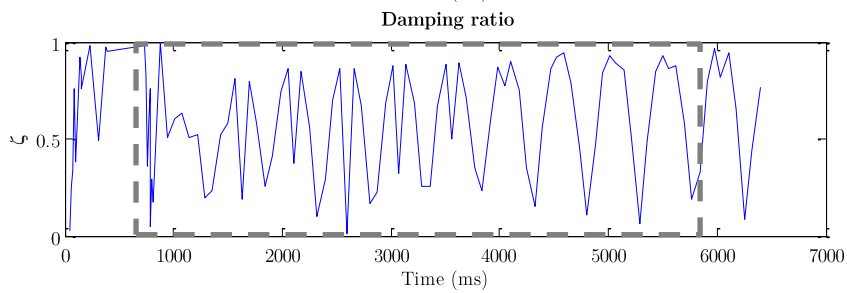


Figure 4-18 Damping ratio of I & II. Range indicated (Side vs. Side)

The two service pipes in area A11 on the other hand experiences the lowest damping. This indicates, as established in the prior sections, that the service pipe connected to the new P12 inlet line are at higher risk of experiencing failure due to fatigue.



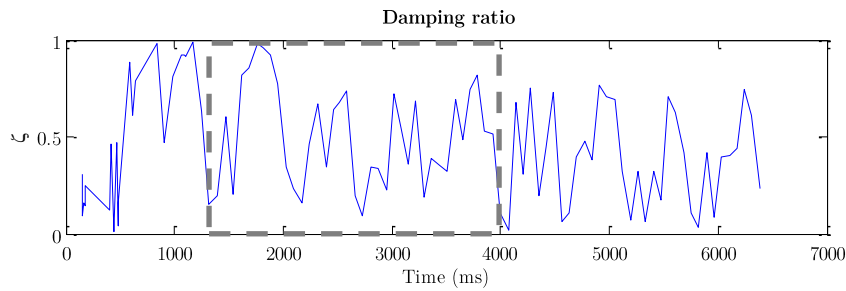


Figure 4-19 Damping ratio of VI & VII. Range indicated (N-S vs. N-S)

Subject III does also exhibit low dampening. Even with the improved geometry of the fitting, both loads and frequencies indicate that failure may occur. One would therefore recommend additional actions to be performed to reduce the risk of failure. One of such actions could be to add a direct support to the top of the flange. Support should always be added in the direction with the lowest damping (Lalanne 2009). As dampening is lowest in the E-W direction, the support should be aimed in this direction. This would reduce the amplitude of vibration and thereby lowering the risk of failure.

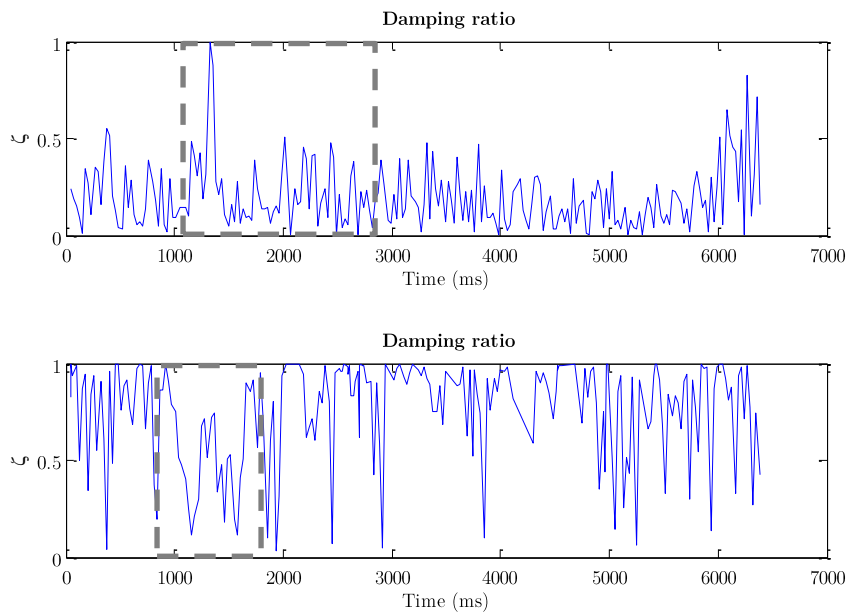


Figure 4-20 Damping ratio of III. Range indicated (E-W vs. N-S)

From the visualization of the results, one can see that the damping ratio fluctuates. This has to do with the calculation of the logarithmic decrement. The MatLab script calculates the logarithmic decrement for all identified peaks

throughout the available data. Focus should therefore be on only the values within the manually set time range. Even with the fluctuating values for the damping ratio, the overall understanding of the interpretation of the results is that the dampening can be considered low. This is especially the case for the test III, VI and VII.

The theory section of the thesis uncovered how the amplitude ratio varies with the damping ratio (ref. Figure 2-12 Variation of  $X$  and  $\phi$  with the frequency ratio  $r$  (Rao 2010)). In the case of the two turboexpanders, the average calculated damping ratio is within the range of 0.4 – 0.55. Within this range, the amplitude ratio is expected to peak at 1.35. This means that the expected amplitude of the service pipe in the case of resonance is only 1.35 time higher than the base excitation outside of the resonance range. As long as these base excitations are similar to the ones measured on site, resonance of these pipes will not dramatically alter the life expectancy of the pipe.

Looking at the instruments connected to the P12 inlet pipeline, the situation is grimmer. With a measured average damping ratio of 0.026363, there are virtually no damping of the vibration of the pipe. The charts available for the amplitude ratio do not cover situations of such low damping. If the instrument were to experience frequencies close to resonance, it would only be a question of time before the failure is a fact.

A set accept criteria of the damping of service pipes can from this be extracted. As the base loads of the individual pipes can be considered low (with the exception of test III in E-W direction), a damping ratio of 0.3 should be considered acceptable. The amplitude ratio at a damping ratio of 0.3 result in a multiplication factor of 1.8 (ref. Figure 2-12 Variation of  $X$  and  $\phi$  with the frequency ratio  $r$  (Rao 2010)). Using the results from the ambient vibration (ref. Table 4-2 Results of vibration testing at ambient conditions), the peak value at identical conditions under resonance can be calculated.

Table 4-5 Estimated results of vibration at resonance

| <i>Test no.</i> | <i>Peak value [mm/s]</i> | <i>Direction</i> |
|-----------------|--------------------------|------------------|
| <b>1</b>        | -7.281                   | Top              |
|                 | 18.99                    | Side             |
| <b>2</b>        | 29.34                    | Top              |
|                 | 18.072                   | Side             |
| <b>3</b>        | 210.96                   | E-W              |
|                 | -23.904                  | N-S              |
| <b>4</b>        | 31.932                   | Side             |
|                 | -21.15                   | Top              |
| <b>5</b>        | 49.842                   | E-W              |
|                 | 48.312                   | N-S              |
| <b>6</b>        | 74.862                   | E-W              |
|                 | 9.576                    | N-S              |
| <b>7</b>        | -14.56                   | E-W              |
|                 | 13.8546                  | N-S              |

## 5 Discussion

Over the course of the working with the master's thesis, several changes from the original project plan was applied. The project would initially be independent of the operator at the different installation. As the project progressed, focus was shifted towards the largest operator on the NCS, Statoil. The reason for this was because of the data accessible to the contractor over the spring of 2012. Aker Solutions, being in a framework agreement with the operator, had access to the plant specific databases known as STID. It was also easier gaining access to the process plant Kollsnes. Still, as the methodology mainly bases itself on regulations valid for all contractors on the NCS the results can be ported for the usage towards other operators in the future.

For the creation of the methodology and the results of the testing, some changes were performed. At the time of the vibration testing and analyzing, the methodology for the screening of service pipes were not completed. This lead to the lack of the calculation of the PoF and CoF for the pipes that were tested in field. Still, one managed to identify service pipes of interest to the contractor for testing.

When analyzing the measured vibration, effort was put on improving the quality of the available data. As the discreet values of the damping ratio fluctuate throughout the measured range, several high- and low pass filters were attempted implemented. Ideally, the filters would help eliminate non-relevant values for the dampening. The results from the individual filter were shown not to improve the quality of the output to an acceptable level.

One also initially measured the vibration at ambient condition. The reason for this was to be able to eliminate the background noise in the case of forced vibration. This was not successfully implemented. The vibration in the tests with forced vibration took a different mode of motion compared to the vibration at ambient conditions. Filtering the signal with the ambient vibration ended in skewed results, impairing the data available for analysis.

The usage of the different filter was thus discarded for a manual approach. For the calculations to be considered conservative, only the five lowest values of the damping coefficient of the established time range were used.

The results from the vibration measurement showed that the damping of the pipes inspected were, for the most part, not sufficient. Based on the determined damping ratio of 0.3, only 5 out of the tested 14 pipes experienced sufficient damping. With an average dampening ratio of 0.0263, test number VI exhibit extremely poor damping. As frequencies of vibration for that test also indicate that the forced induced motion is close to resonance frequency, immediate actions should be implemented. If this advice is not taken, one risks a complete failure of the service pipe due to the increased load from motion at resonance.

The thesis did not take into consideration the effect of insulation on damping. Of the service pipes tested, none of them were close to insulated piping. If further effort should be put on eliminating the impact of fatigue on service pipe, this could be a problem to be addressed.

## 6 Conclusion

With higher focus on maintaining operating activity on the NCS, operators strive to reduce the volume of service pipes failing due to fatigue. Knowledge regarding the technical condition and degradation mechanism affecting equipment onsite will help reducing unplanned production shutdowns. The establishment of a screening methodology for service pipes helps eliminating time consuming and laborious manual inspection on site. It also assists in prioritizing inspection of the various service pipes.

The report has established the principle of fatigue of service pipes situated on the NCS. The dampening properties of the pipes have been derived. From this, a screening methodology has been developed. The methodology can be used for the evaluation of service pipes in regards to risk of failure. The individual steps of the methodology have been explained.

The methodology where used for the testing of the vibration of service pipes on the onshore process plant Kollsnes. The testing was performed in accordance with established methods. From the results of the vibration analysis, the damping of the individual pipes was calculated. Based on the analysis of these results, an acceptance criterion of a damping ratio of 0.3 was identified.

Over the course of the testing in field, service pipes exposed to fatigue was identified. Remedial actions have been suggested and will be forwarded to the responsible body.



## 7 References

- Aker Solutions ASA, 2012a. History - Aker Solutions. Available at:  
<http://www.akersolutions.com/en/Utility-menu/About-us1/History/> [Accessed February 5, 2012].
- Aker Solutions ASA, 2012b. Projects - Aker Solutions. Available at:  
<http://info.enet/projects/pages/default.aspx> [Accessed May 8, 2012].
- American Society of Mechanical Engineers, 2010. ANSI/ASME B31.3-2010 Process Piping.
- Anderson, T.L., 2005. *Fracture Mechanics: Fundamentals and Applications* 3rd ed., Boca Raton: CRC Press Taylor & Francis Group.
- Asheim, H., 2011. Produksjonsbrønner. Available at:  
<http://www.ipt.ntnu.no/~asheim/prodbr.html> [Accessed March 31, 2012].
- Beardmore, R., 2010. Fatigue Life. Available at:  
[http://www.roymech.co.uk/Useful\\_Tables/Fatigue/Fatigue\\_life.html](http://www.roymech.co.uk/Useful_Tables/Fatigue/Fatigue_life.html) [Accessed May 13, 2012].
- Billah, K.Y., 1991. Resonance, Tacoma Narrows bridge failure, and undergraduate physics textbooks. *American Journal of Physics*, 59(2), p.118.
- Blevins, R.D., 1990. *Flow-induced vibration* 2nd ed., Malabar: Krieger Publishing Company. Available at:  
[http://www.osti.gov/energycitations/product.biblio.jsp?osti\\_id=6168070](http://www.osti.gov/energycitations/product.biblio.jsp?osti_id=6168070) [Accessed February 6, 2012].
- Bonney Forge Corporation, 2012a. Sockolet - Bonney Forge®. Available at:  
<http://www.bonneyforge.com/products.php?pg=branch&subpg=sockolet> [Accessed April 26, 2012].
- Bonney Forge Corporation, 2012b. Thredolet - Bonney Forge®. Available at:  
<http://www.bonneyforge.com/products.php?pg=branch&subpg=thredolet> [Accessed April 26, 2012].
- Bonney Forge Corporation, 2012c. Weldolet - Bonney Forge®. Available at:  
<http://www.bonneyforge.com/products.php?pg=branch&subpg=weldolet> [Accessed April 26, 2012].

- British Standards Institution, 1993. *BS 3811:1993 Glossary of terms used in terotechnology*,
- Brustad, S. et al., 2005. OTC 17355 Hydrate Prevention using MEG instead of MeOH: Impact of experience from major Norwegian developments on technology selection for injection and recovery of MEG. In *Offshore Technology Conference*. Houston.
- Callister, W.D., 2006. *Materials Science and Engineering: An Introduction*, Wiley. Available at: <http://www.amazon.com/Materials-Science-Engineering-An-Introduction/dp/0471736961> [Accessed March 31, 2012].
- Central Intelligence Agency, 2012. CIA - The World Factbook. Available at: <https://www.cia.gov/library/publications/the-world-factbook/geos/us.html> [Accessed June 11, 2012].
- Duga, J. et al., 1983. *The Economic Effects of Fracture in the United States*, Washington, DC.; U.S. Department of Commerce.
- Dukkipati, R.V., 2007. *Solving Vibration Analysis Problems Using MATLAB*, New Delhi: New Age International Publishers.
- Emerson Process Management, 2010. *AMS Suite: Machinery Health Manager*,
- Emerson Process Management, 2011. *CSI 2130 Machinery Health Analyzer*,
- Eng-Tips, 2003. Valve engineering - Pressure Valve Chattering. Available at: <http://www.eng-tips.com/viewthread.cfm?qid=65161> [Accessed April 26, 2012].
- Gassco, 2012. Gassco | Kollsnes. Available at: <http://www.gassco.no/wps/wcm/connect/gassco-no/gassco/home/var-virkosomhet/prosessanlegg/kollsnes> [Accessed March 31, 2012].
- International Organization for Standardization, 2006. ISO 14224:2006 Petroleum, petrochemical and natural gas industries - Collection and exchange of reliability and maintenance data for equipment.
- International Organization for Standardization, 2002. NS-EN ISO 17776:2002 Petroleum and natural gas industries - Offshore production installations - Guidelines on tools and techniques for hazard identification and risk assessment.
- Iowa State University, 2009. Palmgren-Miner Rule. , pp.1-3.

- Irwin, G.R., 1961. Plastic Zone Near a Crack and Fracture Toughness. In *Sagamore Research Conference Proceeding*". Syracuse, NY, pp. 63-78.
- Lalanne, C., 2009. *Mechanical Vibration and Shock: Fatigue Damage: 4*, Wiley-Blackwell. Available at: <http://www.amazon.co.uk/Mechanical-Vibration-Shock-Fatigue-Damage/dp/1848211252> [Accessed February 7, 2012].
- Lien, T., 2010. Introduction to offshore technology.
- Markeset, T., 2012. MOM 350 – Condition monitoring and management. , p.523.
- Mathieson, P., 2012. AIM Competence Centres Strategy.
- Mathieson, P., 2007. Small-bore piping fatigue flow for BP Angola FPSO.
- Microsoft Corporation, 2012. A beginner's guide to Visio 2010. Available at: <http://office.microsoft.com/en-au/visio-help/a-beginner-s-guide-to-visio-2010-HA010357067.aspx> [Accessed June 6, 2012].
- NORSOK, 2008. M-601 Welding and inspection of piping. , (April).
- NORSOK, 2007. N-003 Actions and action effects. , (September).
- NORSOK, 2011. Z-008 Risk based maintenance and consequence classification. , (June).
- Nave, R., 2011. First law of thermodynamics. *Department of Physics and Astronomy Georgia State University*. Available at: <http://hyperphysics.phy-astr.gsu.edu/hbase/thermo/firlaw.html> [Accessed May 13, 2012].
- Det Norske Veritas, 2012. Eksplosjonsfarlige omgivelser – ATEX / IECEx. Available at: <http://www.dnvba.com/no/sertifisering/produktsertifisering/Eksplosjonsfarlige-omgivelser/Pages/default.aspx> [Accessed April 22, 2012].
- Det Norske Veritas, 2010a. Fatigue Design of Offshore Steel Structures. *Recommended Practice DNV-RPC203*, (April). Available at: <http://www.advancepipeliner.com/Resources/Pipeline/Fatigue/RP-C203.pdf> [Accessed March 12, 2012].
- Det Norske Veritas, 2010b. *RECOMMENDED PRACTICE DNV-RP-G101: RISK BASED INSPECTION OF OFFSHORE TOPSIDES STATIC MECHANICAL EQUIPMENT*,

- Olsnes, T.-O., 2001. *Inspeksjon av termolommer A-kompressor Troll Gass Kollsnes, Kårstø.*
- Rao, S.S., 2010. *Mechanical Vibrations* 5th ed., Miami: Prentice Hall.
- Reliability Maintenance Solutions Ltd, Vibration Analyser CSI 2130. Available at: [http://www.rms-reliability.com/index.php?option=com\\_content&view=article&id=141:vibration-analyser-csi-2130&catid=66:vibration-analyser&Itemid=200](http://www.rms-reliability.com/index.php?option=com_content&view=article&id=141:vibration-analyser-csi-2130&catid=66:vibration-analyser&Itemid=200) [Accessed April 12, 2012].
- Rice, J.R., 1968. A Path Independent Integral and the Approximate Analysis of Strain Concentration by Notches and Cracks. *Journal of Applied Mechanics*, 35, pp.379-386.
- Rogsnvåg, S. et al., 2005. Common model for Work Permits (WP). , pp.1-44. Available at: [http://www.trainingportal.no/coursecontent/course/olf-trainingportal/courses/atsja\\_1126161031750/dokumenter/Common model for WP.pdf](http://www.trainingportal.no/coursecontent/course/olf-trainingportal/courses/atsja_1126161031750/dokumenter/Common%20model%20for%20WP.pdf).
- Schlumberger, 2012. slug flow: Schlumberger Oilfield Glossary. Available at: [http://www.glossary.oilfield.slb.com/Display.cfm?Term=slug flow](http://www.glossary.oilfield.slb.com/Display.cfm?Term=slug%20flow) [Accessed April 26, 2012].
- Silva, C.W.D., 2007. *Vibration: Fundamentals and Practice* 2nd ed., CRC/Taylor & Francis. Available at: <http://books.google.no/books?id=AKjnOnhGDXYC>.
- Statoil, 2010a. *AS-2672-J-JA-010-01 GENERAL ARRANGEMENT 603 FLOW ORIFICE 10" 900#*,
- Statoil, 2011a. *C030-PH-A00--LP-093-01 OVERALL ONSITE PLOT PLAN*,
- Statoil, 2011b. *C030-PH-A00--PE-101-03 SLUG CATCHER 20-VL302A*.
- Statoil, 2009a. *C030-PH-A00--PT-002-01 GENERAL LEGEND GENERAL NOTES*.
- Statoil, 2012a. *C030-PH-A00--PT-003-01 GENERAL LEGEND NUMBERING CODES (KOP)*.
- Statoil, 2004. *C030-PH-A00--PT-004-01 GENERAL LEGEND EQUIPMENT SYMBOLS*.
- Statoil, 2012b. *C030-PH-A00--PT-005-01 GENERAL LEGEND INSTRUMENT SYMBOLS*.

- Statoil, 2012c. C030-PH-A00--PT-006-01 GENERAL LEGEND INSTRUMENT TYPICALS (KOP).
- Statoil, 2012d. C030-PH-A00--PT-006-02 GENERAL LEGEND INSTRUMENT TYPICALS (KOP).
- Statoil, 2012e. C030-PH-A00--PT-006-03 GENERAL LEGEND INSTRUMENT TYPICALS (KOP).
- Statoil, 2012f. C030-PH-A00--PT-006-04 GENERAL LEGEND INSTRUMENT TYPICALS (KOP).
- Statoil, 2012g. C030-PH-A00--PT-006-05 GENERAL LEGEND INSTRUMENT TYPICALS (KOP).
- Statoil, 2012h. C030-PH-A00--PT-006-06 GENERAL LEGEND INSTRUMENT TYPICALS (KOP).
- Statoil, 2009b. C030-PH-A00--PT-007-01 GENERAL LEGEND PIPING, FIRE PROTECTION AND HVAC SYMBOLS.
- Statoil, 2008. C030-PH-A00--PT-008-01 PIPING DETAILS MANUAL SAMPLE CONNECTIONS.
- Statoil, 2011c. C030-PH-A00-PE-101-02 SEPARATION AND STABILIZATION PIG RECEIVER HEADER SYSTEM 20.
- Statoil, 2010b. *Kollsnes Engineering Numbering System ( Kollsnes ENS )*,
- Statoil, 2007. Kollsnes gas processing plant. Available at:  
<http://www.statoil.com/en/OurOperations/TerminalsRefining/ProcessComplexKollsnes/Pages/default.aspx> [Accessed May 18, 2012].
- Statoil, 2012i. TR2000 PIPING AND VALVE MATERIAL SPECIFICATION.  
 Available at: <http://tr2000.statoil.com/TR2000/index.jsp> [Accessed March 31, 2012].
- Sukaih, N., 2002. A practical, systematic and structured approach to piping vibration assessment. *International Journal of Pressure Vessels and Piping*, 79(8-10), pp.597-609. Available at:  
<http://linkinghub.elsevier.com/retrieve/pii/S0308016102000856>.
- Wells, A.A., 1961. Unstable Crack Propagation in Metals: Cleavage and Fast Fracture. In *Proceedings of the Crack Propagation Symposium*.

- Wieghardt, K., 1906. *Über einen Grenzübergang der Elastizitätslehre und seine Anwendung auf die Staik hochgradig statisch unbestimmter Fachwerke*, Berlin: Leonhard Simion. Available at: [http://www.worldcat.org/title/uber-einen-grenzubergang-der-elastizitatslehre-und-seine-anwendung-auf-die-staik-hochgradig-statisch-unbestimmter-fachwerke/oclc/258682328&referer=brief\\_results](http://www.worldcat.org/title/uber-einen-grenzubergang-der-elastizitatslehre-und-seine-anwendung-auf-die-staik-hochgradig-statisch-unbestimmter-fachwerke/oclc/258682328&referer=brief_results) [Accessed March 10, 2012].
- Yarema, S.Y., 1996. On the contribution of G. R. Irwin to fracture mechanics. *Materials Science*, 31(5), pp.617-623. Available at: <http://www.springerlink.com/content/n588040426n026t6/> [Accessed March 10, 2012].
- Økland, J., 2010. Kollsnes bygger for fremtiden - Offshore.no. *Offshore.no*. Available at: [http://www.offshore.no/sak/Kollsnes\\_bygger\\_for\\_fremtiden](http://www.offshore.no/sak/Kollsnes_bygger_for_fremtiden) [Accessed April 1, 2012].

## 8 Attachments

### 8.1 Deduction of mechanisms for fracture mechanics

What Griffith did was to make the following assumption: “A crack propagates if the potential strain energy of the body  $\delta W$  released in this process is sufficient to compensate the energy required for the formation of new surfaces.” (Yarema 1996)

$$\delta W = \gamma \cdot \delta A \quad 8.1$$

The value  $\gamma$  is the specific surface energy and the multiple  $\delta A$  is an increment in the area of the surfaces of the crack. This gives that the rate of release of strain energy relative to the increment in the area of the crack must be equal to the specific surface energy illustrated here

$$\frac{\delta W}{\delta A} = \gamma \quad 8.2$$

From this, Griffith deduced the formula for the determination of a breaking load,  $p_c$  for an elastic plate with the crack length of  $2 \cdot a$ . This crack is subjected to uniformly distributed form  $p$  perpendicular to the crack

$$p_c = \sqrt{\frac{2 \cdot E_l \gamma}{\pi \cdot A}} \quad 8.3$$

The values of  $E_l$  varies based on whether the plate experiences plane stress state or plane deformation. For plane stressed state;  $E_l = E$  and for plane deformation;  $E_l = \frac{E}{(1-\mu^2)}$ .  $E$  is the Young's modulus of the material and  $\mu$  the Poisson ratio. As stated previously, this was only valid for brittle materials.

Based on the work of Griffith, the scientist G. R. Irwin managed to overcome these difficulties in porting the models to non-brittle materials. Irwin proposed to add the specific surface energy  $\gamma$  to the work of plastic deformation  $\gamma_p$  in just a small zone in front of the crack tip. This newly formed surface had a sum of specific surface energy based on the sums of these energies;

$$\gamma_{eff} = \gamma + \gamma_p \quad 8.4$$

This effective surface energy,  $\gamma_{eff}$ , is no longer a characteristic of the material, but a highly informative parameter for evaluating the crack (Anderson 2005).

In his work “Analysis of stresses and strains near the end of a crack traversing a plate”, Irwin presented that the component of the stress tensor in a small vicinity of the crack tip could be explained by the formula

$$\sigma_{ij} = \sqrt{G \cdot E_t} \cdot \frac{1}{\sqrt{2 \cdot \pi \cdot r}} \cdot f_{ij}(\theta) \quad 8.5$$

Where  $f_{ij}(\theta)$  is the function of the polar angle and  $r$  the distance of a given point from the crack tip. From this, Irwin introduced the stress intensity factor,  $K = \sqrt{G \cdot E_t}$ , independently of the work done by K. Wieghardt 50 years prior to Irwin's discovery (Wieghardt 1906). This led to the formula for the Griffith energy approach

$$G_c = \frac{K_c^2}{E_t} = 2 \cdot \gamma \quad 8.6$$

This formula simplified the work necessary to analyze the fracture processes in linearly elastic bodies as it removed the laborious numerical calculations of strain energy by evaluation of the singular part of the stresses with an already known distribution law. This approach also makes it possible to describe fracture as a process with stage wise fracturing (Yarema 1996).

Building on the works of Irwin and Griffith, scientists such as Paris, Dugdale, Barenblatt and Wells (Anderson 2005) built the foundation of fracture mechanics. As the new discipline got foothold in the early 1960s, several papers were developed for the newly developed linear elastic fracture mechanics (LEFM). As LEFM in principle ceases to be valid when plastic deformation precedes failure, the primary work done by the scientist was to correct the methods for yielding at the crack tip. The Irwin plastic zone correction (Irwin 1961) was a relative simple extension of LEFM which made it possible to do calculations when significant plastic deformation did happen.



Up until 1980 several other methods were developed as well. The most important were the crack-tip-opening displacement (CTOD) developed (Wells 1961) and the J-integral (Rice 1968). Where CTOD was a parameter for the movement of the plastic deformation with the crack face, the J-integral was a parameter to characterize nonlinear material behavior ahead of a crack. The J-integral showed that the nonlinear energy release rate could be expressed as a line integral. By further improving the understanding of the J-integral, Rice and Rosengren showed that the J-integral also could be used as a nonlinear stress-intensity factor in addition to the use as an energy release rate (Anderson 2005). This did in turn lead to a standard procedure for testing J-integrals in metals.

Between 1980 and today, more sophisticated models for material behavior has been developed. The focus is now on time-dependent nonlinear material behavior. An example of this is viscoplasticity and viscoelasticity. The quantum leaps in computational power over the last two decades has also helped with analyzing complex three dimensional finite element analyses of crack-containing structures.

## 8.2 Deduction of mechanisms for damping of vibration

Dealing with time-response methods, the Logarithmic Decrement Method is the most applied method for measuring damping. In this method, an initial excitation is applied to a single-degree-of-freedom oscillatory system with viscous damping. As Figure 2-13 Impulse response of a simple oscillator (Silva 2007) shows, the form of the response as a time decay, which is expressed by the formula 8.7

$$y(t) = y_0 \cdot \exp(-\zeta \cdot \omega_n \cdot t) \cdot \sin(\omega_d \cdot t) \quad 8.7$$

If the response is known, then it is possible to determine the logarithmic decrement  $\delta$  through the formula

$$\delta = \frac{1}{r} \cdot \ln\left(\frac{X_i}{X_{i+r}}\right) = \frac{2 \cdot \pi \cdot \zeta}{\sqrt{1 - \zeta^2}} \quad 8.8$$

Then the damping ratio  $\zeta$  is easily calculated with the formula

$$\zeta = \frac{\delta}{\sqrt{4 \cdot \pi^2 + \delta^2}} \quad 8.9$$

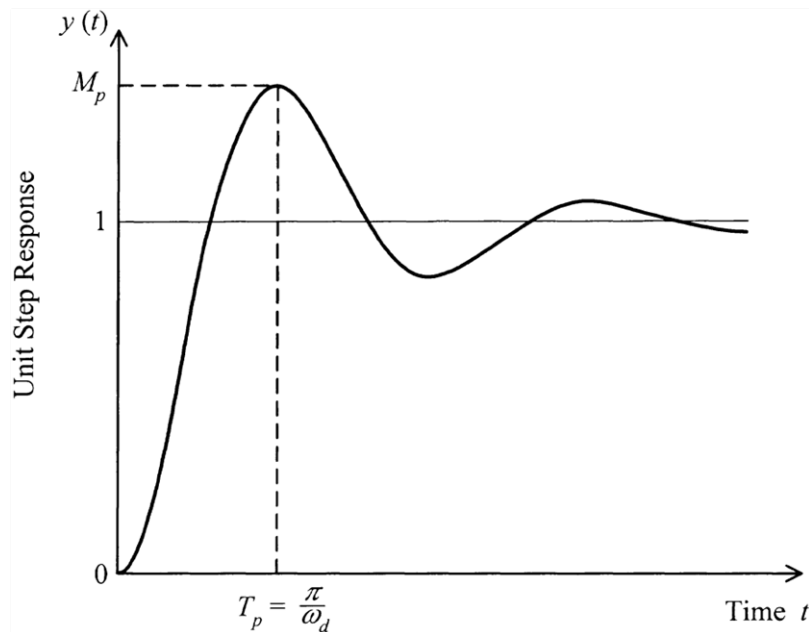


Figure 8-1 Characteristic step response of a simple oscillator (Silva 2007)

As regards the Step-Response Method, a unit step excitation is applied to the single-degree-of-freedom oscillatory system and its time response looks like a typical step-response curve given by the equation

$$y(t) = 1 - \frac{a}{\sqrt{1 - \zeta^2}} \cdot \exp(-\zeta \cdot \omega_n \cdot t) \cdot \sin(\omega_d \cdot t + \varphi) \quad 8.10$$

Damping ration  $\zeta$  can be determined through these three parameters: peak time, ( $T_p$ ), peak value ( $M_p$ ) or percentage overshoot ( $PO$ ). These three parameters are easily obtained from the step response curve. Formulas 8.11, 8.12 and 8.13 show the relation between these three parameters and damping ratio

$$\zeta = \sqrt{1 - \left( \frac{\pi}{T_p \cdot \omega_n} \right)^2} \quad 8.11$$

$$\zeta = \frac{1}{\sqrt{1 + \frac{a}{\left[ \frac{\ln(M_p - 1)}{\pi} \right]^2}}} \quad 8.12$$

$$\zeta = \frac{1}{\sqrt{1 + \frac{a}{\left[ \frac{\ln\left(\frac{PO}{100}\right)}{\pi} \right]^2}}} \quad 8.13$$

The hysteretic Loop Method calculated the energy loss per cycle of oscillation due to steady state harmonic loading. Damping capacity ( $\Delta U$ ) is given by the area of the displacement-force hysteric loop. Then, the loss factor ( $\eta$ ) and the damping ration ( $\zeta$ ) can easily be determined through the formulas

$$\eta = \frac{\Delta U}{2 \cdot \pi \cdot U_{\max}} \quad 8.14$$

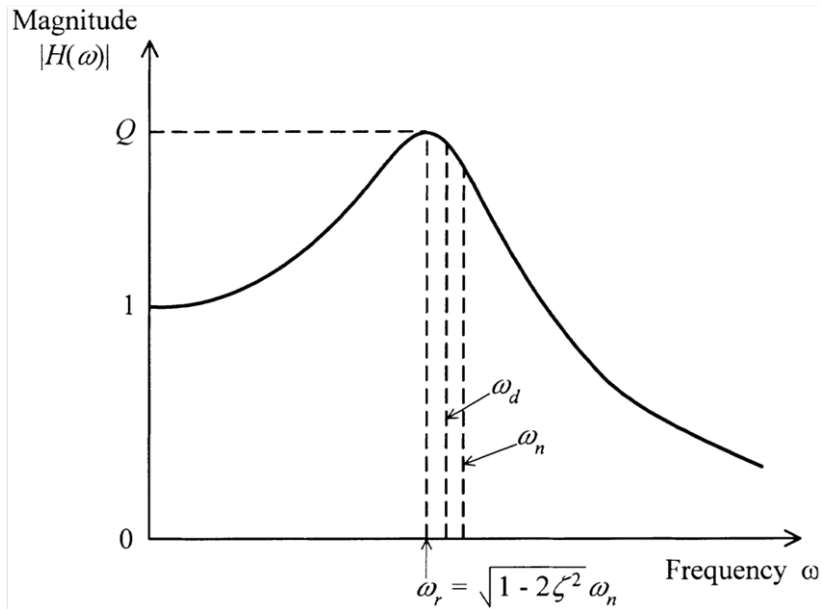


Figure 8-2 Magnification factor method of damping measurement applied to a single-degree-of-freedom system (Silva 2007)

The Magnification-Factor Method is a frequency-response method. The damping ratio ( $\zeta$ ) can be determined on the condition that the magnitude curve of the frequency-response function is known. From this curve it is possible to obtain the amplification factor ( $Q_A$ ), which is the magnitude of the frequency-response function at resonant frequency. Then, damping ratio ( $\zeta$ ) can be determined using expression

$$Q_A = \frac{1}{2 \cdot \zeta \cdot \sqrt{1 - \zeta^2}} \quad 8.16$$

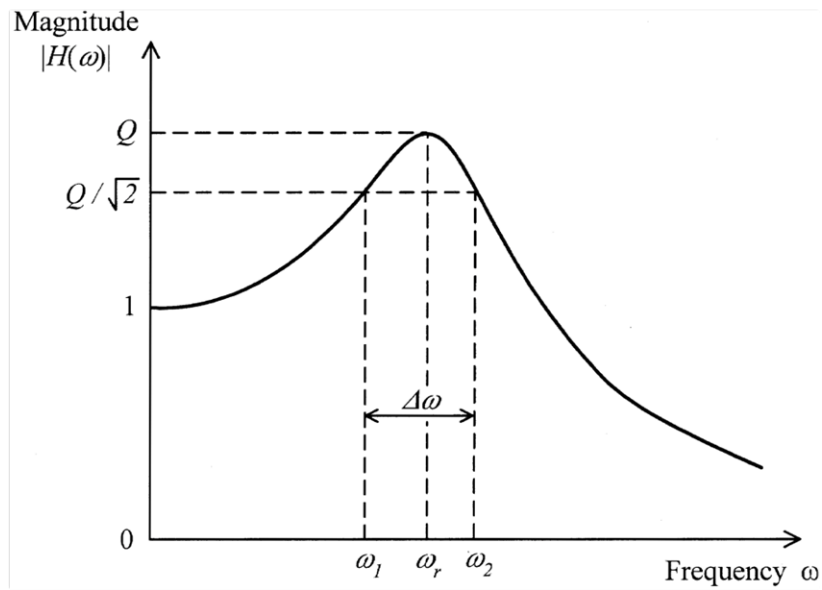


Figure 8-3 Bandwidth method of damping measurement in a single-degree-of-freedom system (Silva 2007)

The last method to estimate damping from frequency domain is the bandwidth method. This method is also based on the magnitude curve of the frequency response function. Bandwidth ( $\Delta\omega$ ) is defined as the width of the frequency-response function when the magnitude is  $\frac{1}{\sqrt{2}}$  time peak value. Then, damping ratio can be determined from bandwidth using the expression

$$\zeta = \frac{1}{2} \cdot \frac{\Delta\omega}{\omega_r} \quad 8.17$$

### 8.3 Plot Plan

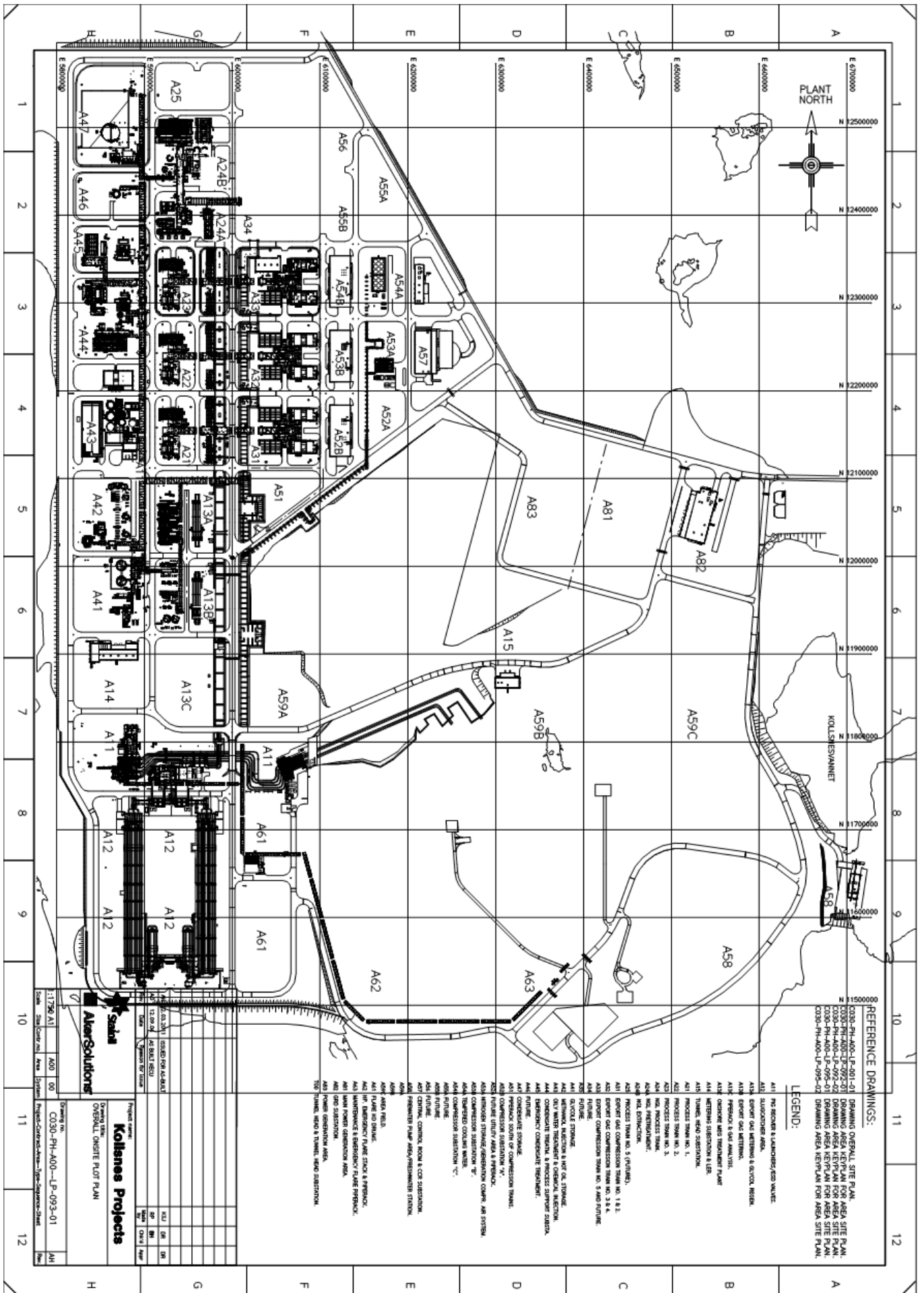


Figure 8-4 Plot Plan Kollsnes (Statoil 2011a)

#### 8.4 Minutes of Meeting Statoil

|                      |   |                      |                |
|----------------------|---|----------------------|----------------|
| <b>Summoner:</b>     | Ekaterina Ponomareva, Statoil   | <b>Location:</b>     | Statoil, NB251 |
| <b>Secretary:</b>    | André Augestad  | <b>Date:</b>         | 22.03.2012     |
| <b>Participants:</b> | André Augestad, AS<br>Nils Petter Dalstø, AS<br>Jonny Hammersland, Statoil<br>Ekaterina Ponomareva, Statoil | <b>Distribution:</b> |                |

| Subject | Description  |
|---------|--|
| 01      | <p><i>Statoil's experiences with vibration and fatigue</i></p> <ul style="list-style-type: none"> <li>- Wave induced vibration</li> <li>- Production induced vibration <ul style="list-style-type: none"> <li>o Oil</li> <li>o Gas</li> <li>o Mechanical equipment</li> </ul> </li> <li>- Vibration of unknown origin <ul style="list-style-type: none"> <li>o 20 and 23 system on Oseberg most exposed <ul style="list-style-type: none"> <li>▪ Comment AS: Possibility for acoustically induced</li> <li>▪ Dependent on pipe length</li> </ul> </li> <li>o Lock-in properties of vibration expected <ul style="list-style-type: none"> <li>▪ Vibration frequencies jump to resonant frequencies.</li> <li>▪ Vibrations can be reduced/eliminated by halting production temporarily. When taken up to full capacity, vibrations are no longer detectable.</li> </ul> </li> </ul> </li> <li>- Examples of vibrations of unknown origin <ul style="list-style-type: none"> <li>o Åsgård: Turret vibrates when dynamic position is combined with specific ship orientations</li> <li>o Kollsnes Dead leg on pig launcher <ul style="list-style-type: none"> <li>▪ Double block and bleed valve</li> <li>▪ Opening of valve increases loop length by 3 meters. Flow in anti-phase; problem eliminated</li> </ul> </li> <li>o Oseberg Delta: Wave induced vibration problem <ul style="list-style-type: none"> <li>▪ 100 dB measured close to the conductors at storms</li> </ul> </li> <li>o Visund: Wave induced vibration problem <ul style="list-style-type: none"> <li>▪ Crack formations</li> </ul> </li> </ul> </li> <li>- Screening methodology</li> </ul> |
| 02      | <p><i>Fatigue in areas of gas processing onsite</i></p> <ul style="list-style-type: none"> <li>- Problems in areas of gas processing <ul style="list-style-type: none"> <li>o Damping of vibration: Recommend the establishment of an accept criteria for damping of vibrations</li> <li>o Screening methodology: Establishment of a screening methodology for the</li> </ul> </li> </ul>  |

|    |  |
|----|--|
|    | <ul style="list-style-type: none"> <li>mapping of areas exposed to fatigue prior to inspection.</li> <li>○ Differences in valve forks: The shattering of vibrations within the resonance frequencies by adding damping material</li> <li>○ Problems with reverberation in vibrating mechanical equipment</li> <li>○ Statoil: Necessary to identify service pipes vulnerable for fatigue <ul style="list-style-type: none"> <li>▪ Currently not offered by any contractors.</li> </ul> </li> </ul>  |
| 03 | <p><i>Inspection of spring support on plants operated by Statoil</i></p> <ul style="list-style-type: none"> <li>- Old stress reports: Can't alter conditions without invalidating stress ISO's</li> <li>- Degrading mechanisms: Elasticity of the springs are not constant over the life time of the spring</li> <li>- Study of accept criteria necessary</li> </ul>   |
| 04 | <p><i>Current procedures at AS in regards to inspection</i></p> <ul style="list-style-type: none"> <li>- Line tag exported from SAP <ul style="list-style-type: none"> <li>○ Add criticality to the individual lines</li> <li>○ Structural support necessary at long periodic amplitudes</li> </ul> </li> </ul>  |
| 05 | <p><i>Testing with strain gauges</i></p> <ul style="list-style-type: none"> <li>- Long life time at low strains</li> <li>- Long-run testing: Costly putting ex-classified equipment in-field for longer periods of time</li> <li>- Metering with accelerometer: Handles long-run testing in field well <ul style="list-style-type: none"> <li>○ Problem with accelerometer metering; measures relative acceleration</li> </ul> </li> </ul>   |
| 06 | <p><i>Fatigue Oseberg Field Centre</i></p> <ul style="list-style-type: none"> <li>- 24.01.2011 Gas leakage Oseberg A <ul style="list-style-type: none"> <li>○ Category: Emergency shutdown 2.0 (NAS): Full shutdown</li> <li>○ Rough weld resulted in crevice of heat affected zone</li> </ul> </li> <li>- Official cause: Unfortunate geometry, fatigue and vibrations <ul style="list-style-type: none"> <li>○ Over 6000 service pipes installed offshore</li> <li>○ A-standard introduced after incident</li> </ul> </li> <li>- Service pipe project Oseberg Field Centre <ul style="list-style-type: none"> <li>○ Revision stop 2007 and 2009: Inspected over 6000 service pipes</li> <li>○ Expectation: 59 service pipes replaced in 2011 <ul style="list-style-type: none"> <li>▪ Mainly system 13 and 20</li> </ul> </li> <li>○ Export of P&amp;ID's: Service pipes identified from existing P&amp;ID's</li> <li>○ Evaluation of repair <ul style="list-style-type: none"> <li>▪ Currently: Weldolet and welds</li> <li>▪ Future: Internal Thore-method: Cutting and grinding of fitting transition <ul style="list-style-type: none"> <li>• Increases area</li> <li>• Reduces risk for crevice corrosion</li> </ul> </li> </ul> </li> <li>○ Internal procedure prepared based on ASME B31.3</li> <li>○ Sockolet to replace Weldolet</li> </ul> </li> </ul> |

## 8.5 Microsoft Visual Basic macros

### 8.5.1 BareData\_\_\_()

Sub BareData\_\_()





```

Selection.End(xlDown).Select
Selection.End(xlDown).Select
Selection.End(xlDown).Select
Selection.End(xlDown).Select
Selection.End(xlDown).Select
Selection.End(xlDown).Select
Selection.End(xlDown).Select
Selection.End(xlUp).Select
Selection.End(xlUp).Select
ActiveCell.Offset(-6, 0).Range("A1").Select
Range(Selection, Selection.End(xlToRight)).Select
Range(Selection, Selection.End(xlToRight)).Select
Range(Selection, Selection.End(xlToRight)).Select
Range(Selection, Selection.End(xlDown)).Select
Range(Selection, Selection.End(xlDown)).Select
Range(Selection, Selection.End(xlDown)).Select
Range(Selection, Selection.End(xlDown)).Select
Selection.Cut
Sheets.Add After:=Sheets(Sheets.Count)
Sheets("Sheet1").Select
Sheets("Sheet1").Name = "KRITISK"
ActiveCell.Select
ActiveSheet.Paste
Sheets("KRITISK").Select
Sheets("KRITISK").Move Before:=Sheets(1)
ActiveCell.Select
Selection.End(xlDown).Select
Selection.End(xlDown).Select
Selection.End(xlDown).Select
Selection.End(xlDown).Select
Selection.End(xlUp).Select
ActiveCell.Offset(2, 2).Range("A1:B1").Select
Range(Selection, Selection.End(xlDown)).Select
Selection.Cut
ActiveCell.Offset(0, -2).Range("A1").Select
Selection.End(xlDown).Select
ActiveCell.Offset(1, 0).Range("A1").Select
ActiveSheet.Paste
Selection.End(xlUp).Select
ActiveCell.Offset(2, 4).Range("A1").Select
Selection.End(xlToRight).Select
Selection.End(xlToLeft).Select
ActiveCell.Range("A1:B1").Select
Range(Selection, Selection.End(xlDown)).Select
Selection.Cut
ActiveCell.Range("A1:A8192").Select
Selection.End(xlToLeft).Select
Selection.End(xlToLeft).Select
Selection.End(xlDown).Select
ActiveCell.Offset(1, 0).Range("A1").Select
ActiveSheet.Paste
Selection.End(xlUp).Select
ActiveCell.Offset(2, 6).Range("A1:B1").Select
Range(Selection, Selection.End(xlDown)).Select
Selection.Cut

```

```

ActiveCell.Offset(0, -6).Range("A1").Select
Selection.End(xlDown).Select
ActiveCell.Offset(1, 0).Range("A1").Select
ActiveSheet.Paste
ActiveCell.Offset(-1, 0).Range("A1").Select
Selection.End(xlUp).Select
ActiveCell.Offset(0, 2).Range("A1:A2").Select
Range(Selection, Selection.End(xlToRight)).Select
Selection.ClearContents
ActiveCell.Offset(0, -1).Range("A1").Select
Selection.End(xlDown).Select
Range(Selection, Selection.End(xlUp)).Select
ActiveSheet.Shapes.AddChart.Select
ActiveChart.ChartType = xlLine
ActiveChart.SetSourceData
Source:=Range("KRITISK!$B$7:$B$32776")
ActiveChart.SeriesCollection(1).XValues =
"=KRITISK!$A$8:$A$32776"
ActiveChart.PlotArea.Select
ActiveCell.Offset(-32769, -
1).Range("B1:B32770,A32759").Select
ActiveCell.Offset(-11, -1).Range("A1").Activate
Selection.End(xlUp).Select
End Sub

```

### 8.5.3 GRAF()

```

Sub GRAF()
'
' GRAF Macro
'
'
Range("C8:D8").Select
Range(Selection, Selection.End(xlDown)).Select
Selection.Cut
Selection.End(xlToLeft).Select
Selection.End(xlDown).Select
Range("A2056").Select
ActiveSheet.Paste
Selection.End(xlUp).Select
Range("E8:F8").Select
Range(Selection, Selection.End(xlDown)).Select
Selection.Cut
Range("A8").Select
Selection.End(xlDown).Select
Range("A4104").Select
ActiveSheet.Paste
Selection.End(xlUp).Select
Range("G8:H8").Select
Range(Selection, Selection.End(xlDown)).Select

```

```

Selection.Cut
Selection.End(xlToLeft).Select
Selection.End(xlToLeft).Select
Selection.End(xlDown).Select
Range("A6152").Select
ActiveSheet.Paste
Selection.End(xlUp).Select
Range("B7").Select
Selection.End(xlDown).Select
Range(Selection, Selection.End(xlUp)).Select
ActiveSheet.Shapes.AddChart.Select
ActiveChart.ChartType = xlLine
ActiveChart.SetSourceData Source:=Range("'Q13-
2_2'!$B$7:$B$8199")
ActiveChart.SeriesCollection(1).XValues = "'Q13-
2_2'!$A$8:$A$8199"
End Sub

```

## 8.6 MatLab datasheet

```

% Start by clearing out the memory of the project
clear; clc;

% Start by correcting font types and sizes
% Change default axes fonts.
set(0, 'DefaultAxesFontName', 'LM Roman 12')
set(0, 'DefaultAxesFontSize', 10)

% Start by defining input of data:
fileName = '.xlsx';
Range =;

Input = xlsread(fileName);

% The relevant amplitude input is defined
Time = Input(:,1); % Time in ms
Amplitude = Input(:,2); % Amplitude in mm/s

if Time(10)-Time(1) < 4;
    x = 2;
else x = 1;
end

% Then define the sampling frequency
Fs = 1280*x; % Hz

% The sample time are found using the inverse of the
frequency

```

```

T = 1/Fs;

% The length of the signal is found
L = length(Amplitude);

% The time vector is calculated
t = (0:L-1)*T;

% One can then plot the amplitude against the time
subplot(4,1,1);
plot(Time,Amplitude)
title('\bf Signal in time domain')
xlabel('Time (ms)')
ylabel('Amplitude (mm/s)')

% The next step is to find the next power of 2 from
% the length of "Amplitude"
NFFT = 2^nextpow2(L);

% One can then perform the fast Fourier transform from the
% function Y = fft(Amplitude,NFFT) that returns the n-point
DFT.
Y = fft(Amplitude,NFFT)/L;
f = Fs/2*linspace(0,1,NFFT/2+1);

% One can then plot the single-sided amplitude spectrum
subplot(4,1,2);
plot(f,2*abs(Y(1:NFFT/2+1)))
xlim([0 Range])
title('\bf Single-Sided Amplitude Spectrum of Signal')
xlabel('Frequency (Hz)')
ylabel('|Y(f)|')

% After the initial plotting, it is necessary to find peaks
of the data
% This is done so that the dampening ratio can be found as a
rolling
% calculation of the data.

% Start by only selecting positive integers of the amplitude
by replacing
% negative integers with 0. Choose not to plot this
PosAmp = Amplitude;
PosAmp(PosAmp < 0) = 0; % Set negative numbers to zero
% subplot(4,1,3);
% plot(Time,PosAmp)
% title('\bf Positive component of signal')
% xlabel('Time (ms)')
% ylabel('Amplitude (mm/s)')

% One then has to find the peaks throughout the plottet data.
% This is done using the built in local maxima function of
MATLAB

```

```

% called findpeaks. To identify the correct peaks, a distance
limit
% is put in place. For reason of analysis, this is set to 500
points.

[PeakValue,PeakLocation] =
findpeaks(PosAmp, 'minpeakdistance', 500);

PeakLocation = PeakLocation/(Fs/1000);

% subplot(4,1,2);
% plot(PeakLocation,PeakValue)
% plot(PeakLocation,PeakValue)
% title('\bf Peaks')
% xlabel('Time (ms)')
% ylabel('Amplitude (mm/s)')

% The last step it to use these peaks to find values for the
% Logarithmic Damping Coeffisient throughout the dataset

for i=(1:length(PeakValue)-1)
    LogDec(i) = 1/(PeakLocation(i+1) -
PeakLocation(i))*log(PeakValue(i)/(PeakValue(i+1)));
end

% The Logarithmic decrement is plotted
subplot(4,1,3);
plot(LogDec)
title('\bf Logarithmic decrement')
xlabel('Peak number')
ylabel('\delta')

% One can then plot the damping raio of the oscillator
DampRat = LogDec./sqrt(4*pi^2+LogDec.^2);
subplot(4,1,4);
plot(DampRat)
title('\bf Damping ratio')
xlabel('Peak number')
ylabel('\zeta')

% The figure are now ready for export

```

## 8.7 Results from analysis

| <i>Area</i> | <i>Description</i>                  | <i>Line tag</i>         | <i>Acc.orient</i>    | <i>Range</i>      |
|-------------|-------------------------------------|-------------------------|----------------------|-------------------|
| A21         | Turboexpander 1<br>(Out of service) | CA-25-5111-FS20A        | Top                  | Auto range        |
|             |                                     | <b>Valve tag</b>        | <b>Valve orient.</b> | <b>Excitation</b> |
|             |                                     | Q-B-L-1100-04C Item 329 | Horizontal           | None              |

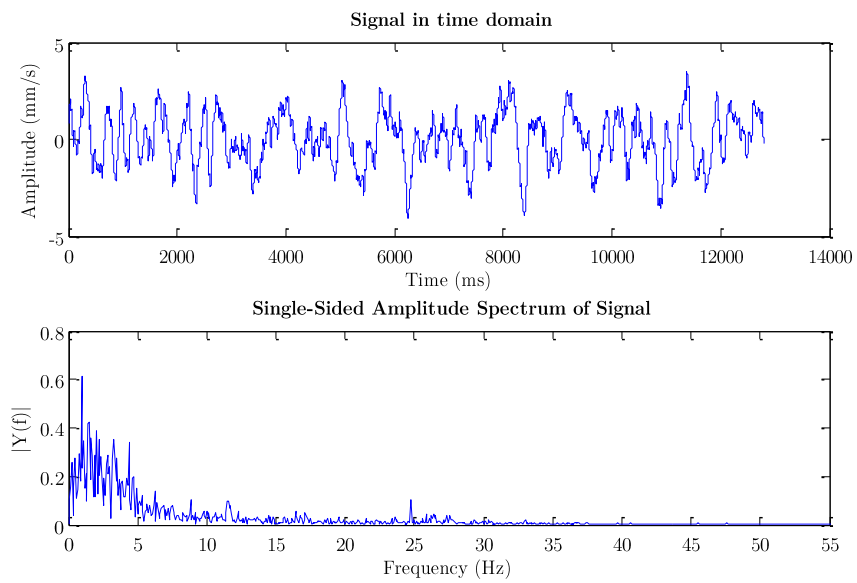


Figure 8-5 Result Non-induced vibration CA-25-5111-FS20A, A21, top

| <i>Area</i> | <i>Description</i>                     | <i>Line tag</i>         | <i>Acc.orient</i>    | <i>Range</i>      |
|-------------|--|-------------------------|----------------------|-------------------|
| <b>A21</b>  | Turboexpander<br>1 (Out of<br>service) | CA-25-5111-FS20A        | Top                  | 200 mm/s          |
|             |  | <b>Valve tag</b>        | <b>Valve orient.</b> | <b>Excitation</b> |
|             |  | Q-B-L-1100-04C Item 329 | Horizontal           | Stroke            |

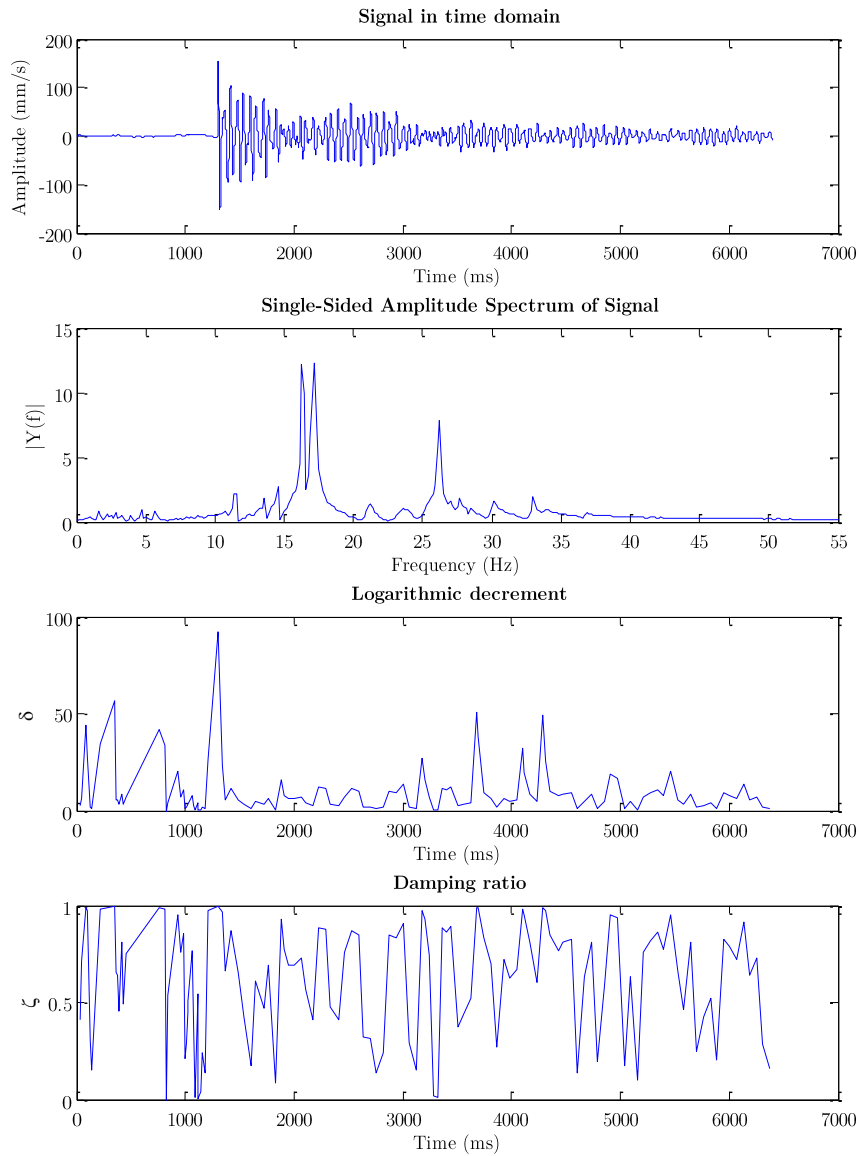


Figure 8-6 Result Induced vibration CA-25-5111-FS20A, A21, top



| <i>Area</i> | <i>Description</i>                     | <i>Line tag</i>         | <i>Acc.orient</i>    | <i>Range</i>      |
|-------------|--|-------------------------|----------------------|-------------------|
| <b>A21</b>  | Turboexpander<br>1 (Out of<br>service) | CA-25-5111-FS20A        | Side                 | Auto range        |
|             |  | <b>Valve tag</b>        | <b>Valve orient.</b> | <b>Excitation</b> |
|             |  | Q-B-L-1100-04C Item 329 | Horizontal           | None              |

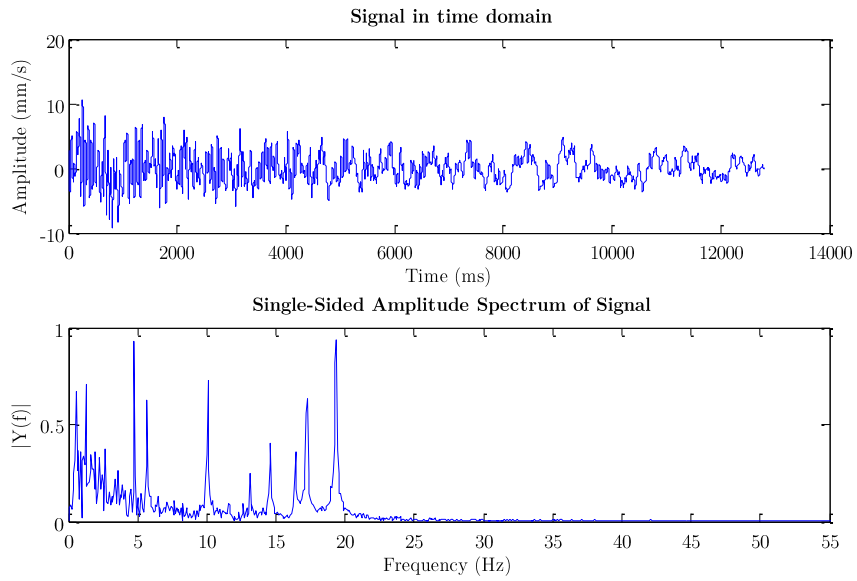


Figure 8-7 Result Non-induced vibration CA-25-5111-FS20A, A21, side

| <i>Area</i> | <i>Description</i>                     | <i>Line tag</i>         | <i>Acc.orient</i>    | <i>Range</i>      |
|-------------|--|-------------------------|----------------------|-------------------|
| <b>A21</b>  | Turboexpander<br>1 (Out of<br>service) | CA-25-5111-FS20A        | Side                 | 200 mm/s          |
|             |  | <b>Valve tag</b>        | <b>Valve orient.</b> | <b>Excitation</b> |
|             |  | Q-B-L-1100-04C Item 329 | Horizontal           | Stroke            |

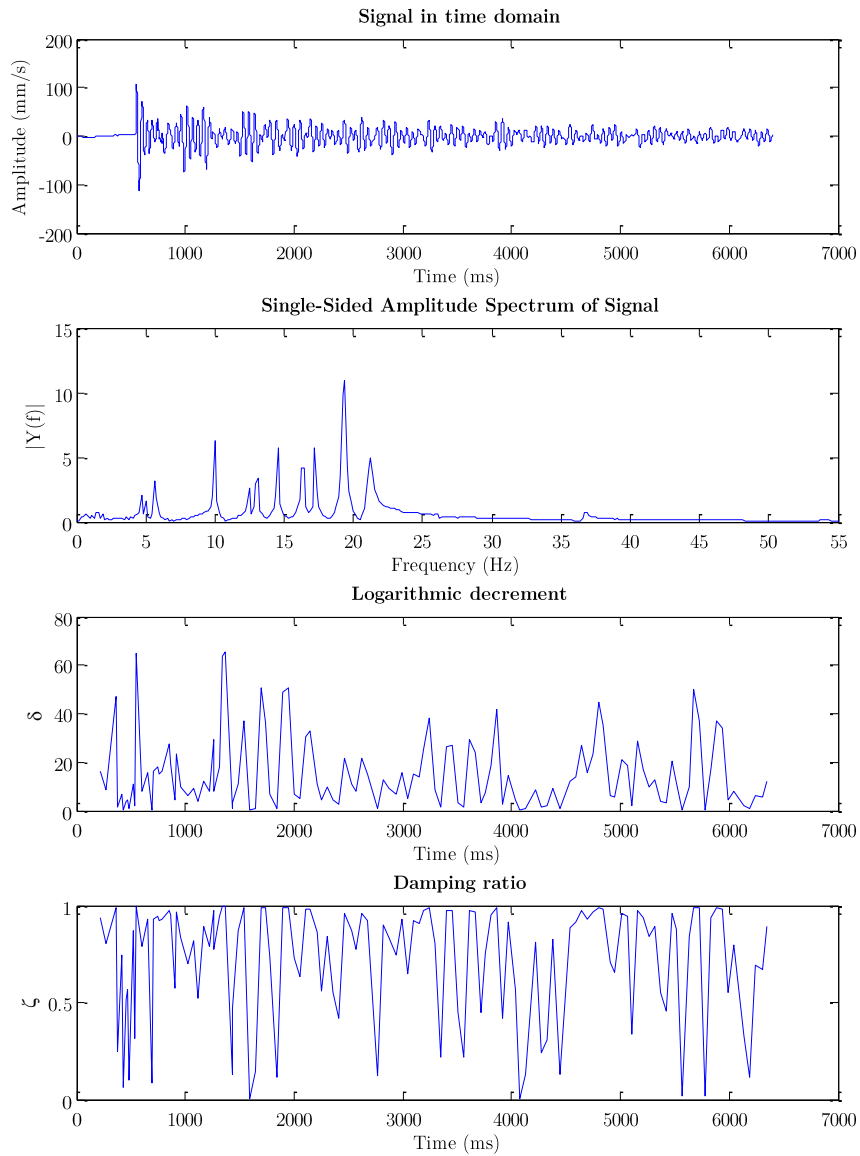


Figure 8-8 Result Induced vibration CA-25-5111-FS20A, A21, side

| <i>Area</i> | <i>Description</i> | <i>Line tag</i>         | <i>Acc.orient</i>    | <i>Range</i>      |
|-------------|--------------------|-------------------------|----------------------|-------------------|
| <b>A22</b>  | Turboexpander<br>2 | CA-25-5110-FS20A        | Top                  | Auto range        |
|             |                    | <b>Valve tag</b>        | <b>Valve orient.</b> | <b>Excitation</b> |
|             |                    | Q-B-L-1100-04C Item 329 | Horizontal           | None              |

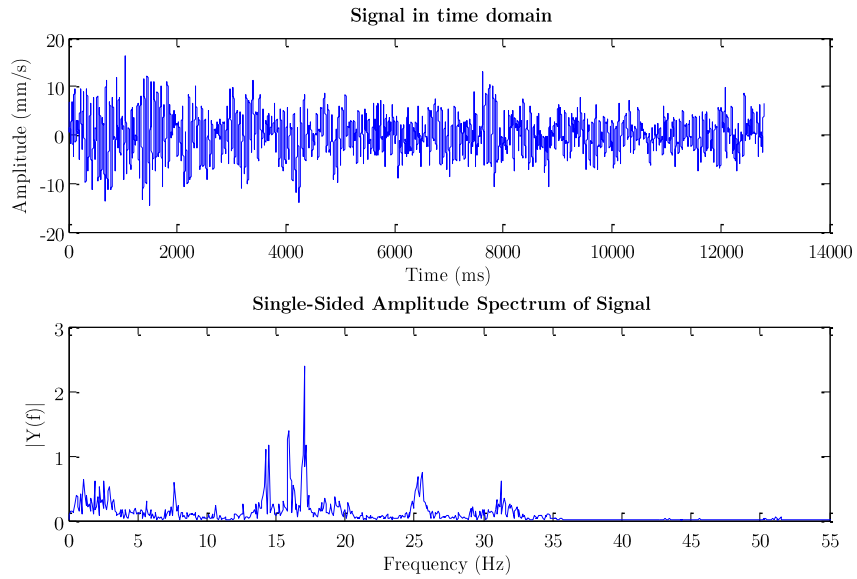


Figure 8-9 Result Non-induced vibration CA-25-5110-FS20A, A22, top

| <i>Area</i> | <i>Description</i> | <i>Line tag</i>         | <i>Acc.orient</i>    | <i>Range</i>      |
|-------------|--------------------|-------------------------|----------------------|-------------------|
| <b>A22</b>  | Turboexpander<br>2 | CA-25-5110-FS20A        | Top                  | 200 mm/s          |
|             |                    | <b>Valve tag</b>        | <b>Valve orient.</b> | <b>Excitation</b> |
|             |                    | Q-B-L-1100-04C Item 329 | Horizontal           | Stroke            |

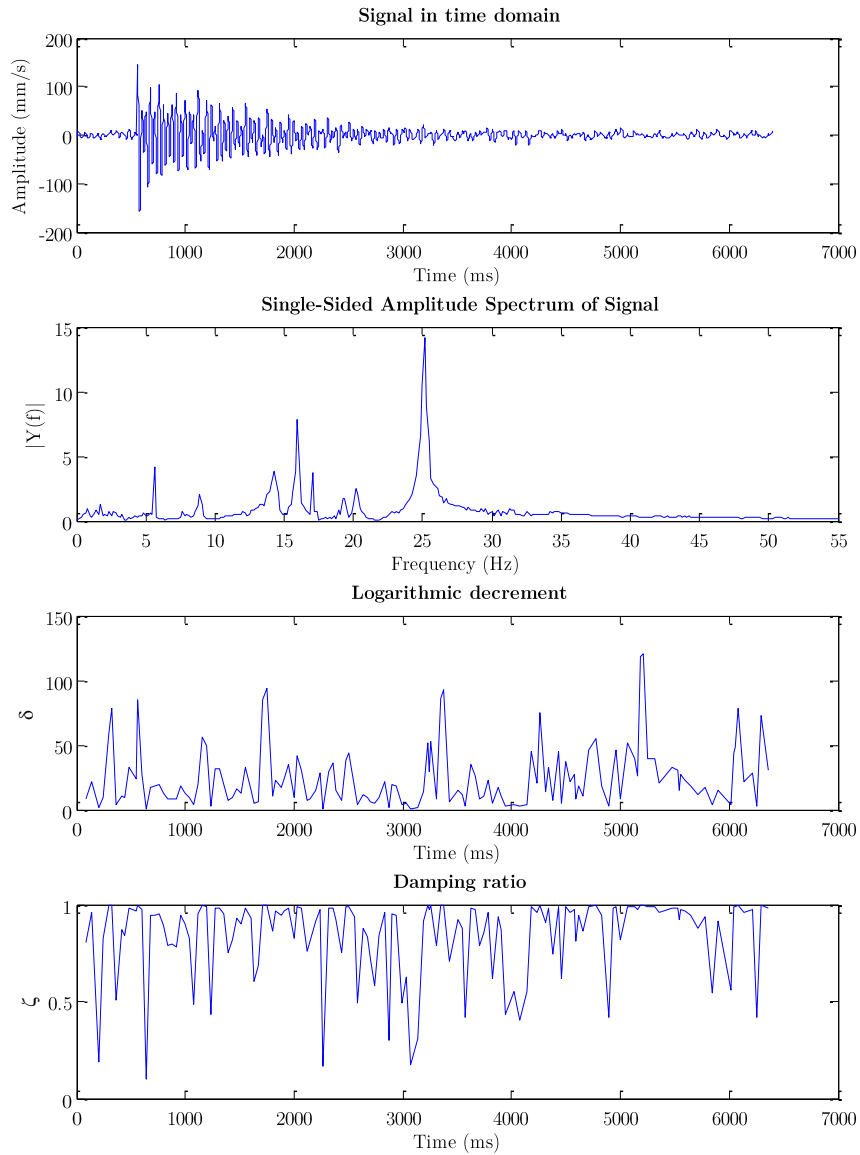


Figure 8-10 Result Induced vibration CA-25-5111-FS20A, A22, top

| <i>Area</i> | <i>Description</i> | <i>Line tag</i>         | <i>Acc.orient</i>    | <i>Range</i>      |
|-------------|--------------------|-------------------------|----------------------|-------------------|
| <b>A22</b>  | Turboexpander<br>2 | CA-25-5110-FS20A        | Side                 | Auto range        |
|             |                    | <b>Valve tag</b>        | <b>Valve orient.</b> | <b>Excitation</b> |
|             |                    | Q-B-L-1100-04C Item 329 | Horizontal           | None              |

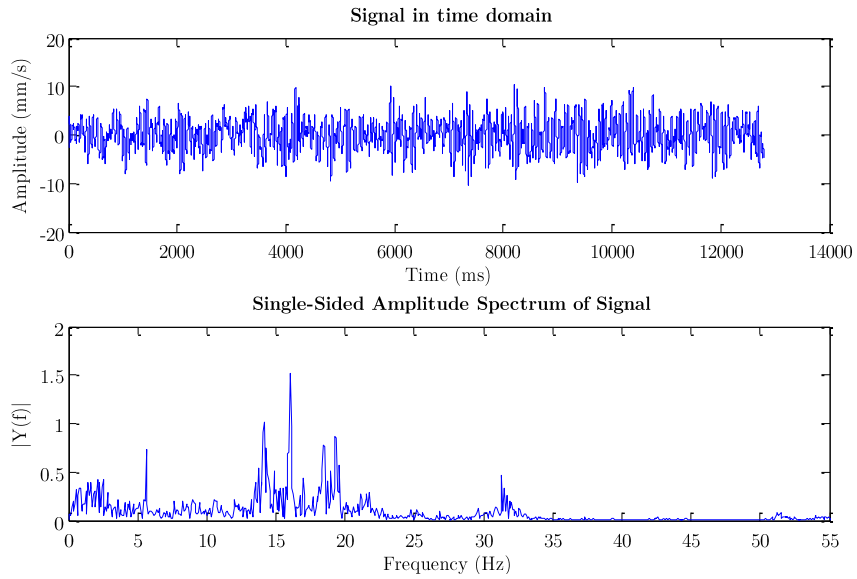


Figure 8-11 Result Non-induced vibration CA-25-5110-FS20A, A22, side

| <i>Area</i> | <i>Description</i> | <i>Line tag</i>         | <i>Acc.orient</i>    | <i>Range</i>      |
|-------------|--------------------|-------------------------|----------------------|-------------------|
| <b>A22</b>  | Turboexpander<br>2 | CA-25-5110-FS20A        | Side                 | 200 mm/s          |
|             |                    | <b>Valve tag</b>        | <b>Valve orient.</b> | <b>Excitation</b> |
|             |                    | Q-B-L-1100-04C Item 329 | Horizontal           | Stroke            |

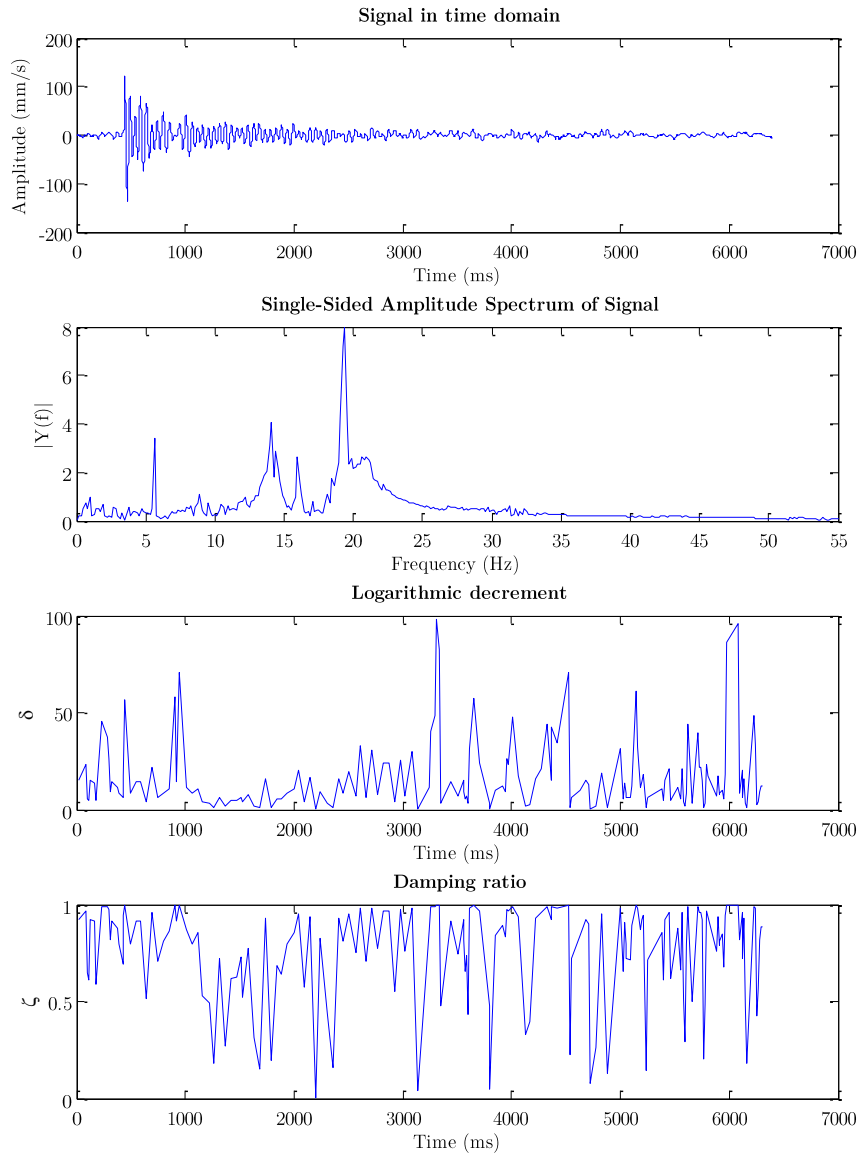


Figure 8-12 Result Induced vibration CA-25-5110-FS20A, A22, side

| <i>Area</i> | <i>Description</i> | <i>Line tag</i>   | <i>Acc.orient</i>    | <i>Range</i>      |
|-------------|--------------------|-------------------|----------------------|-------------------|
| <b>A24</b>  | NGL<br>extraction  | PV-25-8287-ES20A  | East-West            | Auto range        |
|             |                    | <b>Valve tag</b>  | <b>Valve orient.</b> | <b>Excitation</b> |
|             |                    | 25-8287/1-2 SP2-2 | Vertical             | None              |

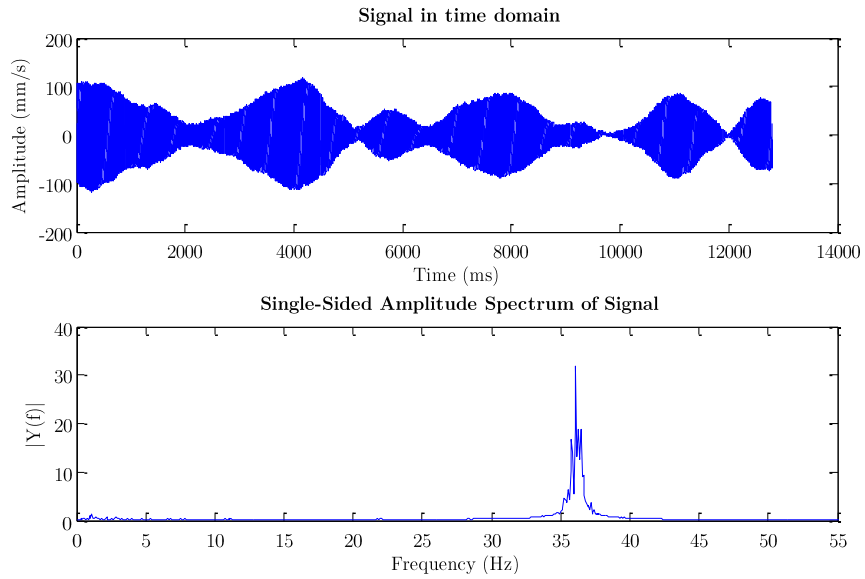


Figure 8-13 Result Non-induced vibration PV-25-8287-ES20A, A24, E-W

| <i>Area</i> | <i>Description</i> | <i>Line tag</i>   | <i>Acc.orient</i>    | <i>Range</i>      |
|-------------|--------------------|-------------------|----------------------|-------------------|
| <b>A24</b>  | NGL<br>extraction  | PV-25-8287-ES20A  | East-West            | 300 mm/s          |
|             |                    | <b>Valve tag</b>  | <b>Valve orient.</b> | <b>Excitation</b> |
|             |                    | 25-8287/1-2 SP2-2 | Vertical             | Stroke            |

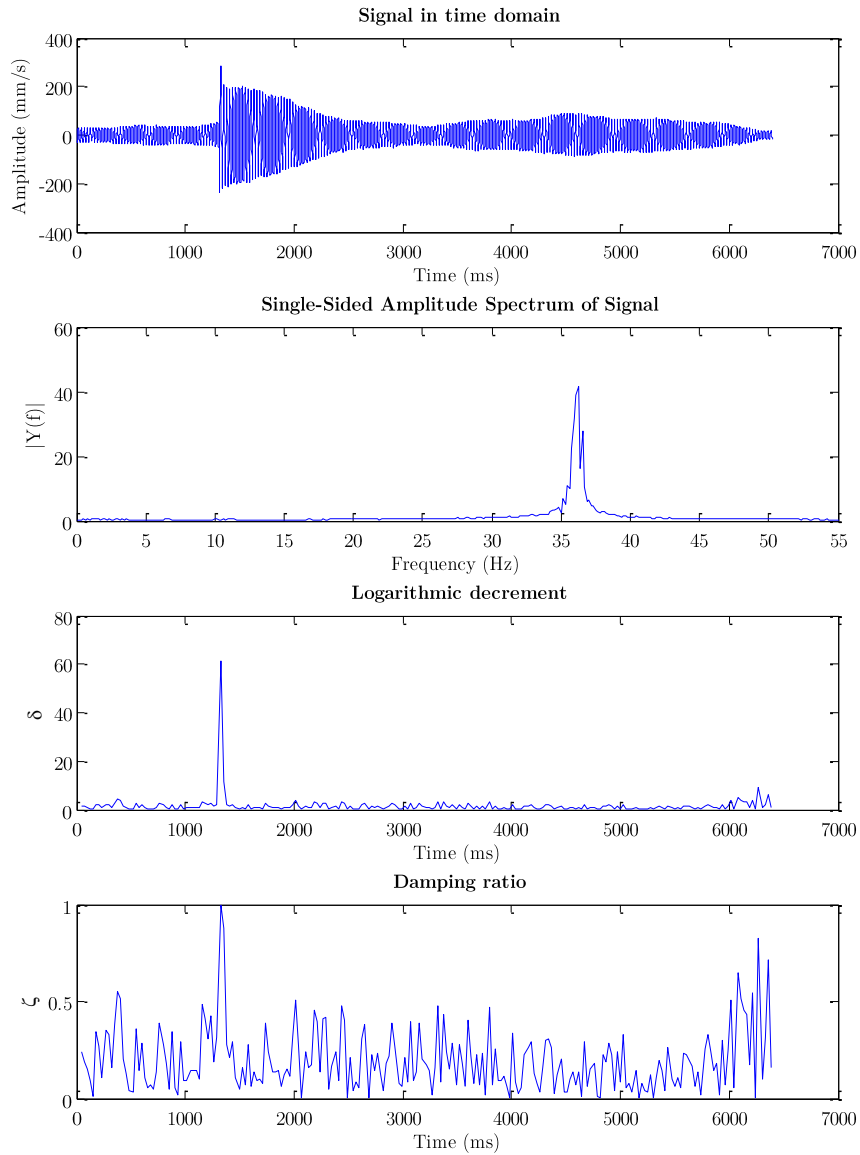


Figure 8-14 Result Induced vibration PV-25-8287-ES20A, A24, E-W



| <i>Area</i> | <i>Description</i> | <i>Line tag</i>   | <i>Acc.orient</i>    | <i>Range</i>      |
|-------------|--------------------|-------------------|----------------------|-------------------|
| <b>A24</b>  | NGL<br>extraction  | PV-25-8287-ES20A  | North-South          | Auto range        |
|             |                    | <i>Valve tag</i>  | <i>Valve orient.</i> | <i>Excitation</i> |
|             |                    | 25-8287/1-2 SP2-2 | Vertical             | None              |

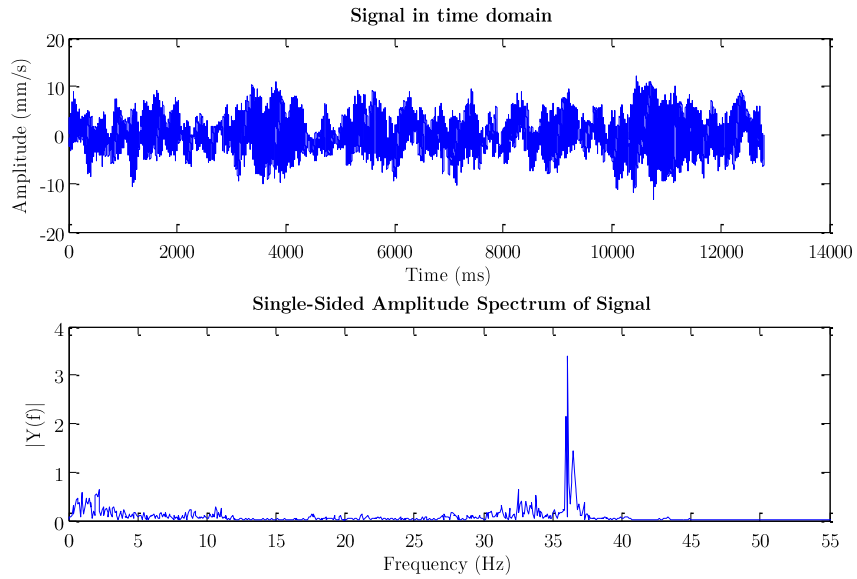


Figure 8-15 Result Non-induced vibration PV-25-8287-ES20A, A24, N-S

| <i>Area</i> | <i>Description</i> | <i>Line tag</i>   | <i>Acc.orient</i>    | <i>Range</i>      |
|-------------|--------------------|-------------------|----------------------|-------------------|
| <b>A24</b>  | NGL<br>extraction  | PV-25-8287-ES20A  | North-South          | 300 mm/s          |
|             |                    | <b>Valve tag</b>  | <b>Valve orient.</b> | <b>Excitation</b> |
|             |                    | 25-8287/1-2 SP2-2 | Vertical             | Stroke            |

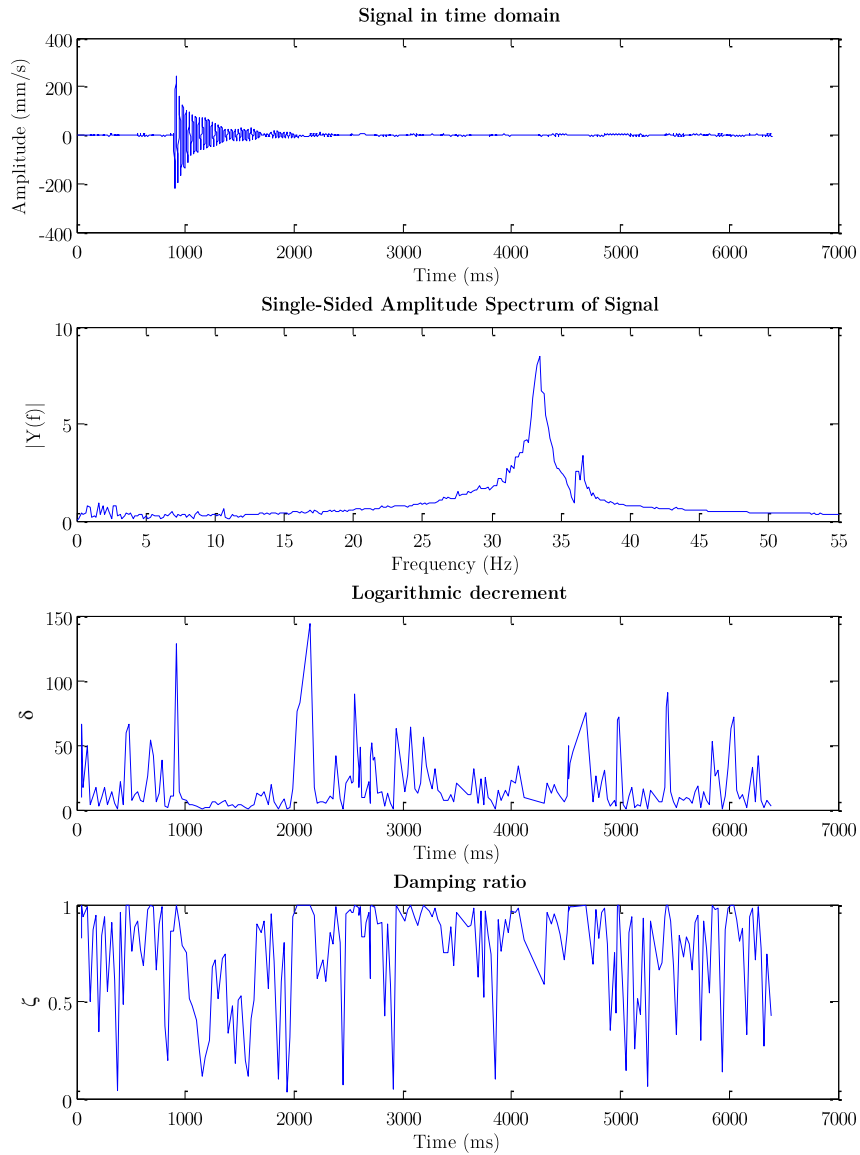


Figure 8-16 Result Induced vibration PV-25-8287-ES20A, A24, N-S

| <i>Area</i> | <i>Description</i> | <i>Line tag</i>  | <i>Acc.orient</i>    | <i>Range</i>      |
|-------------|--------------------|------------------|----------------------|-------------------|
| <b>A24</b>  | NGL<br>extraction  | PL-25-8501-BC21A | Side                 | Auto range        |
|             |                    | <i>Valve tag</i> | <i>Valve orient.</i> | <i>Excitation</i> |
|             |                    | NA               | Horizontal           | None              |

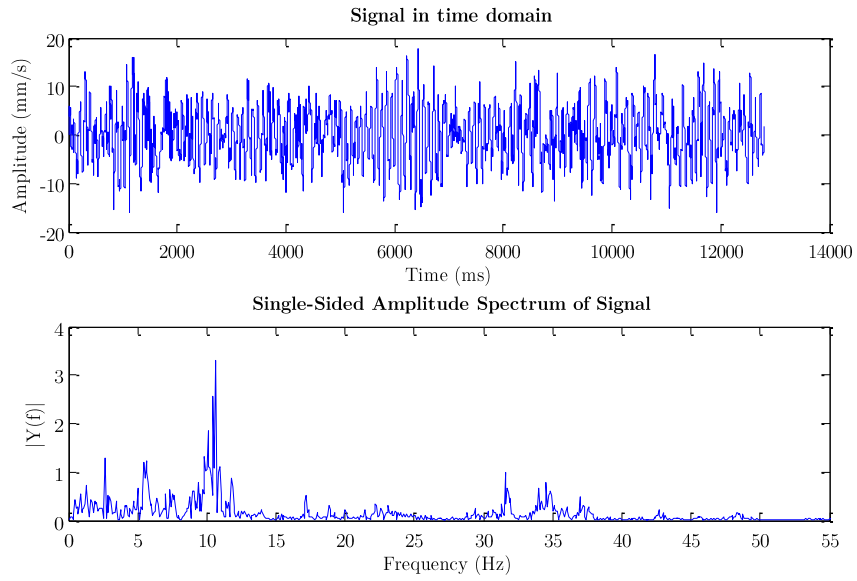


Figure 8-17 Result Non-induced vibration PL-25-8501-BC21A, A24, side

| <i>Area</i> | <i>Description</i> | <i>Line tag</i>  | <i>Acc.orient</i>    | <i>Range</i>      |
|-------------|--------------------|------------------|----------------------|-------------------|
| <b>A24</b>  | NGL<br>extraction  | PL-25-8501-BC21A | Side                 | 300 mm/s          |
|             |                    | <b>Valve tag</b> | <b>Valve orient.</b> | <b>Excitation</b> |
|             |                    | NA               | Horizontal           | Stroke            |

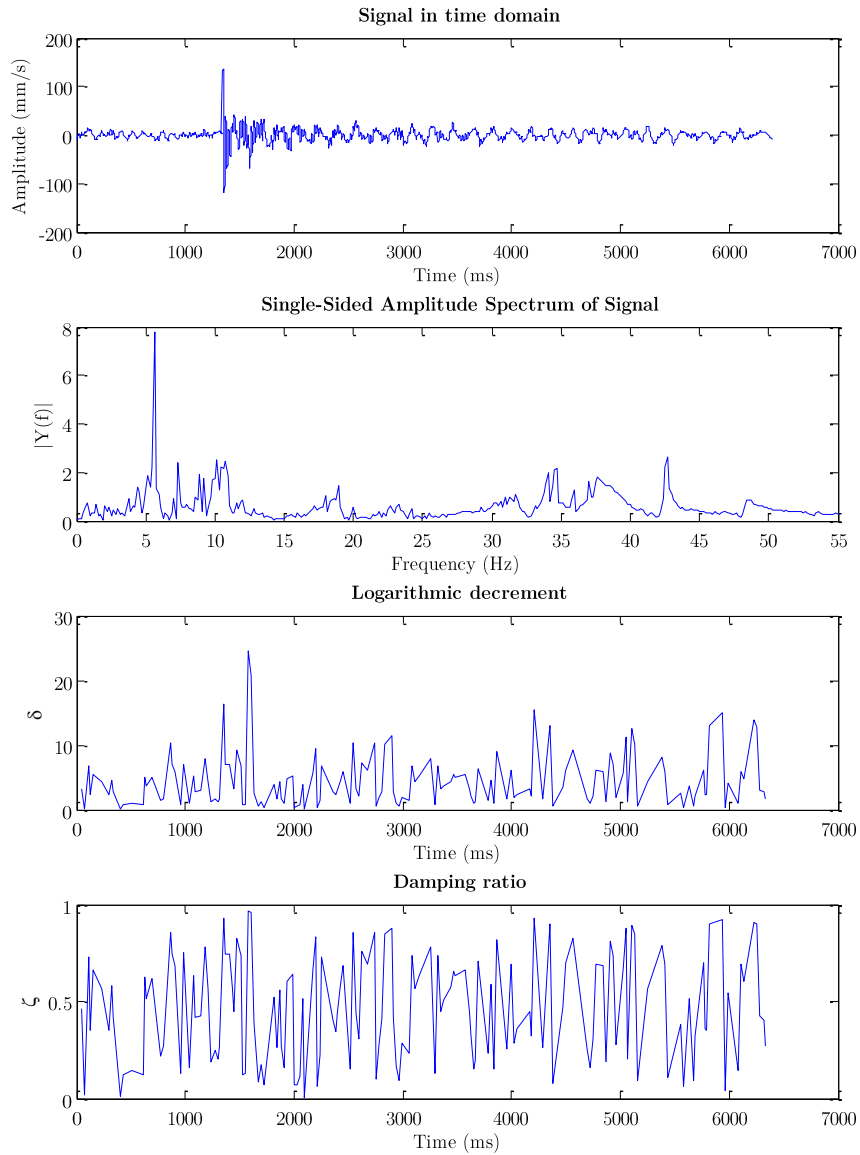


Figure 8-18 Result Induced vibration PL-25-8501-BC21A, A24, top

| <i>Area</i> | <i>Description</i> | <i>Line tag</i>  | <i>Acc.orient</i>    | <i>Range</i>      |
|-------------|--------------------|------------------|----------------------|-------------------|
| <b>A24</b>  | NGL<br>extraction  | PL-25-8501-BC21A | Top                  | Auto range        |
|             |                    | <b>Valve tag</b> | <b>Valve orient.</b> | <b>Excitation</b> |
|             |                    | NA               | Horizontal           | None              |

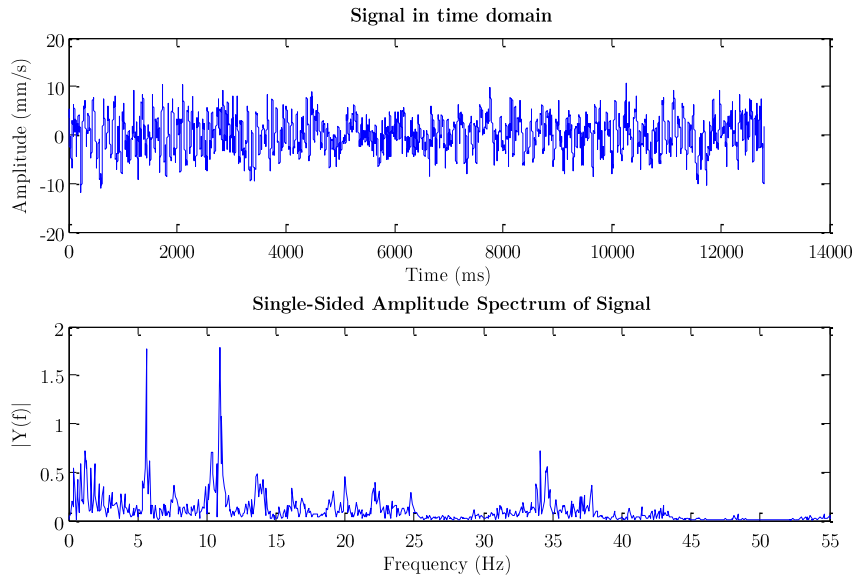


Figure 8-19 Result Non-induced vibration PL-25-8501-BC21A, A24, top

| <i>Area</i> | <i>Description</i> | <i>Line tag</i>  | <i>Acc.orient</i>    | <i>Range</i>      |
|-------------|--------------------|------------------|----------------------|-------------------|
| <b>A24</b>  | NGL<br>extraction  | PL-25-8501-BC21A | Top                  | 300 mm/s          |
|             |                    | <b>Valve tag</b> | <b>Valve orient.</b> | <b>Excitation</b> |
|             |                    | NA               | Horizontal           | Stroke            |

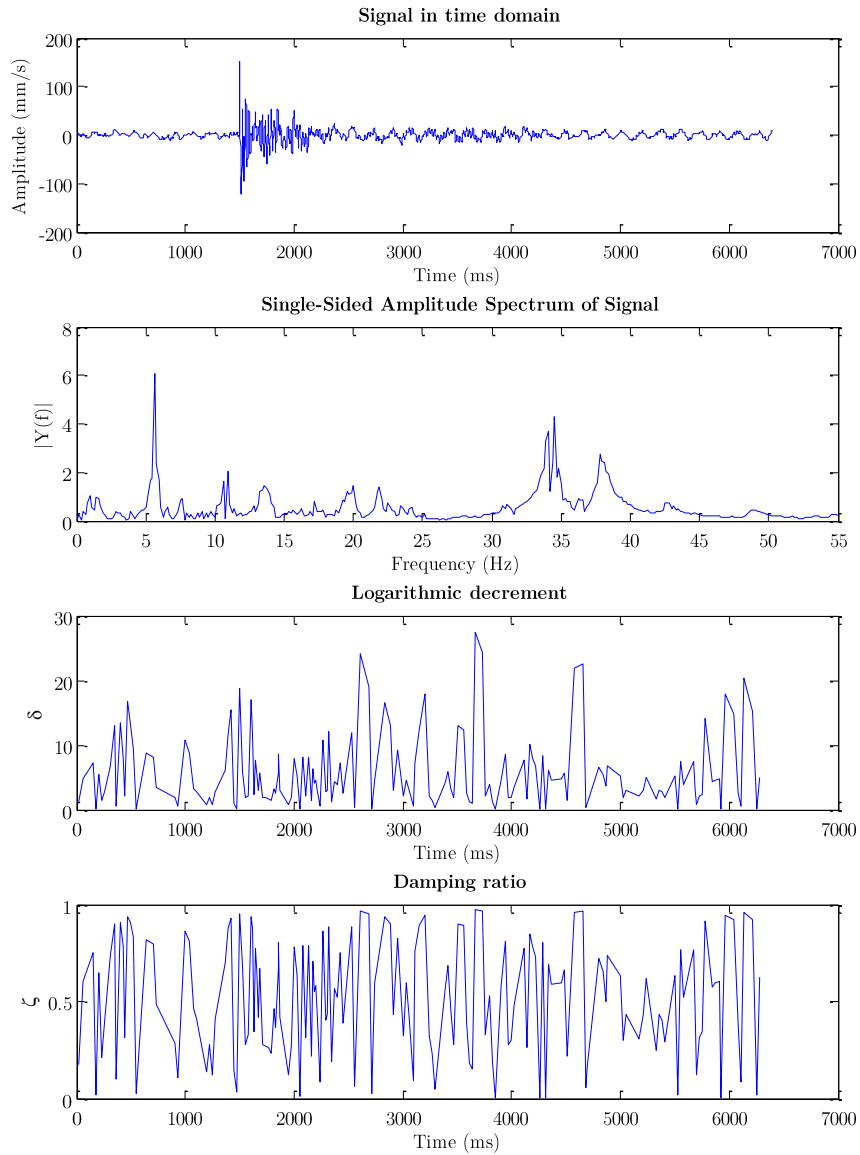


Figure 8-20 Result Induced vibration PL-25-8501-BC21A, A24, top

| <i>Area</i> | <i>Description</i> | <i>Line tag</i>  | <i>Acc.orient</i>    | <i>Range</i>      |
|-------------|--------------------|------------------|----------------------|-------------------|
| <b>A24</b>  | NGL<br>extraction  | PV-25-8107-DC11A | East-West            | Auto range        |
|             |                    | <b>Valve tag</b> | <b>Valve orient.</b> | <b>Excitation</b> |
|             |                    | NA               | Vertical             | None              |

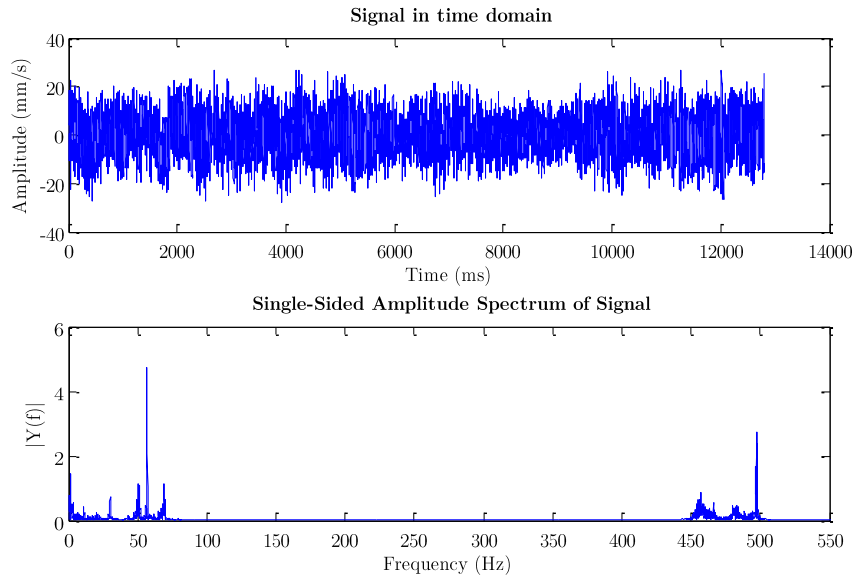


Figure 8-21 Result Non-induced vibration PV-25-8107-DC11A, A24, E-W

| <i>Area</i> | <i>Description</i> | <i>Line tag</i>  | <i>Acc.orient</i>    | <i>Range</i>      |
|-------------|--------------------|------------------|----------------------|-------------------|
| <b>A24</b>  | NGL<br>extraction  | PV-25-8107-DC11A | East-West            | 300 mm/s          |
|             |                    | <b>Valve tag</b> | <b>Valve orient.</b> | <b>Excitation</b> |
|             |                    | NA               | Vertical             | Stroke            |

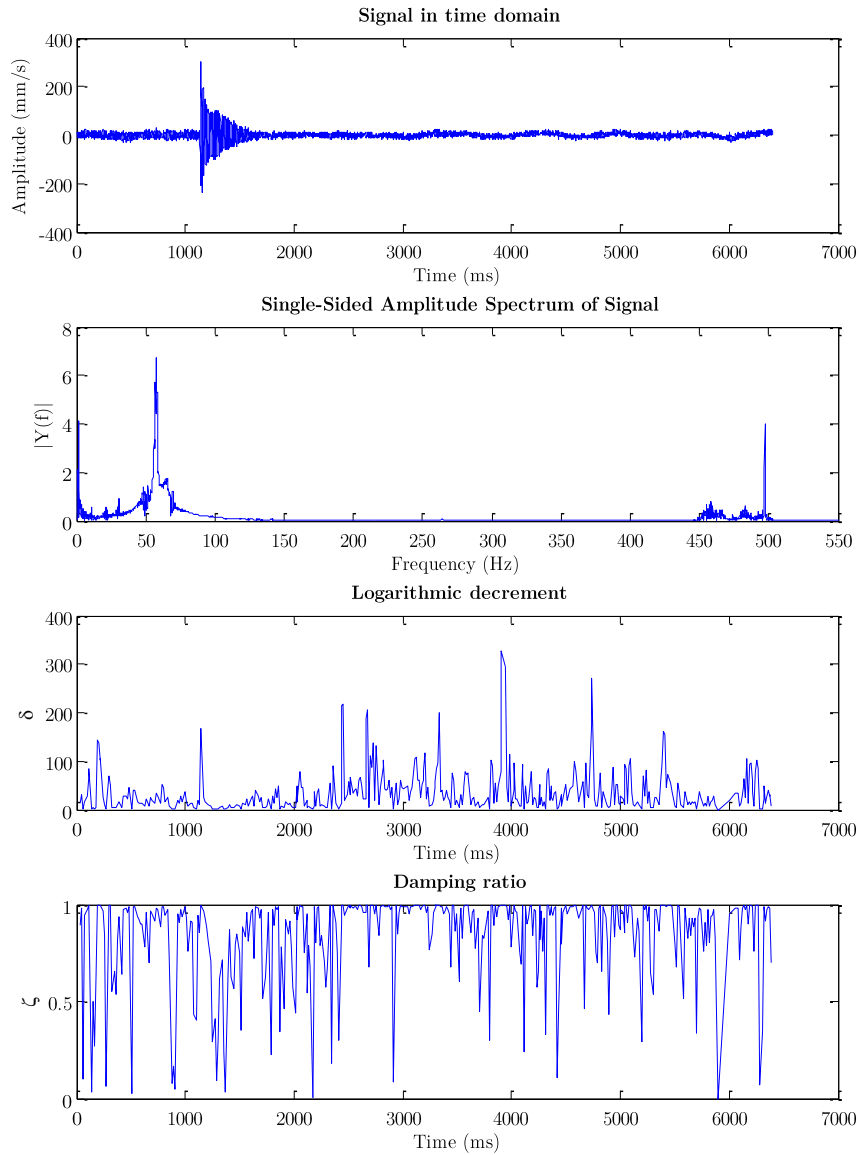


Figure 8-22 Result Induced vibration PV-25-8107-DC11A, A24, E-W



| <i>Area</i> | <i>Description</i> | <i>Line tag</i>  | <i>Acc.orient</i>    | <i>Range</i>      |
|-------------|--------------------|------------------|----------------------|-------------------|
| <b>A24</b>  | NGL<br>extraction  | PV-25-8107-DC11A | North-South          | Auto range        |
|             |                    | <i>Valve tag</i> | <i>Valve orient.</i> | <i>Excitation</i> |
|             |                    | NA               | Vertical             | None              |

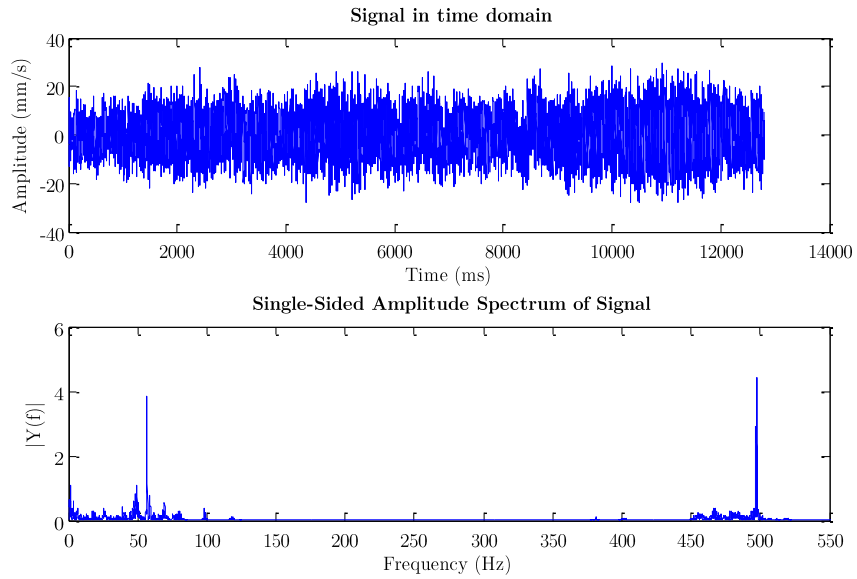


Figure 8-23 Result Non-induced vibration PV-25-8107-DC11A, A24, N-S

| <i>Area</i> | <i>Description</i> | <i>Line tag</i>  | <i>Acc.orient</i>    | <i>Range</i>      |
|-------------|--------------------|------------------|----------------------|-------------------|
| <b>A24</b>  | NGL<br>extraction  | PV-25-8107-DC11A | North-South          | 300 mm/s          |
|             |                    | <i>Valve tag</i> | <i>Valve orient.</i> | <i>Excitation</i> |
|             |                    | NA               | Vertical             | Stroke            |

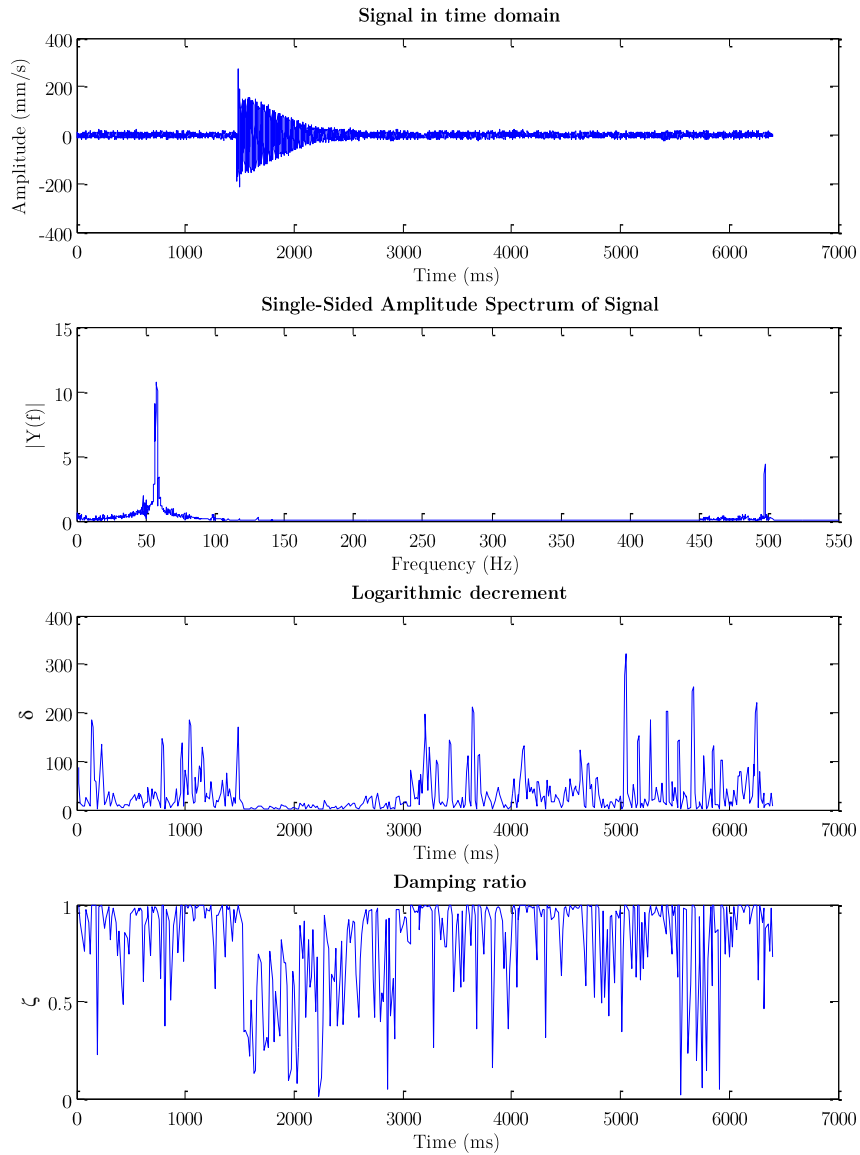


Figure 8-24 Result Induced vibration PV-25-8107-DC11A, A24, N-S

| <i>Area</i> | <i>Description</i>                  | <i>Line tag</i>                 | <i>Acc.orient</i>                | <i>Range</i>              |
|-------------|-------------------------------------|---------------------------------|----------------------------------|---------------------------|
| <b>A11</b>  | Pig receiver & Launchers/ESD valves | 10"-PR-20-5347-EC19AX           | East-West                        | Auto range                |
|             |                                     | <b>Valve tag</b><br>20-FE5228-1 | <b>Valve orient.</b><br>Vertical | <b>Excitation</b><br>None |

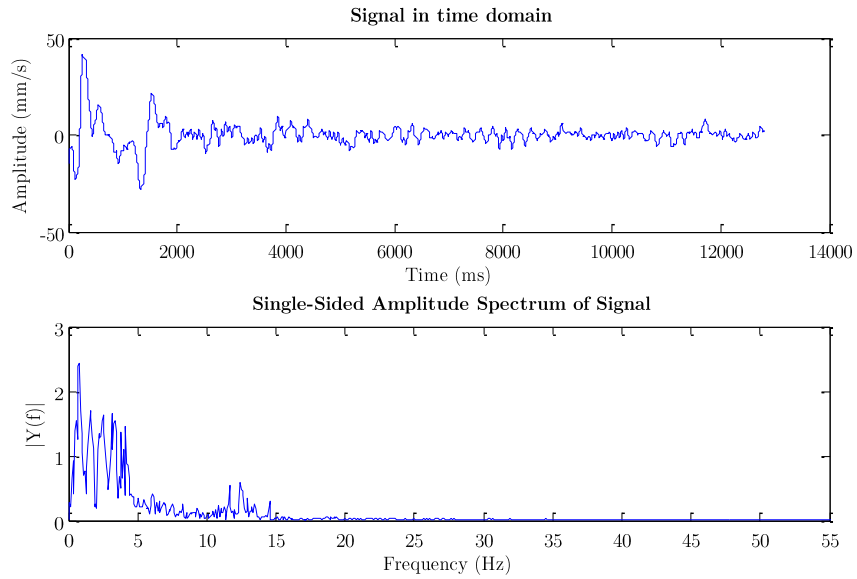


Figure 8-25 Result Non-induced vibration PR-20-5347-EC19AX, A11, E-W

| <i>Area</i> | <i>Description</i>                  | <i>Line tag</i>                 | <i>Acc.orient</i>                | <i>Range</i>                |
|-------------|-------------------------------------|---------------------------------|----------------------------------|-----------------------------|
| <b>A11</b>  | Pig receiver & Launchers/ESD valves | 10"-PR-20-5347-EC19AX           | East-West                        | 300 mm/s                    |
|             |                                     | <b>Valve tag</b><br>20-FE5228-1 | <b>Valve orient.</b><br>Vertical | <b>Excitation</b><br>Stroke |

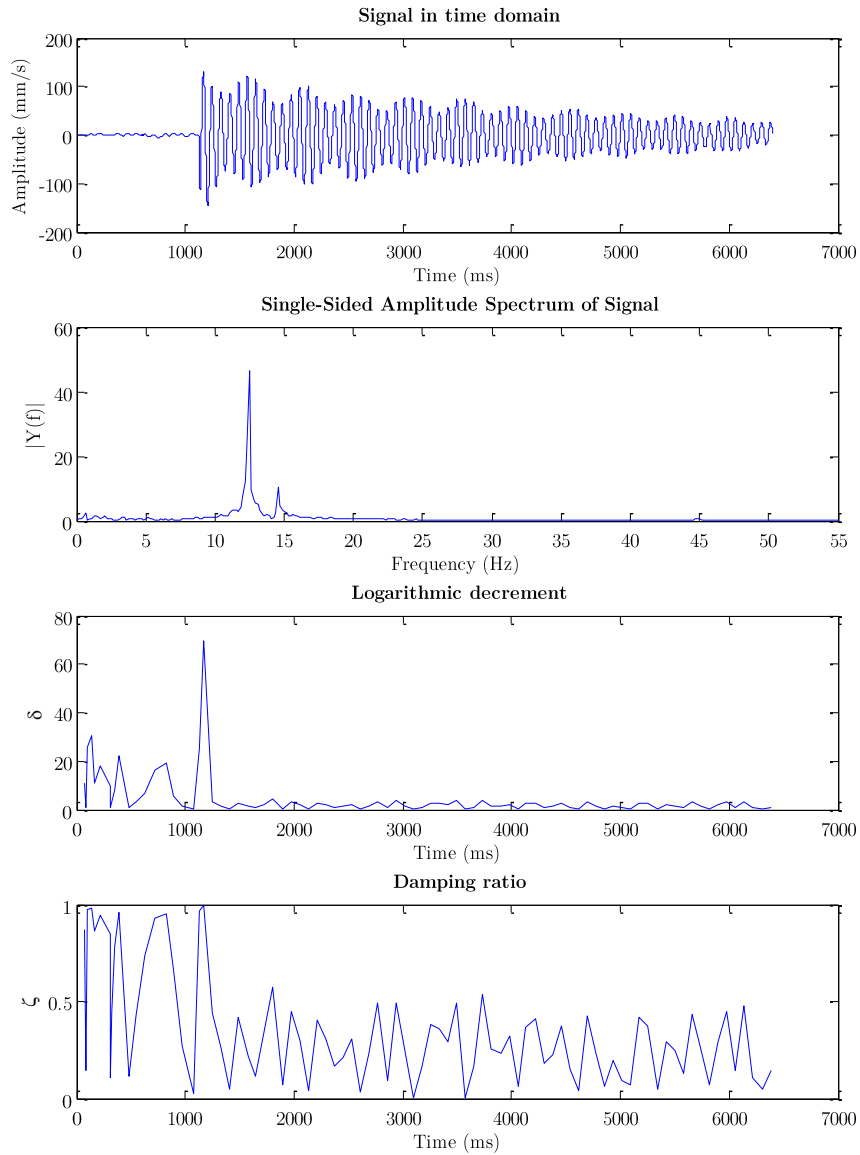


Figure 8-26 Result Induced vibration PR-20-5347-EC19AX, A11, E-W

| <i>Area</i> | <i>Description</i> | <i>Line tag</i>       | <i>Acc.orient</i>    | <i>Range</i>      |
|-------------|--------------------|-----------------------|----------------------|-------------------|
| <b>A11</b>  | Pig receiver &     | 10"-PR-20-5347-EC19AX | North-South          | Auto range        |
|             | Launchers/ESD      | <b>Valve tag</b>      | <b>Valve orient.</b> | <b>Excitation</b> |
|             | valves             | 20-FE5228-1           | Vertical             | None              |

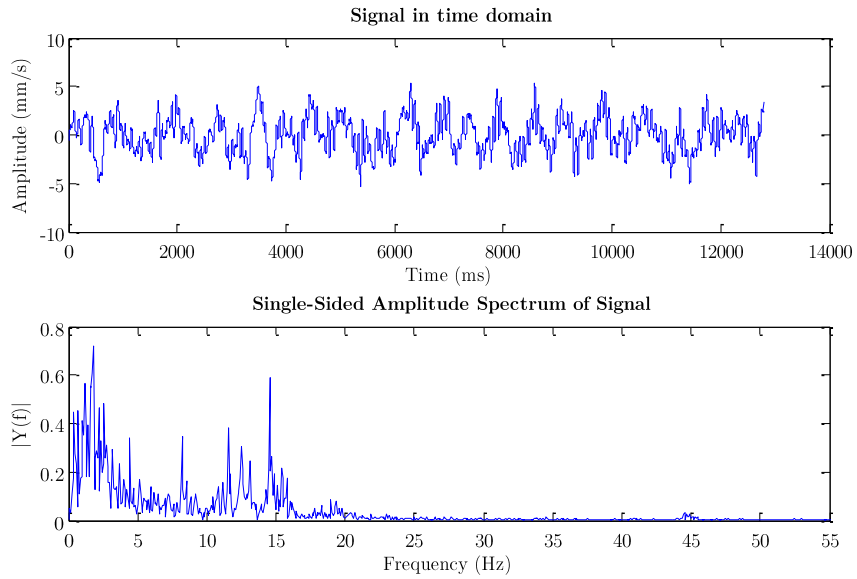


Figure 8-27 Result Non-induced vibration PR-20-5347-EC19AX, A11, N-S

| <i>Area</i> | <i>Description</i>                  | <i>Line tag</i>                 | <i>Acc.orient</i>                | <i>Range</i>                |
|-------------|-------------------------------------|---------------------------------|----------------------------------|-----------------------------|
| <b>A11</b>  | Pig receiver & Launchers/ESD valves | 10"-PR-20-5347-EC19AX           | North-South                      | 300 mm/s                    |
|             |                                     | <b>Valve tag</b><br>20-FE5228-1 | <b>Valve orient.</b><br>Vertical | <b>Excitation</b><br>Stroke |

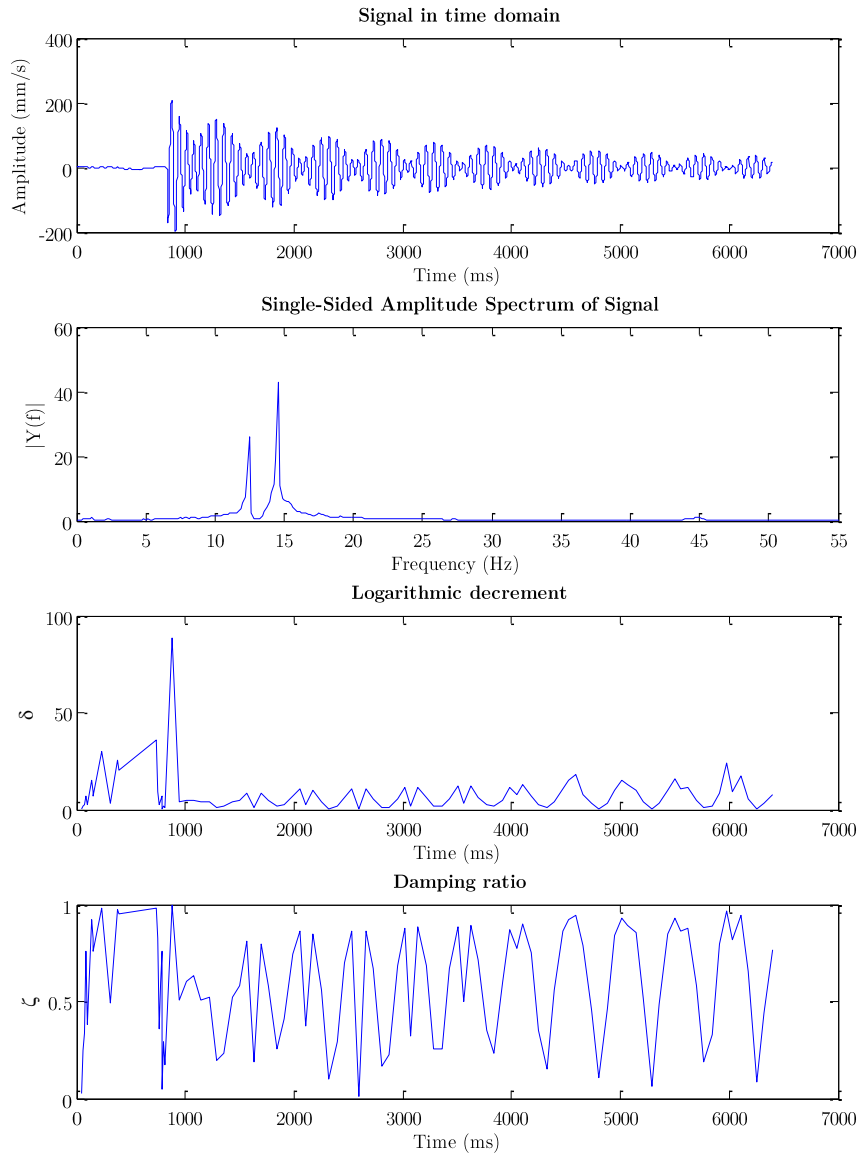


Figure 8-28 Result Induced vibration PR-20-5347-EC19AX, A11, N-S

| <i>Area</i> | <i>Description</i>                  | <i>Line tag</i>                 | <i>Acc.orient</i>                | <i>Range</i>              |
|-------------|-------------------------------------|---------------------------------|----------------------------------|---------------------------|
| <b>A11</b>  | Pig receiver & Launchers/ESD valves | 10"-PR-20-5347-EC19AX           | East-West                        | Auto range                |
|             |                                     | <b>Valve tag</b><br>20-FE5228-2 | <b>Valve orient.</b><br>Vertical | <b>Excitation</b><br>None |

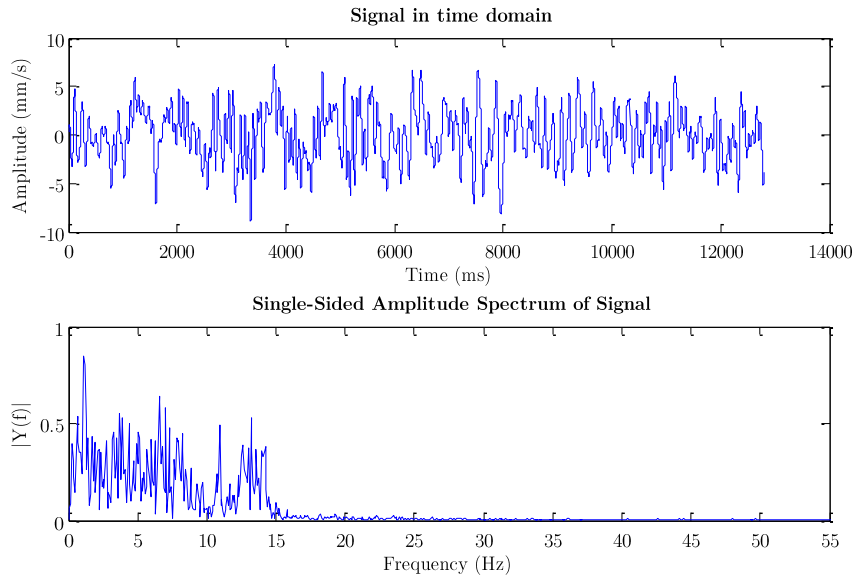


Figure 8-29 Result Non-induced vibration PR-20-5347-EC19AX, A11, E-W

| <i>Area</i> | <i>Description</i>                  | <i>Line tag</i>                 | <i>Acc.orient</i>                | <i>Range</i>                |
|-------------|-------------------------------------|---------------------------------|----------------------------------|-----------------------------|
| <b>A11</b>  | Pig receiver & Launchers/ESD valves | 10"-PR-20-5347-EC19AX           | East-West                        | 300 mm/s                    |
|             |                                     | <b>Valve tag</b><br>20-FE5228-2 | <b>Valve orient.</b><br>Vertical | <b>Excitation</b><br>Stroke |

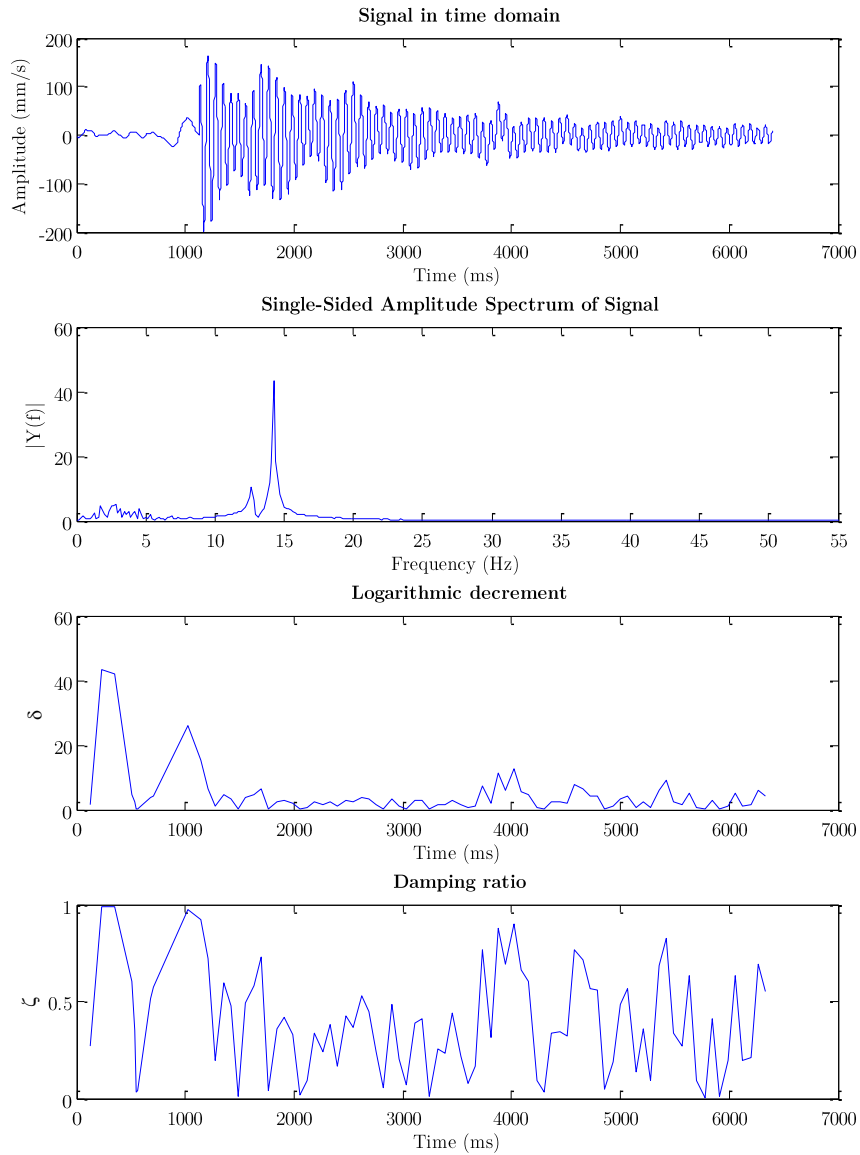


Figure 8-30 Result Induced vibration PR-20-5347-EC19AX, A24, E-W



| <i>Area</i> | <i>Description</i>                  | <i>Line tag</i>                 | <i>Acc.orient</i>                | <i>Range</i>              |
|-------------|-------------------------------------|---------------------------------|----------------------------------|---------------------------|
| <b>A11</b>  | Pig receiver & Launchers/ESD valves | 10"-PR-20-5347-EC19AX           | North-South                      | Auto range                |
|             |                                     | <b>Valve tag</b><br>20-FE5228-2 | <b>Valve orient.</b><br>Vertical | <b>Excitation</b><br>None |

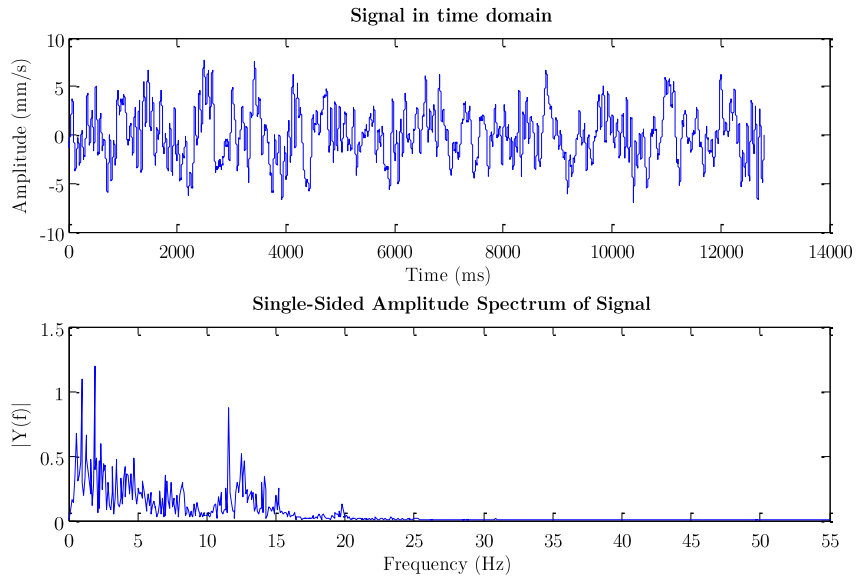


Figure 8-31 Result Non-induced vibration PR-20-5347-EC19AX, A11, N-S

| <i>Area</i> | <i>Description</i>                  | <i>Line tag</i>                 | <i>Acc.orient</i>                | <i>Range</i>                |
|-------------|-------------------------------------|---------------------------------|----------------------------------|-----------------------------|
| <b>A11</b>  | Pig receiver & Launchers/ESD valves | 10"-PR-20-5347-EC19AX           | North-South                      | 300 mm/s                    |
|             |                                     | <b>Valve tag</b><br>20-FE5228-2 | <b>Valve orient.</b><br>Vertical | <b>Excitation</b><br>Stroke |

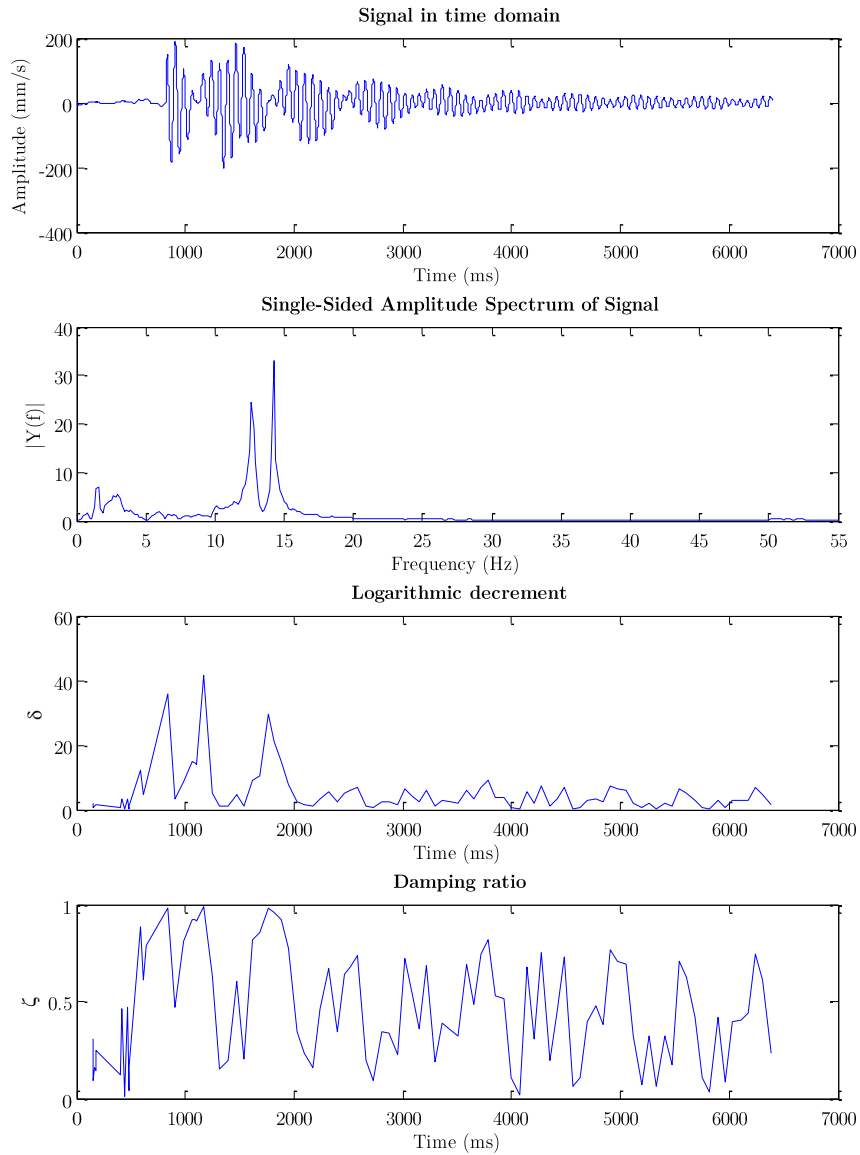


Figure 8-32 Result Induced vibration PR-20-5347-EC19AX, A11, N-S